Assessment of Functional Magnetic Resonance Imaging as a Tool to Detect Neuronal Activity in the Spinal Cord

BY
Jane M. Lawrence Dewar

A Thesis
Submitted to the Faculty of Graduate Studies
in Partial Fulfilment of the Requirements for the Degree of

Doctor of Philosophy

Department of Physiology
University of Manitoba
Winnipeg, Manitoba

Assessment of Functional Magnetic Resonance Imaging as a Tool to Detect Neuronal Activity in the Spinal Cord

BY

Jane M. Lawrence Dewar

A Thesis/Practicum submitted to the Faculty of Graduate Studies of The University of Manitoba in partial fulfillment of the requirement of the degree

Of

DOCTOR OF PHILOSOPHY

ABSTRACT

Functional Magnetic Resonance Imaging (fMRI) is an indirect, non-invasive tool that has been used to detect areas of neuronal activity in the brain during a stimulus or task. Regions of activity are identified based on a hemodynamic effect. Coupling between the metabolic demands of neuronal activity and the hemodynamic response results in localized increases in blood oxygenation as the areas of activity receive a much larger supply of oxygenated blood than is needed. Oxyhemoglobin and deoxyhemoglobin have different magnetic susceptibilities therefore the localized increases in blood oxygenation are detectable by fMRI. More recently, the technique has been developed for use in the spinal cord. Spinal cord imaging is subject to more confounds than brain imaging. Examples of additional problems include motion due to respiration and the flow of cerebral spinal fluid (CSF). For these reasons the technique must be verified by comparison with "gold standards" in order to demonstrate that spinal fMRI can detect regions of neuronal activity.

In Chapter 2, a chronic experimental model for fMRI imaging of the rat spinal cord is described. This section is critical for later parts of the thesis as well as future studies as currently, alpha-chloralose is the most commonly used anesthetic during animal fMRI studies. Recovery of the animal is not possible therefore limiting experimental design. The areas of functional activity in the cervical spinal cord were compared in alpha-chloralose and halothane anesthetized rats during electrical forepaw stimulation. The expression of c-fos, a known marker of neuronal activity, was used to observe the regions of the spinal cord in which activity was observed. Correspondence between functional activity and c-fos expression was found in the rostral-caudal

direction. The results indicate that halothane anesthesia can be used during animal spinal fMRI studies.

In Chapter 3, the fMRI response in the rat spinal cord to different intensities of thermal stimuli is characterized. A comparison between alpha-chloralose and halothane anesthesia was also repeated in order to confirm our previous findings that halothane could be used for animal spinal fMRI. The most striking results demonstrate that the intensity of stimulation could be identified by the magnitude of the percentage signal change observed. Regardless of type of anesthesia, greater percentage signal change was observed during noxious thermal stimulation as compared to innocuous thermal stimulation. Results confirmed that functional activity could be observed in the rat spinal cord under halothane anesthesia. As in Chapter 2, c-fos expression was used to verify the presence and identify the rostral-caudal distribution of neuronal activity.

Finally, we have used local field potentials to localize areas of neuronal activity and compare to areas of functional activity identified by fMRI in the rat lumbar spinal cord during electrical stimulation of the hind paw. Generally, fMRI revealed a similar rostral-caudal distribution of active pixels compared to the distribution of negative local field potentials. The correlation within the slices was limited, however, the two measurements were not taken simultaneously therefore a direct site-to-site match between active pixels and negative local field potentials may not be possible. Further work is needed to investigate the causes of disagreement between the two techniques that is observed in some areas. Electrophysiology reveals neuronal activity within the deeper layers of the cord and on the contralateral side. This provides a better assessment of spinal fMRI than the comparison to c-fos labeling alone. This work advances our

understanding of what the functional maps obtained by spinal fMRI represent. In turn, a better understanding of spinal fMRI will help further the acceptance of the technique as a useful clinical tool for assessing pathological conditions of the spinal cord.

ACKNOWLEDGEMENTS

Many thanks to all those involved in this project in one way or another over the past years. In particular:

My supervisor Kris Malisza, without her never ending patience, encouragement, support, and guidance this work would not have been possible.

My advisory committee: Patrick Stroman for the countless hours of writing programs, fixing them when I can't get them to work, and his continuous support and patience. Phil Gardiner, who welcomed me into his lab and provided guidance through the electrophysiology studies. Larry Jordan, for his support, helpful discussions, and always ensuring I stay on track.

All of those who provided support in the preparation for, and completion of these experiments including, Saro Bascaramurty, Marco Gruwel, Allan Turner, Kalan Gardiner, and Slava Vyacheslav. I would like to also thank Uta Sboto-Frankenstein for always being a supportive friend.

Thank you to my fellow graduate students in the physiology department who saved my sanity. I am especially grateful to Jennifer Kornelsen, Myriam Lafreniere-Roula, and Katinka Stecina. I am extremely fortunate to work with such a great source of support and to be able to share in each other's successes along the way.

I would like to thank my family. My mother, Sharon, and grandparents, Lillian, and James, who have a constant source of encouragement throughout my studies. Finally, I would like to that my husband Mark, for his unwavering support, encouragement and devotion during my studies.

TABLE OF CONTENTS

LIST OF TABLES

CHAPTER 2

List of Figures

Chapter 1

Chapter 2

Chapter 3

CHAPTER 4

APPENDIX 1

CHAPTER 1: GENERAL INTRODUCTION

Thesis Overview

Spinal cord injury affects over 41,000 Canadians and each year there are approximately 1,100 new injuries (Rick Hansen Foundation, 2004). The majority of spinal cord injury research focuses on recovery and regeneration. With the development of new methods of intervention, better techniques for assessing spinal cord function are needed. Currently the American Spinal Injury Association (ASIA) scale is the most common and accepted method. This scale generally surveys the extent to which motor and sensory modalities are present or absent and then estimates the extent of injury in the cord. A more detailed method is needed in order to provide more comprehensive information about the level and areas of neuronal activity in the spinal cord.

Functional Magnetic Resonance Imaging (fMRI) is an accepted noninvasive method for determining areas of neuronal activity in the brain. The field of fMRI is rapidly expanding as it is proving a powerful tool for examining both healthy and pathological conditions. It has been used clinically to assess brain functioning in stroke patients as well as in presurgical planning in epileptics. FMRI has several advantages over other neuroimaging techniques including that it is completely non-invasive. Cerebral blood oxygenation is used as an endogenous contrast agent making an injection of radioactive isotopes, such as used in Positron Emission Tomography (PET) studies, unnecessary. The application of fMRI to the spinal cord provides a noninvasive method of observing areas of neuronal activity making it a useful tool for assessment of function in spinal cord injury and disease. Furthermore, as rehabilitation and treatment methods

for spinal cord injury improve, an accurate tool is required that will provide a specific report on any progress in recovery. Spinal fMRI yields a map of changes in neuronal activity and may be used to assess spinal cord function.

The application of fMRI to the spinal cord is recent. Therefore, in order for the technique to become widely accepted by the clinical and scientific communities, a comparison with "gold standard" techniques must be performed to verify that spinal fMRI non-invasively detects areas of neuronal activity. In brain fMRI, functional maps were validated by comparison with other techniques such as $H_2{}^{(15)}O$ PET (Ramsey et al. 1996) and local field potentials (Logothetis et al. 2001).

Functional maps obtained in the rat spinal cord were compared with other methods of detecting neuronal activity. Chapters 2 and 3 outline areas of functional activity in the spinal cord compared with the expression of c-fos, a nuclear protein and accepted marker of neuronal activity. Chapter 4 compares functional maps with the areas of extracellular local field potentials. The results of this work assess the relationship between the two techniques in order to determine the level of correspondence.

Spinal cord anatomy and physiology

As part of the central nervous system, the spinal cord relays and integrates messages between the body and brain and from the environment. Sensory information is relayed from muscle, joints, and skin. Motor information is transmitted for both voluntary movements and involuntary reflexes. The spinal cord, like the brain, is composed of white and gray matter. The outer portion, composed of white matter, surrounds the inner, butterfly-shaped gray matter. The white matter is subdivided into dorsal, lateral, and ventral funiculi. These longitudinal tracts of myelinated axons carry sensory information to the brainstem and brain through ascending pathways and descending tracts carry information from the supraspinal levels to various levels of the cord. The gray matter, which contains the cell bodies of nerve cells, is subdivided into dorsal and ventral horns and an intermediate zone. The dorsal horns contain sensory neurons, which receive input from the body. The ventral horns contain interneurons as well as being the location of motor neurons whose axons innervate skeletal muscle. Interneurons in the gray matter integrate somatosensory information from the trunk and limbs to the brain, information from the brain back to the periphery, as well as between motor neurons.

As in the brain, there are three meningeal layers surrounding the spinal cord, the pia mater, arachnoid mater, and dura mater. The subarachnoid space around the spinal cord is filled with cerebral spinal fluid (CSF). Near the center of the cord is a small central canal also filled with CSF. The flow of CSF occurs in pulsations related to the cardiac cycle (Henry-Feugeas et al. 1993). The spinal cord is housed in the spinal canal of the spine. Between each adjacent vertebra is a space, or foramen, through which the spinal nerves exit from the spinal canal and go out to innervate the body. The dorsal root

ganglia, made up of the cell bodies of primary afferent neurons, are housed within the intervertebral foramina.

The rat spinal cord is on average 119.9 mm long and contains 34 spinal cord segments (Hebel R and Stromberg, 1986). There are five regions of the spinal cord: cervical, thoracic, lumbar, sacral, and coccygeal. The rat spinal cord consists of eight cervical (C) segments, thirteen thoracic (T) segments, six lumbar (L) segments, four sacral (S) segments and three coccygeal segments. The spinal cord is shorter than the vertebral column and spinal cord segments smaller that the vertebra. Therefore, the spinal cord segments do not necessarily align with the vertebra of the same number (Figure 1). While the first cervical vertebra is in alignment with the first cervical spinal cord segment, the first thoracic spinal cord segment aligns with the last cervical vertebra. The first lumbar segment begins at the distal end of the eleventh thoracic vertebra (Hebel R and Stromberg, 1986). Each spinal cord segment projects two dorsal and two ventral roots. A dorsal and ventral root unit on either side of the spinal cord to form a spinal nerve which exits the vertebral column through the intervertebral foramina. The spinal nerves later branch to innervate the body. The third to sixth lumbar spinal cord segments project motor fibers to the hind limb and receive sensory fibers. The hind limb is innervated by two major nerves, the cutaneous surae lateralis and the tibialis (Figure 1). The cutaneous surae lateralis is a nerve which arises from the fibularis (peroneal) nerve. The fifth cervical to first thoracic spinal cord segments receive forelimb sensory input and project motor fibers to this area via the medianus and ulnaris nerves (Figure 1).

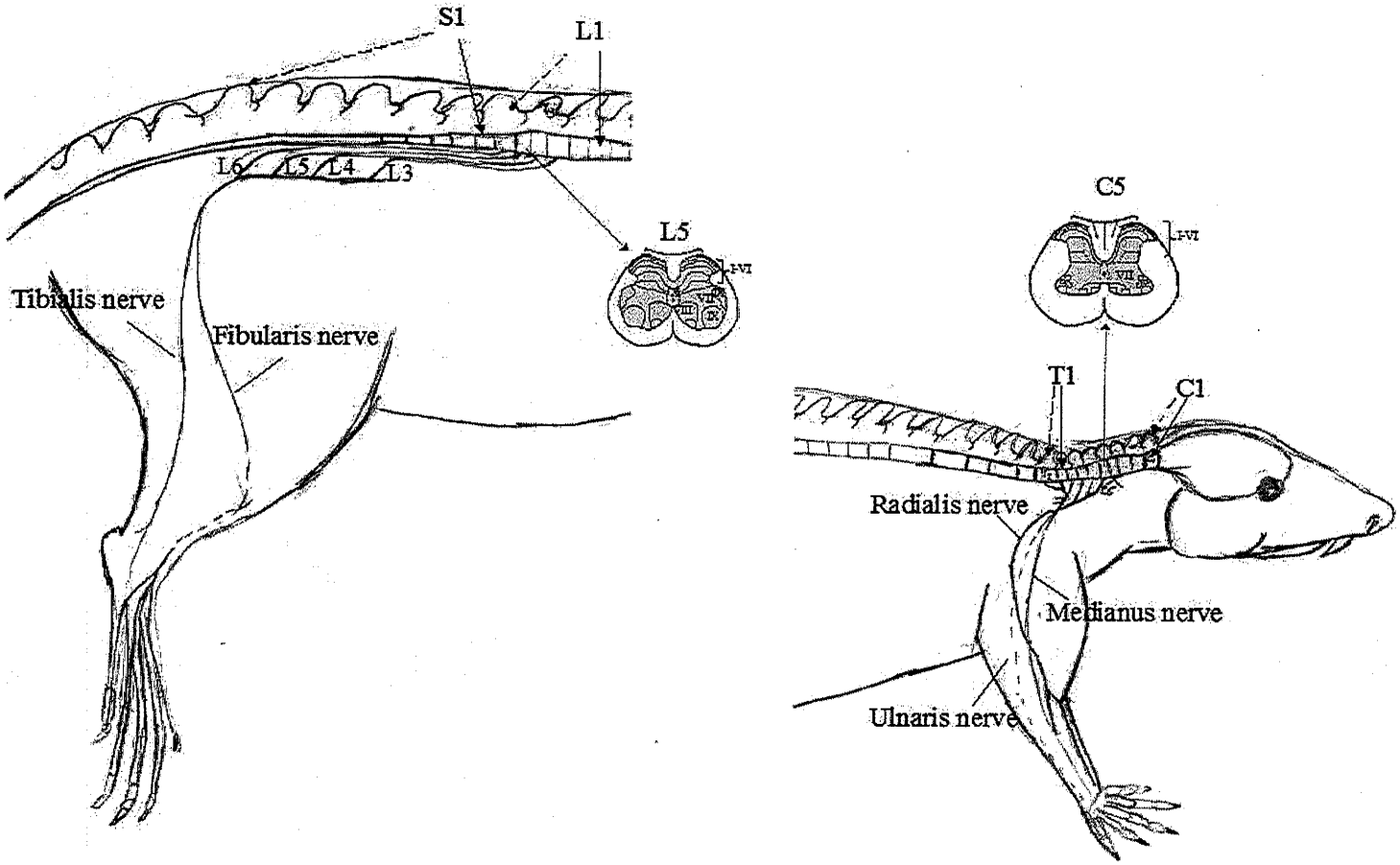

Figure 1. General neuroanatomy of the rat involved in this dissertation. Solid arrows indicate the labeled spinal cord levels. Dashed errors indicate the labeled verebral levels. Laminar organization is identified on cross sections of the spinal cord at levels of interest to this thesis.

The gray matter of the spinal cord is divided into 10 regions called Rexed laminae based on the cytoarchitecture determined by the morphology and distribution of Nissl-stained cell bodies in cross-sections (Rexed, 1952; Rexed, 1954). Although Rexed described the laminar system in the cat his organization has since been applied to the rat spinal cord (Molander and Grant, 1995). The rat spinal cord consists of ten laminae (Figure 1). The dorsal horn consists of lamina I through VI. The position of laminae V and VI is different in different spinal cord segments. They are located in either the dorsal horn or in the intermediate zone. The intermediate zone contains lamina VII. The ventral horns contain laminae VIII and IX. The gray matter surrounding the central canal contains lamina X.

Vasculature of the spinal cord

The arterial system that supplies the spinal cord is very similar to that of humans. Three vessels, a single ventral spinal artery, and two dorsal arteries run longitudinally along the length of the spinal cord.

The ventral spinal artery lies in the surface of the ventromedial fissure. At regular intervals the ventral spinal artery gives off branches called sulcal arteries. The vessels ascend the ventromedial sulcus to reach where the ventral horn meets the gray commissure. The sulcal arteries form numerous branches supplying the gray matter, as well as one or more branches projecting into the white matter (Scremin, 1995).

The pial arterial network sends perforating arteries to supply other areas of the spinal cord. They are arranged in radial orientation and travel through the white matter to the gray matter (Scremin, 1995).

The gray matter of the spinal cord is more vascularized than the white matter. The majority of blood supply to the gray matter comes from the sulcal arteries. The dorsal horns receive blood from the posterior spinal arteries, posterior medullary feeders and perforating pial branches.

Transduction of somatosensory stimuli

There are three types of cutaneous receptors: mechanoreceptors, thermoreceptors, and nociceptors. Cutaneous mechanoreceptors respond to mechanical touch of the skin. Differences in surface temperature stimulate cutaneous thermoreceptors. Nociceptors respond to stimuli that threaten or cause injury to tissue.

Nociceptors are classified according to the types of stimuli to which they respond and to the size of the afferent fiber that innervates them (Willis and Coggeshall, 2004). There are two main classes of nociceptors, Aδ and C polymodal nociceptors, in addition to a variety of other classes. Aδ and C refer to the fibre type of the primary neuron. Aδ fibres are finely myelinated and conduct signals more quickly than small-diameter, C fibres that are not myelinated.

The receptors responding to heat stimuli have been divided into three categories: warming units, warming/noxious heat units, and noxious heat units (Menetrey et al. 1979). Warming units respond to innocuous warm temperatures below 42.5°C. Innocuous thermal stimuli cause firing of Aδ afferent fibres. The theshold for warming/noxious heat units have a maximal response above 42.5°C. Noxious heat units have a threshold between 42.5°C and 48°C and firing rate increases with increased temperature (Menetrey

et al. 1979). Noxious thermal stimulation results in the firing of both Aδ and C afferent fibers.

Pathways involved in the transmission of somatosensory pain and temperature

The principle pathway mediating information regarding noxious and thermal stimuli is the anterolateral system. The anterolateral system is composed of three ascending tracts: the spinothalamic, spinoreticular, and spinomesencephalic (Willis et al., 1995). A fourth tract, the spinocervical tract, ascends the spinal cord in the dorsolateral fasciculus and is also involved in carrying noxious and thermal information (Willis et al., 1995). The origins of these tracts are in various laminae of the spinal cord. Nociceptive afferents terminate primarily within the dorsal horn of the spinal cord. Aδ nociceptive fibres terminate within lamina I and V (Light and Perl, 1979). C nociceptive fibers terminate mainly in lamina I and II (Sugiura et al. 1986). There are also neurons in lamina VII and VIII that respond to noxious stimuli (Chaouch et al., 1983). The properties of these neurons are more complicated as their inputs are polysynaptic and many of the neurons in lamina VII respond to stimuli applied to either side of the animal.

The spinothalamic tract

The spinothalamic tract carries information regarding pain and temperature. Noxious primary afferent neurons terminate in lamina I, II and V-VII and synapse with spinothalamic tract neurons. The primary afferents also send collaterals to deeper lamina in the cord. Some of these neurons in deeper lamina project back to lamina I, and interneurons in lamina II that in turn project to other laminae. Innocuous thermal

stimulation results in activity of subpopulations of spinothalamic neurons, primarily in lamina I (Christensen and Perl, 1970; Craig and Kniffki, 1985).

The axons that make up the spinothalamic tract ascend in the ventral and lateral funiculi (Giesler, Jr. et al. 1981). The spinothalamic tract has three sites of termination in the thalamus: the ventroposterolateral nucleus, the intralaminar nuclei and posterior complex.

The spinoreticular tract

There are three groups of spinoreticular neurons. Two groups respond primarily to noxious inputs. The first group of neurons originate in laminae V, VII, VIII (Chaouch et al. 1983) and X (Nahin and Micevych, 1986) and project to the medial pontomedullary reticular formation. They are often referred to as the medial spinoreticular tract. Many of the cells overlap in response properties and location with spinothalamic neurons. The axons of the cells originating in lamina X will ascend the spinal cord ipsilaterally in the ventrolateral funiculus. The second group of spinoreticular neurons originate in laminae I, V-VIII, and X and project to the dorsal reticular nucleus of the medulla. They respond to noxious input. The third group of neurons is often associated with motor control because many of the neurons respond to joint movement and project to the lateral reticular nucleus, which in turn projects to the cerebellum. A large proportion of these neurons are excited by noxious inputs (Menetrey et al. 1984). Most neurons in this group originate in lamina X and project to the lateral reticular nucleus.

Axons of the spinoreticular tract synapse in the reticular formation of the pons and medulla. The higher order neurons from the reticular formation then terminate in the intralaminar and posterior nuclei of the thalamus and in other areas of the brain such as the diencephalon and hypothalamus.

The spinomesencephalic tract

The spinomesencephalic tract projects to three areas of the midbrain: the superior colliculi, the periaqueductal gray (PAG), and the midbrain reticular formation. The PAG and midbrain reticular formation receive noxious inputs and form part of the neural circuitry involved in the descending control of pain.

Neurons which project to the PAG originate in laminae I, III, V-VII and X and in the lateral spinal and lateral cervical nuclei (Liu, 1983). The lateral spinal and lateral cervical nuclei are located lateral to the dorsal horn in the dorsal region of the lateral funiculus. The lateral spinal nucleus is present in all spinal cord segments. The lateral cervical nucleus is present only between C1 and C3 and is found just lateral to the lateral spinal nucleus (Molander and Grant, 1995). The axons of the spinomesencephalic tract ascend to the brainstem in the ventrolateral funiculus. Neurons which originate in lamina I project to the PAG in the contralateral dorsolateral fasiculus (Baker and Giesler, Jr., 1984).

Neurons which project to the midbrain reticular formation originate in similar locations as those that project to the PAG. Cells which originate in lamina I have axons which ascend in the contralateral dorsolateral fasiculus and send collateral branches to the cuneiform nucleus.

The spinocervical tract

The spinocervical tract has been well described in the cat (Brown et al., 1983). In the rat, spinocervical neurons originate in the ipsilateral dorsal horn in laminae III-V at all spinal cord levels caudal to the lateral cervical nucleus(Baker and Giesler, Jr., 1984). The axons ascend in the dorsolateral fasiculus and terminate in the lateral cervical nucleus in the rostral cervical spinal cord. The nucleus and tract are smaller in the rat than in the cat. While the tract is mainly associated with other modalities, some cells were found to respond to noxious mechanical or thermal stimuli (Willis et al., 1995).

Spinal organization of reflexes

Painful stimulation may also elicit a withdrawal reflex. Withdrawal reflexes involve the whole limb, therefore, afferent information must spread over several spinal segments to stimulate several muscle groups. Cutaneous reflexes cause the excitation of one muscle group and the inhibition of anatagonist muscles groups. This action is referred to as reciprocal innervation (Sherrington, 1906). In addition, reflexes have crossed effects. As a flexor reflex is evoked on one side, extension occurs on the contralateral side to strengthen postural support (Kandel et al. 2000). Therefore, the effects of stimulation may result in widespread activity across several spinal cord segments and on both sides of the cord.

Direct measurements of neuronal activity

To verify that functional MRI can be used to non-invasively observe areas of neuronal activity, a comparison with "gold-standards" must be performed. This involves the use of direct measurements of neuronal activity in order to observe the patterns of activity that are evoked with the type, and intensity of stimulation we are using during imaging. The neurophysiological basis of the BOLD signal in the brain was compared to single-unit recordings, multi-unit recordings, and local field potentials (Logothetis et al. 2001). Logothetis et al. found that the fMRI signal best corresponded to local field potentials as they reflect a population response within a recording area (2001). In this thesis two methods are used to observe areas of neuronal activity, the labeling of the protein c-fos, and local field potentials.

C-fos expression

The fos protein was first identified in virology research in 1982 and classified as an oncogene. It was thought to be involved in the neuroplastic process of Finkel-Biskis Jinkins murine osteosarcoma virus (Curran and Teich, 1982). Over time it was found that the fos protein is not exclusively expressed in growing cells and so it is now classified as an "immediate-early gene" from virology nomenclature. The term "early" is used because expression occurs before replication of the viral genome. The term "immediate" originates from the rapid expression of viral genes after cell infection regardless of the presence of protein synthesis inhibitors. The viral and cellular genes were since distinguished by the terms "viral immediate-early gene" (v-fos) and "cellular immediate-

early gene" (c-fos) for cellular genes rapidly induced in the presence of protein synthesis inhibition (Chiasson et al. 1997).

C-fos was linked to cell protection (Giovannelli et al. 1998), cell death by apoptosis (Inada et al. 1998) and may also be involved in communication between the immune and nervous systems (Goehler et al. 1998). It is often associated with stress response although it is present under basal conditions in many tissues, but at very low levels.

C-fos expression is rapidly induced within some neurons upon repetitive stimulation. Sensory neurons in the dorsal horn lamina and interneurons in lamina X express c-fos protein. Motor neurons do not transcribe the c-fos gene and so very little labeling is observed in the ventral horn. Increased intracellular Ca^{2+} leads to a second messenger pathway that results in the transcription of c-fos RNA (figure 2). Its translation to protein in spinal cord sensory neurons reaches a peak approximately two hours following stimulation. The c-fos protein can be visualized using immunocytochemical techniques, and its use as an activity-dependent marker is now well established (Herdegen and Leah, 1998).

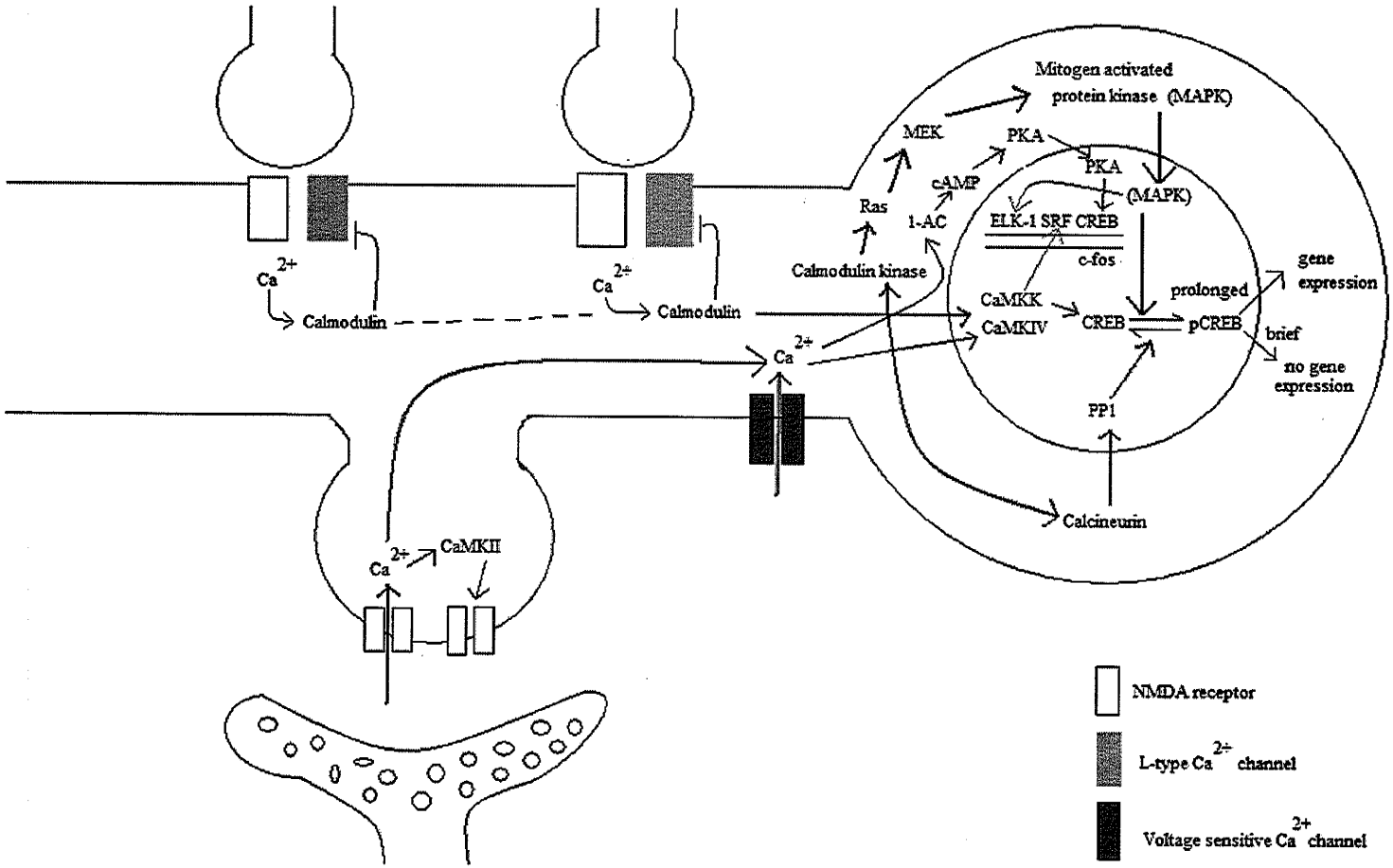

Figure 2. Depolarization-activated second messenger pathway leading to c-fos transcription

Several different types of stimuli induce the expression of c-fos, including patterns of electrical stimulation (Sheng et al. 1993). Other types of noxious stimulation employed to induce c-fos expression in the spinal cord include thermal, mechanical and chemical stimuli (Herdegen and Leah, 1998; Hunt et al. 1987). Patterns of immunolabeling of the rat spinal cord were determined following noxious mechanical stimulation of both the hind paw and forepaw (Bullitt, 1991; King and Apps, 2000). These studies demonstrated that the mediolateral somatotropy of forelimb and hind limb inputs into the spinal cord are similar. Both rostrocaudal and mediolateral somatotropic organization appears to be present in nociceptive neurons of the rat dorsal horn.

Within this dissertation, the observation of c-fos positive cells will be used to verify that neuronal activity is present in the imaged region of the spinal cord. We anticipate similarities in the distribution of c-fos labeled cells to fMRI activity in the rostral-caudal direction. Comparisons between the two techniques cannot be made, however, within cross-sections of the cord. This is due to the limitations of using c-fos. Not all neurons transcribe the c-fos gene, or do so selectively under certain conditions. Therefore, labeling of c-fos protein does not account for all neuronal activity.

Local field potentials

Predating the use of cellular markers, field potentials were used to determine the presence of neuronal activity. Local field potentials reveal the events occurring simultaneously from a large population of neurons. The net movement of ion currents near a recording electrode is observed extracellularly (Figure 3). Prior to any activity a flat base line is observed as there is no change in current. The potential observed

depends on the net events that occur in the population of cells near the recording electrode. If the recording electrode is near an area where the threshold for postsynaptic action potentials has been reached, a large negative potential is observed extracellularly due to flow of positive charged particles into the neuron (Figure 3A). These areas where current is flowing from the extracellular space into the neurons are also referred to as 'current sinks'. If the recording electrode is far away from postsynaptic potentials a positive field potential will be observed as positive charge will move into the extracellular space (Figure 3B). These areas are called 'current sources'.

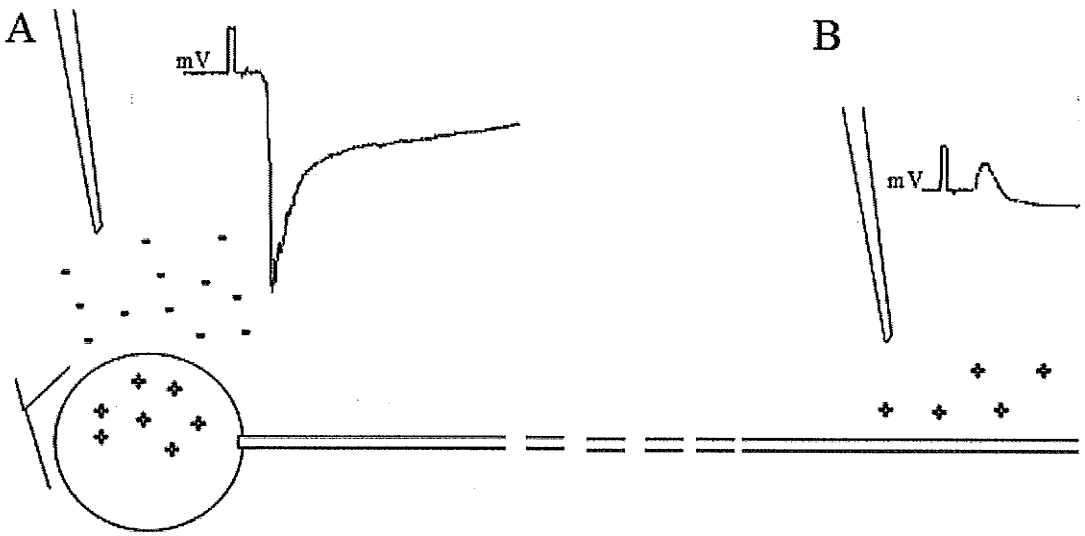

Figure 3. Extracellular events observed by local field potentials near neuronal activity (A) and at distances further away (B).

Inhibition of a neuron is caused by hyperpolarization or a net outward positive current. As a result, one may expect to observe a positive potential to be observed extracellularly. A positive voltage potential due to inhibition can be distinguished from a current source in several ways. The two causes have different temporal characteristics.

Therefore, a current source will occur in the same frame in time as the negative current sink. Postsynaptic inhibition, however, will experience a synaptic delay and therefore would be observed later in time than a current sink. The amplitude in voltage of a current source will also be proportional to that of a current sink in response to a graded stimulus. That is to say, a sink and source will be at half amplitude with half of a given intensity of stimulation. Postsynaptic inhibition involves modulation and therefore differences in amplitude will not vary linearly. In addition, much smaller currents are involved in postsynaptic inhibition and because the technique records from a population of neurons, the response would likely be masked.

In addition to excitatory and inhibitory synaptic events, there are other influences that contribute to local field potentials. The dimensions and orientations of dendrites were found to play a role in field fluctuations (Fromm and Bond, 1967; Logothetis and Pfeuffer, 2004). Voltage-dependent membrane oscillations and spike after-potentials were also shown to contribute in brain recordings (Buzsaki, 1931; Buzsaki and Gage, 1988; Kamondi et al. 1998; Kobayashi et al. 1997). As a result the responses represent input into the observed areas as well as local excitatory and inhibitory processing.

Local field potentials were used to examine neuronal activity in the spinal cord although more so in a cat model (Edgely and Jankowska, 1987; Schaible et al, 1986; Noga et al., 1995) than in the rat (Fitzgerald, 1982). Fitzgerald used extracellular recordings to characterize the response of dorsal horn cells to focal application of capsaicin to the sciatic nerve. In this thesis, we aim to identify the regions of negative local field potentials in order to further understand the basis of neuronal activity that underlies the maps obtained by fMRI.

Principles of Magnetic Resonance Physics

Nuclear Magnetic Resonance (NMR) is capable of detecting a small signal from the interaction of nuclei that have a magnetic moment, with a main static magnetic field. In the absence of a magnetic field, the nuclei of hydrogen are oriented randomly. Nuclei have an inherent property called 'spin'. Since the proton has charge and spin, it acts like a small magnet. Not all nuclei have a net nuclear momentum, (e.g. ^{12}C) and therefore do not contribute toward the NMR signal. Hydrogen has a sole proton and therefore a net magnetic moment. Hydrogen is an ideal element for biological imaging and spectroscopy experiments because of the abundance of water in the body.

Nuclei placed in a main, static magnetic field (B_0) will align parallel or anti-parallel to the field. More nuclei will align parallel to the field as this is a low energy state, whereas anti-parallel alignment is a higher energy state. A net magnetic moment is produced due to the greater number of nuclei aligned with the field. The induction of the main external field causes the protons to precess, or follow a circular path around the magnetic field. The precessional frequency can be calculated by the Larmor equation:

$$\omega_o = \gamma B_0$$

Where ω_o is the precessional frequency, B_0 is the magnetic field strength of the MRI (7T, for example), and γ is the gyro magnetic ratio (for a hydrogen proton = 42.5 MHz/T) (Jezzard et al. 2001). Therefore the precessional rate is determined by the strength of the main magnetic field and at greater strengths there will be a greater precessional frequency.

In order to obtain a MR signal, a condition called 'resonance' must be established. Resonance occurs when an object is exposed to an oscillating perturbation that has a frequency close to its own natural frequency of oscillation (ω_o). A weaker, alternating magnetic field (B_1) is applied perpendicular to the B_0 field. The applied B_1 field oscillates at a radio frequency (RF) determined by the Larmor equation. As a result the spins are excited and start to precess in phase and establish a transverse magnetization. It is the transverse magnetization that can be detected by a receiving coil. When the RF pulse is turned off, a strong signal can be observed if the spins are in phase. If the precessional frequency of the spins is different, they will begin to dephase and there will be a decrease in signal. The absorbed energy in the sample is given up over time and the nuclei relax back to the main magnetic field (Jezzard et al. 2001).

The ways and times in which the signal relaxes are exploited to produce the desired contrast in the image. Relaxation back to alignment with the main magnetic field occurs in the longitudinal (z axis) and transverse (xy plane) directions. The return of longitudinal magnetization to equilibrium is also called spin-lattice or T1 relaxation. Spin-lattice refers to the interaction and exchange of energy between the spins and the surrounding environment. As a result, different tissues will have different T1 values depending on the efficiency of how this interaction takes place. The T1 recovery is described by

$$M_z=M_0[1-\exp(-t/T1)]$$

In an environment where random motions can occur more freely (e.g. cerebrospinal fluid) the local molecular motion is much higher than the Larmor frequency. As a result the T1 relaxation is very slow. T1 is also affected by field strength. At higher field strengths the

Larmor frequency is greater. The relaxation pathways are less efficient and so T1 values are longer.

Net magnetization that decays exponentially in the transverse plane is called spin-spin or T2 decay. The T2 decay curve is

$$M_{xy}=M_0\exp(-t/T2)$$

The name spin-spin, refers on the interaction between neighbouring nuclei due to random fluctuations in the Larmor frequency. If a nucleus is near a neighbour that spins at a higher frequency, it will spin faster. Likewise, if the neighbouring nucleus has a lower frequency of spin, it will slow down. When the neighbouring spins have moved away from each other they will return to their own Larmor frequency, however, they will no longer be in phase. (Jezzard et al. 2001). The dephasing causes the signal to decay and once the moments point in all directions the net signal if zero. T2 is less dependent on the main magnetic field than T1 however, it is determined by the chemical environment. Therefore each tissue type has a different T2 value.

T2* relaxation is the decay due to large scale variations in the applied magnetic field in addition to the spin-spin interactions. These can result from physical imperfections with the magnet or more often are due to the geometry and composition of the sample. Within the head there are various interfaces between neural tissue, bone, air occupied spaces (the sinuses) and fluid filled spaces (the ventricles). Similarly, the spinal cord is surrounded by CSF, the spine, the musculature and fat of the back, and air filled spaces such as near the lungs in some areas. As the materials have different compositions they also have different magnetic susceptibilities. The areas in which different materials meet can cause artifacts or signal dropout within an image. Functional imaging of the

frontal lobe can be problematic due to signal dropout around the sinuses. While T2* may seem undesirable, it can be useful in some instances. T2* is affected by the concentration of deoxyhemoglobin; making it an endogenous contrast agent.

The desired contrast of an MR image is obtained by manipulating the factors that affect the T1 and T2 relaxation times. The manipulations are written with the pulse sequences used for imaging. Commonly, the timing and number of RF or gradient pulses are altered. There are two basic types of pulse sequences that are used within MR imaging: spin-echo and gradient echo. As only spin-echo sequences are used in the spinal cord functional MRI studies described, the components of a basic spin-echo sequence will be reviewed.

During spin echo sequences, a 90° pulse emitted from the transmitting coil tips the net magnetization into the transverse plane sending the spins into phase (Figure 4A). The signal begins to dephase (Figure 4B), and after a time TE/2, a 180° pulse is applied which flips the magnetization about the xy plane (Figure 4C), interchanging the slow and fast spins such that at time TE the spins are refocused producing the echo (Figure 4D). The time between the initial excitation pulse and the echo that is detected is referred to as the echo time (TE). A diagram of the sequence, the effects on the spins, and the observed signal are shown in Figure 4. The effects of T2 relaxation cannot be refocused in this sequence since they depend on random interactions. Therefore, any loss in transverse magnetization is due to T2. An advantage to the spin echo sequence is that because it refocuses large bulk effects, some sources of interference can be eliminated.

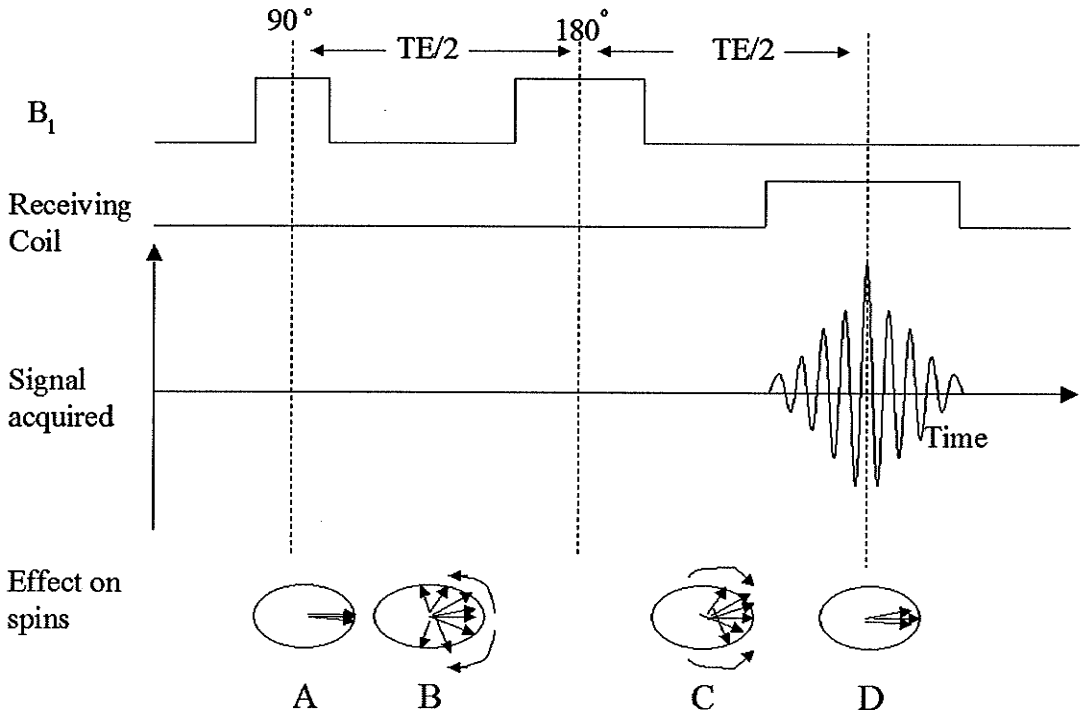

Figure 4. A simplified spin echo sequence. A 90° excitation causes spins to move from the z plane to the xy plane. When the pulse ends, the spins begin to dephase. An 180° pulse causes the spins to flip about the x-axis (or the y-axis depending on the pulse) and refocuses the signal. The peak of the echo is observed at TE.

During a gradient echo sequence, an RF pulse is used to flip the magnetization into the xy-plane and then a gradient pulse, rather than an 180° pulse is used to refocus the net magnetization. A strong signal can be detected while a gradient is on, as this is when the spins are in phase. Once the RF is turned off the signal decays exponentially. Applying a negative gradient dephases the spins and the signal decays faster. The opposite gradient is then applied to reverse the effect, and refocuses the signal (Jezzard et al., 2001). The signal acquired is dependent on T2*.

In the 1970s a method was developed that made it possible to create an image from an NMR signal. Paul Lauterbur developed the 2D back projection technique which was the first method used to reconstruct the NMR signal into an image (Lauterbur, 1973). The method applied gradients in several directions in order to obtain a spatially encoded NMR signal along lines from a variety of angles. The spectra were then compared and an image could be created. In 2003, Lauterbur was awarded the Nobel Prize in Medicine along with Peter Mansfield for their development of Magnetic Resonance Imaging. Mansfield was awarded the prize for his work in applying gradients to the magnetic field and developing faster imaging techniques.

Lauterbur and Mansfield were able to develop images from NMR spectra based on the principles of spatial specificity. Magnetic field gradients vary linearly in intensity along the 3 directional axes but are parallel to main static field. By making the main magnetic field vary in the z-plane, the Larmor frequency at which the nuclei precess is dependent on their spatial location in the main magnetic field. Therefore, even a homogeneous sample, such as a tube of water, will produce many different frequencies spread over its spatial distribution.

Since Lauterbur's discovery there have been many advances in the reconstruction of NMR images. The 2D back projection technique is no longer used as it takes long periods of time and is susceptible to signal artifacts. Current techniques use Fourier imaging. The Fourier transform breaks down the NMR signal into several sine and cosine waves. These Fourier coefficients are used to construct a 2D matrix that can later be reconstructed into an image using an inverse Fourier transform.

The 2D matrix in which the Fourier coefficients of the sample are collected and plotted is called k-space. The Fourier coefficients are plotted according to coordinates in phase and frequency encoding directions (Jezzard et al. 2001). The way in which each coordinate in k-space is collected is determined by the pulse sequence used. The parameters of the gradients are manipulated so that each location can be sampled. Once all areas have been sampled the data in k-space is reconstructed using an inverse Fourier transform. The data can then be plotted to spatially encode signal intensities from spin densities giving a recognizable image of the object.

K-space is 2 dimensional. Usually, the x-axis is called the frequency encoding direction while the y-axis is the phase encoding direction, however, this depends on the image orientation. The size of k-space is determined by the matrix size determined in the pulse sequence. The matrix size is one of three parameters that determine the resolution of the image acquired. The other parameters include the slice thickness, which determines the depth of a voxel in the z-plane, and the field of view. The in-plane resolution of an image can then be determined by dividing the field of view by the matrix size. For example, an image with a field of view of 30 mm^2 and matrix size of 128 x 128 will consist of voxels that are 0.23 mm^2.

Exploiting the relaxation rates of different tissues can produce image contrast. Without any weighting of relaxations, contrast can be obtained by proton density changes. To achieve this, the TR must be longer than T1 to ensure that the longitudinal relaxation fully recovers between repetitions and the TE must be shorter than T2 so that there is little signal decay. In these images contrast is based on the water content of different tissues. Manipulation of the TE and TR allows the weighting of the image to be

changed. Different materials have different relaxation times. A T1 weighted imaged is obtained by using a short TR, short TE, and a high flip angle. In a T1 weighted image CSF appears dark because the long T1 of CSF does not allow time for the CSF to fully recover during a short TR period. Tissues with short T1 (white matter and fat) will appear brighter, since they can recover more fully during the short TR period. T2 weighted images can be obtained by using a long TR and long TE. Stronger signal is obtained from tissues with longer relaxation times (Jezzard et al. 2001). If the echo time is made longer, the signal amplitude decreases as defined by the T2. Tissues with long T2 appear brighter (CSF, fat) whereas those with short T2 are darker (liver, white matter tracts). In images with T2-weighting, TR should be long to avoid any T1-weighting. Similarly, T1-weighted images should have a short TE to reduce T2-weighting.

T2* weighting is typically used during functional imaging in order to obtain signal based on the local concentration of deoxyhemoglobin. It is obtained by using a gradient echo sequence with a TE approximately equal to T2* in order to obtain optimal contrast-to-noise (Jezzard et al. 2001). The T2* of oxygenated and deoxygentated blood is different, providing a contrast mechanism for functional imaging.

Functional Magnetic Resonance Imaging

Functional Magnetic Resonance Imaging (fMRI) can be used to observe a map of neural activity that occurs in neural tissue in space and time. The technique uses an endogenous contrast agent as the T2* of the blood is affected by the ratio of deoxyhemoglobin and oxyhemoglobin. The fact that the method is non-invasive makes fMRI more appealing than other imaging methods such as Positron Emission

Tomography (PET) which requires a bolus injection of radioactive tracer. Functional MRI has greater spatial resolution than EEG and MEG and is capable of detecting neuronal activity in deep brain structures such as in the basal ganglia. The temporal resolution of fMRI is limited compared to electrophysiological techniques as the signal is an indirect measure of neuronal activity. In the brain, the time to reach from baseline to the peak of response is approximately six seconds. This is known as the hemodynamic response. The basis of the contrast mechanism makes an assumption of the relationship between neuronal activity and localized increases in cerebral blood flow. Several studies have investigated and verified the neural-hemodynamic coupling relationship in the brain.

Neuronal activity is an energy expensive process. In the central nervous system, ATP utilization is an oxidative process requiring a constant supply of glucose and oxygen. These materials are supplied, and waste products removed, by the vascular system. The brain and spinal cord are highly vascularized with many branching small vessels and capillaries. It is at the capillaries where exchange of oxygen and carbon dioxide takes place. This close spatial relationship at the level of capillaries between neuronal activity and the blood oxygen saturation can be utilized to indirectly detect areas of neuronal activity.

Blood Oxygenation Level Dependent Effect

The hemodynamic effect that is the primary basis of the fMRI signal is known as the Blood Oxygen Level Dependent (BOLD) effect. The BOLD effect is based on the magnetic properties of iron in the heme of hemoglobin. In oxyhemoglobin the iron is

diamagnetic, however, in deoxyhemoglobin it is paramagnetic (Pauling and Coryell, 1936). Diamagnetism is the state in which a material has a tendency to counteract the presence of an applied magnet field in order to minimize the effect of the magnet field. Most constituents of tissue are diamagnetic and therefore would not contribute to the fMRI signal (Ogawa et al. 1990). In contrast, paramagnetic materials align with the magnetic field producing an internal magnetic field. In a magnetic field, deoxyhemoglobin results in some field distortion due to susceptibility differences relative to the surrounding area, which cause local magnetic field gradients. In turn this leads to intravoxel phase dispersions. Therefore, a decrease in the amount of oxygen, or increase in the concentration of deoxyhemoglobin, is known to decrease T2 (Thulborn et al. 1982) and T2* of a sample. Ogawa found that the greater ratio of oxyhemoglobin to deoxyhemoglobin during neuronal activity resulted in an increase in the T2* of the blood and therefore an increased fMRI signal, which he called the BOLD signal (Ogawa et al. 1992).

Neuronal activity results in a local increase in blood flow. After the first few seconds of activity the blood flow is much larger than the rate of oxygen consumption, resulting in a net increase of local oxygen (Ogawa et al. 1990). In contrast to the basal state, an area of activity will have a much higher proportion of oxyhemoglobin compared to deoxyhemoglobin. Functional MRI examines the differences between rest and active states. However, the methodology is not a simple subtraction of the resting state from the activation state. Several repeated measures of rest and activity must be observed within one fMRI experiment in order to observe a representative change and increase statistical

significance. This type of design is called a 'block design' experiment as several repeated image volumes are acquired during alternating periods of rest and stimulation.

The neurophysiological basis of the BOLD effect in the brain was investigated by comparing the response in visual cortex of monkey with electrophysiological recordings (Logothetis et al. 2001). Since then there were several reviews by Attwell and Iadecola (2002), Logothetis and Wandell (2004), Nair (2005), and Raichle and Mintun (2006) that are useful for more information about the relationship between neuronal activity and the BOLD response. Further work is still needed in order to fully understand all of the influences of the BOLD effect. Differences in metabolic demands from different types of cells should be considered as they may influence the overall response (Logothetis and Wandell, 2004). Large projection neurons may have larger energy requirements compared to glial cells. The mechanisms that constitute the overall increased metabolic demand should be considered.

The dependency of the BOLD contrast mechanism on changes in blood flow and oxygenation means that the signal is vulnerable to any manipulations of the vascular system. Dilation of blood vessels has been observed in upstream arterioles outside the area of neuronal activity (Iadecola et al., 1997). Vascular effects that take place further away interfere with the specificity of the signal. Blood flow can also be altered by modulations to the autonomic nervous system. Anesthetics, or drugs that modulate aspects of the normal functioning of autonomic signals may also alter the capacity to which the vascular system can react to changes in oxygen demand. Factors affecting the blood gas concentrations are critical. Within animal studies careful monitoring is important to ensure animals are not hypercapnic as accurate changes in blood

oxygenation are needed to observe a dependable fMRI signal. Any of the above concerns can alter the coupling between neuronal activity and the BOLD response and lead to either false positive or false negative signals.

Signal Enhancement by Extravascular Protons

The local increase in blood flow to an area of neuronal activity also results in a local increase in blood pressure. The increase in blood pressure may result in a small amount of water moving from the intravascular space to the extravascular space. This movement of water has been observed in PET studies (Fujita et al. 1997; Ohta et al. 1996). Furthermore, evidence has shown that in an area of neuronal activity, glial cells, specifically astrocytes, swell with water uptake associated with the movement of ionic currents (Amiry-Moghaddam and Ottersen, 2003). By using an extremely short echo time the signal of the functional image will be limited to the proton density, as there will be no relaxation weighting. In this case, the fMRI signal is produced by the water protons and therefore from the movement of water. This second contrast mechanism is called Signal Enhancement by Extravascular Protons (SEEP) (Stroman et al. 2003).

The existence of a second contrast mechanism, SEEP, has been debated within the fMRI community. However, there are several sources of evidence that suggest another contributor to contrast exists in addition to BOLD. In a study performed by Stroman et al. consistent signal change was observed at low field and at very short TE where no signal should be observed if BOLD was the only contributor (2003). More recently, others confirmed the existence of a second contrast mechanism (Li et al. 2005; Ng et al. 2006).

The SEEP contrast mechanism was first observed during human spinal fMRI studies. In those studies, spin-echo sequences with extremely short echo times are used in order to minimize artifacts in spinal cord imaging. In brain fMRI the sequence provides smaller more localized areas of activity as the signal originates near the capillaries. SEEP was proposed as a complementary contrast mechanism to BOLD. In the spinal cord, SEEP is extremely valuable as traditional BOLD imaging methods, using gradient echo sequences, would result in severely distorted images.

Within this dissertation we anticipate a contribution to the signal from SEEP as spin-echo techniques are employed. At higher field strengths it is difficult to achieve a short enough echo time to obtain purely proton density weighted images. Therefore the fMRI obtained in the experiments presented here have substantial contributions from BOLD effect as well.

Spinal fMRI

Functional imaging of the spinal cord is more complicated than that of the brain. Imaging of the spinal cord is difficult because it is more prone to movement, and there are a number of interfaces between tissue, bone, and fluid. Movement results in blurring of images and renders them difficult if not impossible to analyze. Some movement due to respiration is unavoidable; however, it can be minimized. The pulsatile flow of CSF surrounding and within the cord can also cause motion artifacts. The CSF flow was found to correlate to the cardiac cycle (Henry-Feugeas et al. 1993). Therefore with an increased heart rate, as may be observed under stimulation conditions, the rate of CSF

flow will also increase. Finally, susceptibility differences occur at the interfaces of bone and tissue, which also affects the MR signal.

FMRI of the spinal cord is a relatively new technique developed at the Institute for Biodiagnostics (Stroman and Ryner, 2001) and was used to study the patterns of activity elicited in the human and rat spinal cord during a variety of tasks. Human spinal fMRI studies have employed motor tasks and thermal stimulation (Kornelsen and Stroman, 2004; Stroman et al. 2002; Stroman and Ryner, 2001). When subjects squeezed a rubber bulb in their hand ipsilateral activity at the eighth cervical vertebrae as well as some localized contralateral activity at the seventh cervical vertebrae was observed (Stroman and Ryner, 2001). Thermal stimulation applied to the hand resulted in ipsilateral and contralateral activation at the eighth cervical spinal cord. Human studies have also investigated activity in response to vibration (Lawrence et al., 2005), acupuncture (Li et al. 2005) and von Frey filament (Brooks et al., 2004) stimuli as well as electric median nerve stimulation (Kollias et al., 2004). Differences were observed during spinal fMRI studies investigating sensory and motor tasks between spinal cord injury patients in comparison to control subjects (Kornelsen and Stroman, 2004; Stroman et al. 2004). Recent advances using sagittal slices enable a larger region of the cord to be imaged (Stroman et al. 2005). Unfortunately, due to the limitations in imaging the rat spinal cord at 7T, it is not possible at the present to translate this method to the animal studies presented here.

Animal spinal fMRI

Animal studies play an important role as they allow some conditions to be studied that are not permissible in humans. One confound of animal spinal fMRI is the requirement of anesthesia in order to reduce stress and motion. Therefore, the response observed in animals must also be fully characterized. Animal spinal fMRI studies have investigated the patterns of functional activity during different types of stimulation. Existing animal spinal fMRI studies have examined activity due to capsaicin injection (Malisza and Stroman, 2002). Capsaicin injected into the left dorsal forepaw of the rat resulted in ipsilateral activation from the sixth to the eighth cervical spinal cord segments mainly in the dorsal region of the spinal cord. Some activations were also noted on the contralateral side of the spinal cord, however, the main activations which corresponded to the paradigm involved the ipsilateral side of the spinal cord (Malisza and Stroman, 2002). Functional MRI studies involving animals have also demonstrated activity in the 6^{th} to 8^{th} cervical (C) spinal cord segments (corresponding to C5-C7 vertebrae) and 3^{rd} lumbar (L) to 1^{st} sacral (S) spinal cord segments (corresponding to the 13^{th} thoracic (T) to 1^{st} lumbar vertebrae) following electrical stimulation of the forepaw and hind paw, respectively (Malisza et al. 2003; Malisza and Stroman, 2001). Other studies have investigated areas of activity within the rat spinal cord and brain (Lilja et al. 2006; Majcher et al. 2006). The pharmacological modulation of nociception in the rat spinal cord was observed following administration of morphine (Lilja et al. 2006).

The areas of functional activity in the lumbar and cervical spinal cord of the rat were compared with the expression of c-fos protein during electrical stimulation of the right hind paw and forepaw, respectively (Lawrence et al. 2004). Functional activity in

the lumbar spinal cord was observed between the L3 and L6 spinal cord segments. The greatest amount of fMRI activity was observed between the L4 and L6 spinal cord segments. C-fos labeled cells were observed in the dorsal horns between the L4 and L6 spinal cord segments bilaterally. Control experiments revealed that labeling on the contralateral side of stimulation was likely due to surgery performed to cannulate the femoral artery and vein. During forepaw stimulation, functional activity was observed mainly between the C5 and C7 spinal cord segments in the ipsilateral dorsal horn and contralateral ventral horn. The greatest amount of fMRI activity in the dorsal horn was noted in spinal cord segment C5, with significant activations that extended from C5 to C7. Consistent areas of activity were also observed in the right dorsal horn, left ventral horn and around the central canal between spinal cord segments C3/C4 and C7. Typical fMRI signal changes resulting from electrical stimulation are in the range of 10 to 15%, which corresponds well with previous results (Malisza and Stroman, 2002). Small clusters of c-fos positive cells were observed on the ipsilateral side in cervical spinal cord segments C4, C7 and C8 and in large clusters in spinal cord segments C5 and C6. Correlation of histology and fMRI of the spinal cord supports the hypothesis that spinal fMRI demonstrates sites of neuronal activity. Functional MRI of the rat spinal cord demonstrated activity within areas of the cervical and lumbar spinal cord in agreement with physiology, previous observations and immunohistological findings of neuronal activity.

Specific Objectives

Spinal fMRI has obvious clinical and research applications in the area of spinal cord injury and neurodegenerative disease. The ultimate goal of this dissertation is to assess the relationship between areas of signal change observed by functional MRI and areas of neuronal activity in the spinal cord. Areas of signal change observed by fMRI will be referred to as "functional activity" in the following chapters. The term "neuronal activity" will be used to refer to responsive cells determined by immunohistochemistry or electrophysiology.

Animal fMRI studies are complicated by the need for anesthesia in order to reduce motion and stress. Traditionally, alpha-chloralose is the anesthetic of choice as it has been shown to best preserve the neuronal-hemodynamic coupling. In order to develop a chronic animal model it is first necessary to examine different anesthetics agents. In chapter 2, it was demonstrated that halothane can be used for anesthesia during spinal fMRI studies without compromising the quality of results. The presence of c-fos labeled cells confirmed the presence of neuronal activity within the imaged regions of the spinal cord.

The response observed by fMRI must be characterized by comparisons with other types of stimuli. In chapter 3, neuronal activity elicited by innocuous and noxious thermal stimulation to the forepaw was investigated. To date, all animal spinal fMRI studies have investigated responses evoked by electrical or chemical stimuli (Lawrence et al. 2004; Lilja et al. 2006; Majcher et al. 2006; Malisza and Stroman, 2002). The results presented expand upon the repertoire of stimuli used in animal spinal fMRI studies. A

comparison between intensities of heat aids in the further understanding of the observation of nociception by spinal fMRI. Animals anesthetized with alpha-chloralose were compared to those anesthetized with halothane in order to confirm findings using these different types of stimuli. C-fos expression was used to verify the presence of neuronal activity within the region of the spinal cord that was imaged. In chapter 4, spinal fMRI during noxious hind paw stimulation was compared to areas of negative local field potentials within same rats. This is the first comparison between fMRI and electrophysiology in the spinal cord. While direct correlations may be limited as the two techniques were not performed simultaneously, valuable information can be gained.

CHAPTER 2: FUNCTIONAL MAGNETIC RESONANCE IMAGING OF THE CERVICAL SPINAL CORD IN THE HALOTHANE ANESTHETIZED RAT DURING FOREPAW ELECTRICAL STIMULATION

Introduction

Functional magnetic resonance imaging (fMRI) can be used to non-invasively detect regions of the spinal cord (spinal fMRI) that are functionally active due to a given stimulus. Previous studies have determined that fMRI can be used to detect functional activity in the human and animal spinal cord (Malisza et al. 2003; Malisza and Stroman, 2002; Stroman et al. 2002a; Stroman et al. 2002b). Recently, functional activity was compared with areas of c-fos labeled neuronal activity demonstrating that spinal fMRI is able to detect areas related to changes in neuronal activity (Lawrence et al. 2004). Functional MRI studies of the rat spinal cord have demonstrated functional activity in the 6th to 8th cervical (C) spinal cord segments with electrical stimulation of the rat forepaw during alpha-chloralose anesthesia (Lawrence et al. 2004; Malisza and Stroman, 2002).

The experimental design of animal studies is often limited by the need and choice of anesthetic agents. Alpha-chloralose is commonly used for animal fMRI studies because in comparison to other anesthetics it has been found to best preserve neural-metabolic coupling (Ueki et al. 1992). Conversely, it is invasive to administer and its hallucinogenic effects lengthen recovery, making it unsuitable for chronic experiments. An ideal anesthetic for fMRI studies would not depress the nervous system, could be administered non-invasively (i.e. inhalation), and would allow rapid recovery. Such an anesthetic would reduce the number of animals required for fMRI experiments as well as allow chronic studies to be performed.

Anesthetics act on several parts of the central nervous system to produce unconsciousness. These agents have several effects on physiological parameters including the metabolic rate of glucose, which has been shown to be decreased by both alpha-chloralose (Dudley et al. 1982) and halothane (Shapiro et al. 1978). The spinal cord appears to be an important site of action of volatile anesthetics in the inhibition of motor response to noxious stimulation (Collins et al. 1995). Inhalants such as halothane depress neuronal activity significantly, but not entirely. The purpose of this study was to determine if an inhalation anesthetic could be used during functional imaging of the spinal cord. Based on the literature we chose halothane because of its use in previous immunohistochemical studies (Jinks et al. 2002).

Several studies have compared different types of anesthetics during brain fMRI, but no such studies have been performed to determine the effect in spinal cord imaging. The purpose of this study is to determine if areas of functional activity can be observed in the rat spinal cord during halothane anesthesia. The present study compares fMRI of the rat spinal cord during alpha-chloralose and halothane anesthesia. The use of halothane during spinal fMRI studies would enable chronic studies and allow more flexibility in experimental design. In order to verify that areas of signal change are representative of neuronal activation, immunohistochemistry was performed following imaging experiments to verify c-fos expression.

C-fos is an immediate early gene expressed within the nucleus of some types of neurons following repetitive noxious stimulation (Hunt et al. 1987). Its translation into protein peaks at approximately two hours and labeling as a marker for neuronal activity is now well established (Herdegen and Leah, 1998). The patterns of c-fos expression in the

spinal cord have been well studied with different peripheral stimuli (Herdegen and Leah, 1998) and under different anesthetics (Jinks et al. 2002).

Methods

Animal Preparation

Specific pathogen-free Sprague-Dawley rats were obtained from Charles River, Canada, and acclimatized for a minimum of seven days. Animals were treated according to the Canadian Council for Animal Care guidelines following approval by local animal care committees. Twelve animals were imaged and of these, immunohistochemistry was performed on eight. The animals were divided into two groups according to type of anesthesia.

Anesthesia protocols

In the alpha-chloralose group (n=6), each animal was anesthetized with isoflurane (3-4%) induction, 1.5%-2% maintenance) in oxygen (0.4 L/min) and nitrogen (0.6 /min). Catheters (PE 50) containing heparinized saline were placed in the left femoral artery and vein. Bupivacaine (0.25%) was administered into the wound site prior to closure. Alpha-chloralose (30 mg/ml, 80 mg/kg) was administered intravenously over approximately 5 minutes and the isoflurane was discontinued. Anesthesia was maintained with additional doses of alpha-chloralose (40 mg/kg every 90 minutes).

In the halothane group (n=6), each animal was anesthetized with halothane (3-4% induction, 1.5%-2% maintenance) in oxygen (0.4 L/min) and nitrogen (0.6 /min). A catheter (PE 50) containing heparinized saline was placed in the femoral artery for collection of blood gases.

The rectal temperature of all animals was monitored and maintained at 37 ± 0.5 °C with a circulating water blanket and heating lamp. All animals were intubated and ventilated using a small animal ventilator (Columbus Instruments, Ohio, USA). The ventilation volume (3-4 ml) was adjusted to maintain the animal at normal arterial blood gases (PO_2 of 100 – 120 mmHg; PCO_2 of 35-45 mmHg) while keeping a ventilation rate (60/min) constant. Arterial blood samples were obtained from the arterial catheter and the mean arterial blood pressure and heart rate were measured. Physiological parameters were recorded every 10 minutes.

Two small needle electrodes were placed subcutaneously between the 2nd and 3rd, and 3rd and 4th digits on the right dorsal forepaw for delivery of the electrical stimulus (15 V (6.6 ± 0.5 mA) 0.3 ms duration, 3 Hz), and secured with surgical tape. A noxious stimulus was desired in order to maximally elicit c-fos expression. Each animal was examined for a toe twitch in response to stimulation before being placed in the bore of the magnet in order to ensure proper stimulus administration and consistency between experimental animals.

fMRI Measurements

FMRI experiments were performed using a 7 Tesla horizontal bore magnet (Magnex, U.K.) and 205/120 gradient insert (Bruker, Germany) with an Avance console, and a surface coil tuned and matched to 300 MHz. Rats were placed supine with the cervical spinal cord centered over the surface coil and secured by a water blanket over the animal taped across its shoulders to restrict motion.

Sagittal scout images were acquired and used to select transverse slices through the spinal cord with the slices centered on the vertebrae and the intervertebral discs. For spinal fMRI images, a fast spin echo sequence (field of view = 3 cm, 128 x 64 matrix, 2 shot, TE_{eff} 49 - 60 ms, TR 1800 ms, RARE phase encoding) was used with acquisition triggered by the

respiration. Six, 2 mm thick transverse slices separated by 0.6 mm spanning from the fourth cervical to second thoracic spinal cord segments were acquired. A series of 40 time points were acquired using an asymmetric block paradigm of alternating rest and electrical stimulation conditions (10-8-6-9-7, electrical stimulation off-on-off-on-off, respectively) applied to the right forepaw. Experiments were repeated for a total of two hours (the time at which c-fos expression was expected to be maximal) with 5 minutes rest between each series.

Immunohistochemistry

Following imaging, animals were given 0.5 ml of sodium pentobarbital (65 mg/kg i.p.) and transcardially perfused at room temperature with a prefixative solution (150 mL consisting of 100 mL distilled water, 10 mL 9% saline, 0.1 g sodium nitrite, and 10 μL of 10,000 i.u. Heparin) followed by 600 mL of 4% paraformaldehyde in 0.1 M phosphate buffer at pH 7.4. Spinal cords were removed and post-fixed for 24 hours in fixative. They were then transferred to 0.5 M phosphate buffered saline (PBS) containing 15% sucrose with 500 μL 1% sodium azide. Regions of interest were identified, isolated and stored in 15% sucrose solution. Serial transverse sections were cut (20μm thick) and collected on 6 slides. As a result, 6 nearly identical slides were obtained with all sections of any individual slide being approximately 120μm (20μm x 6 slides) away from the next subsequent slice on the same slide. Multiple slides are needed in order to perform omission controls to verify that the secondary antibody is binding specifically to the primary antibody.

Prior to processing, slides were warmed to room temperature, washed for 1 hour in 0.1 M PBS and blocked with 3% donkey serum. Primary incubations were carried out at room temperature for 24 hours in which slides were placed in Rabbit anti c-fos (Santa Cruz

Biotechnology) in PBS (1:1000 dilution) with 1% donkey serum and then were washed for 30 minutes in 1% Triton in 0.1 M PBS. Secondary incubations were carried out at room temperature for two hours in FITC Affinipure Donkey Anti Rabbit IgG (Can/Bio) in PBS (1:100 dilution) with 1% donkey serum. Slides were then washed for 20 minutes in PBS, followed by 20 minutes in 50 mM Tris-HCl buffer. Negative control slides used to confirm there was no non-specific labeling of the secondary antibody were incubated in 1% donkey serum in PBS instead of the diluted primary antibody and incubated in a different coplin jar to avoid any cross contamination of the primary antibody.

To account for c-fos labeled activity due to surgical procedures, control experiments were performed for each anesthetic group (n=4) in which anesthetized rats were monitored following surgery for the same duration as the experimental group without any stimulation prior to perfusion. The animals were then perfused and c-fos staining completed as described above.

Stained sections were viewed with a Nikon Eclipse E600 microscope under a B-1E cube (excitation range of 470-490 nm) for FITC. The number of c-fos labeled cells observed was counted for each region of the cord and averaged within the experimental group.

Data Analysis

Functional MRI time course data were analyzed for each animal by means of direct correlation on a pixel-by-pixel basis to the paradigm using custom-made software developed in IDL (Interactive Data Language, Research Systems Inc. Boulder, Co). A correlation coefficient threshold, R, of 0.312 was used, resulting in $P \leq 0.05$.

Functional activation maps for each rat were obtained in three separate experiments. All maps were combined in order to observe areas where voxels were repetitively found to

be active. Individual maps were manually aligned with an anatomical reference image. Maps were then summed with each pixel being identified as active (1) or not active (0), and the result was smoothed within each slice over a 3 x 3 pixel region. Smoothing was applied to account for imperfect alignment of individual activation maps and differences in anatomy between rats. The resulting combined activity map reflects the number of times a given voxel, or its immediate neighbors, was observed to be active across repeated experiments. In order to display combined results overlaid on an anatomical reference image, only pixels above a selected threshold are displayed as being active. The threshold was selected as that which most clearly demonstrates consistent areas of activity across repeated experiments. With the threshold set too low, additional areas with more variation obscure the pattern of reliable activity. Conversely, no single voxel was observed to be active in all experiments, thus setting the threshold too high also diminishes clear demonstration of the pattern of regions that are repetitively active. The threshold that most clearly demonstrates the general pattern of activity was typically around 50% of the number of experiments. In the alpha–chloralose group, a threshold as high as 12 could be used to produce a map clearly discerning regions that were repetitively active. A threshold of 12 means that a pixel in the resulting map is only shown as active if it, or its immediate neighbors in the same slice, is observed to be active at least 12 times in the 18 combined experiments. A threshold of ten was used in functional data analysis of the halothane anesthetized group. Thresholds greater than ten in this group greatly reduced the visible regions of activity. As mentioned earlier, no single voxel was observed to be active in all experiments. Therefore, for each conditional group a separate threshold must be established as determined by the amount of variability within the group. A color scale was then applied to demonstrate the degree of consistency in activity above the set threshold, with red indicating greatest amount of

activity, and decreasing in spectral order with activity. Areas of activation from each animal were mapped onto a reference image and observed regions of functional activation were compared with known spinal cord physiology and histology.

Results

Physiological parameters

Blood gases were maintained within normal physiological range throughout the experiments. Arterial CO_2 and O_2 concentrations were recorded and the averages for the two anesthetic groups are shown in table 1.

Table 1. Mean physiological parameters obtained during fMRI experiments with alpha-chloralose (n=6) and halothane (n=6) anesthetized rats. Data are presented as the mean ± S.D.

Anesthetic	pH	pCO2 (mmHg)	pO2 (mmHg)	Mean Arterial Blood Pressure (mmHg)	Heart rate (beats/min)
α-chloralose	7.42 ± 0.03	42.12 ± 4.38	96.65 ± 4.85	78.15 ± 15.6	313.56 ± 29.25
halothane	7.39 ± 0.03	53.83 ± 8.94	108.51 ± 16.51	71.24 ± 5.88	331.54 ± 34.66

Functional MRI

The greatest areas of overlap between alpha-chloralose anesthetized subjects occurred between spinal cord segments C5 and C7 (Figure 1A). Most active pixels were observed in the dorsal horn on the ipsilateral side and in the contralateral the ventral horn.

Some areas of overlapping active pixels were observed in the right ventral horn and near the central canal in C5. Average percentage signal change during stimulation conditions ranged between 15% and 18% (Figure 1C). Average time courses of the six individual alpha-chloralose anesthetized animals varied between animals (Figure 2A).

The combined fMRI activation map of halothane anesthetized rats is shown in figure 1B. The greatest number of active pixels was observed in the contralateral ventral horn of C5 and C6 and ipsilateral dorsal horn of C7 and C8. Functional activity was also observed near the central canal between C5 and C8. Average percentage signal change during stimulation conditions ranged between 10% and 15% (Figure 1C). Average time courses of the individual halothane anesthetized animals were very similar with the exception of one animal (Figure 2B).

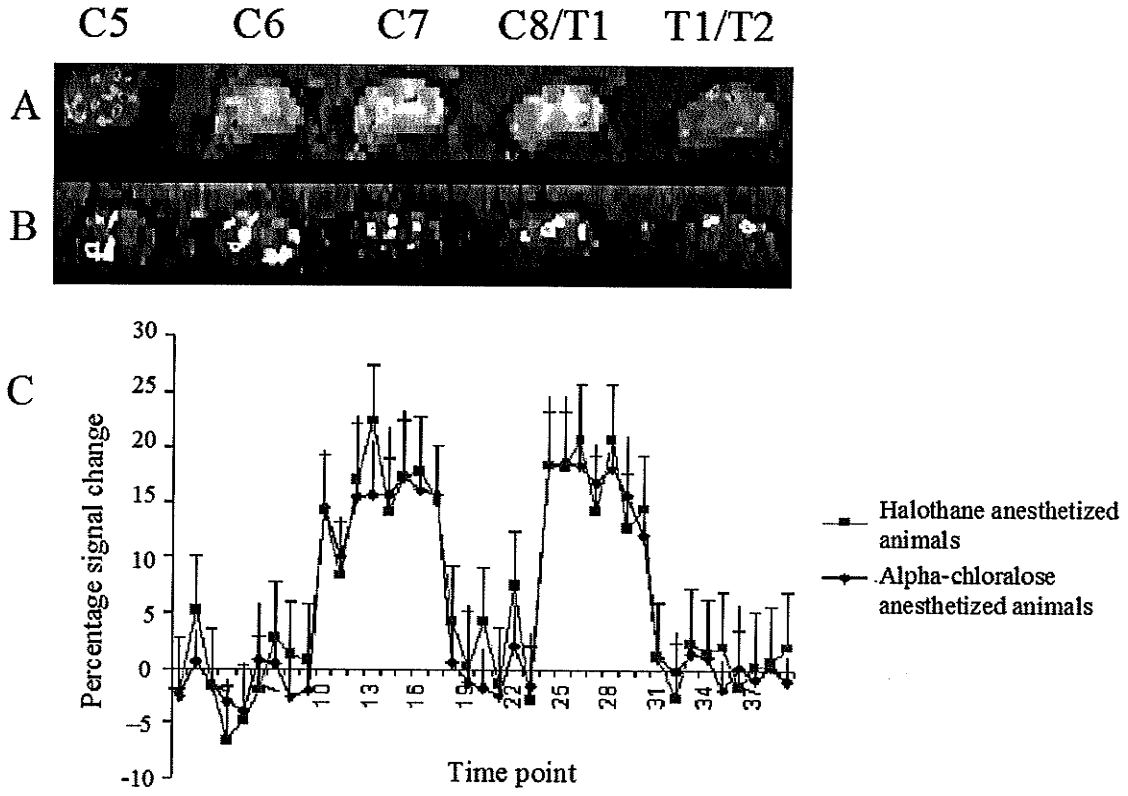

Figure 1. Combined functional activation maps from spinal cord segments C5-T2 in A) alpha-chloralose (n=6) and B) halothane (n=6) anesthetized rats during electrical stimulation of the right forepaw. The images are oriented so that dorsal is up, ventral is down, left is on the left, and the right side is on the right. Red indicates areas of the most overlap followed by yellow and green. Labels indicated the approximate spinal cord segment the slice is positioned in. The average time courses of the combined maps are shown in C).

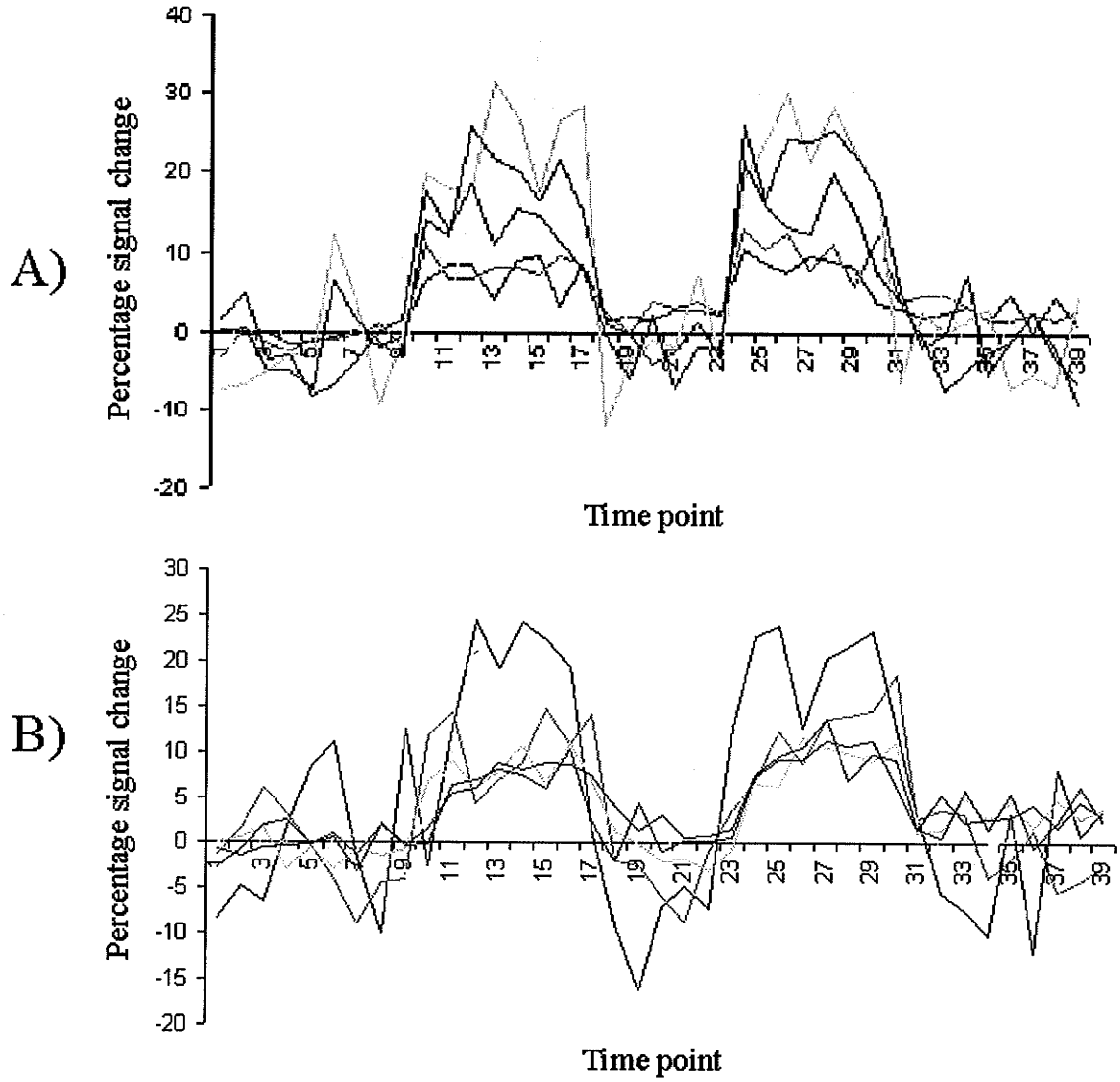

Figure 2. Time courses illustrating percentage signal change over the course of the fMRI paradigm of the A) alpha-chloralose (n=6) and B) halothane (n=6) anesthetized animals. Each individual time course is an average of three functional experiments.

Figure 3 shows a single functional map from one alpha-chloralose (A) and one halothane (B) anesthetized animal. Within the individual maps, the greatest number of active pixels were observed bilaterally in the dorsal horn between spinal cord segments C5 and C7. Fewer active pixels were observed in adjacent slices. Some pixels were also observed in the ventral horn and central canal.

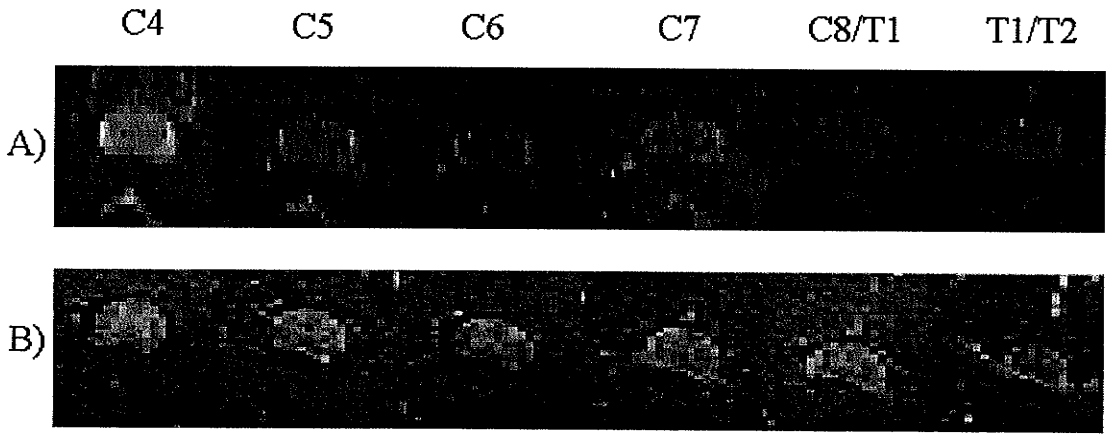

Figure 3. An individual functional activation map from an A) alpha-chloralose and B) halothane anesthetized animal. The images are oriented so that dorsal is up, ventral is down, left is on the left, and the right side is on the right. Labels indicated the approximate spinal cord segment the slice is positioned in.

Immunohistochemistry

In alpha-chloralose anesthetized animals, c-fos staining revealed clusters of cells in the dorsal horn ipsilateral to the side of stimulation between spinal cord segments C4 and C8. As with sites of functional activation, areas of greatest c-fos stained cells were between spinal cord segments C5 and C7 (Figure 4). A small number of c-fos positive cells were observed in spinal cord segment C4. Larger numbers of labeled cells were observed in C5 and then numbers decreased again in C7 and C8. C-fos labeling was not observed in the control group anesthetized with alpha-chloralose.

In halothane anesthetized rats, greatest amount of c-fos labeling was observed in the right dorsal horn of spinal cord segments C5 and C6 (Figure 4). Smaller numbers of labeled cells were observed in the right dorsal horn in spinal cord segments C3 and C4 as well as C7 to the first thoracic spinal cord segment (T1).

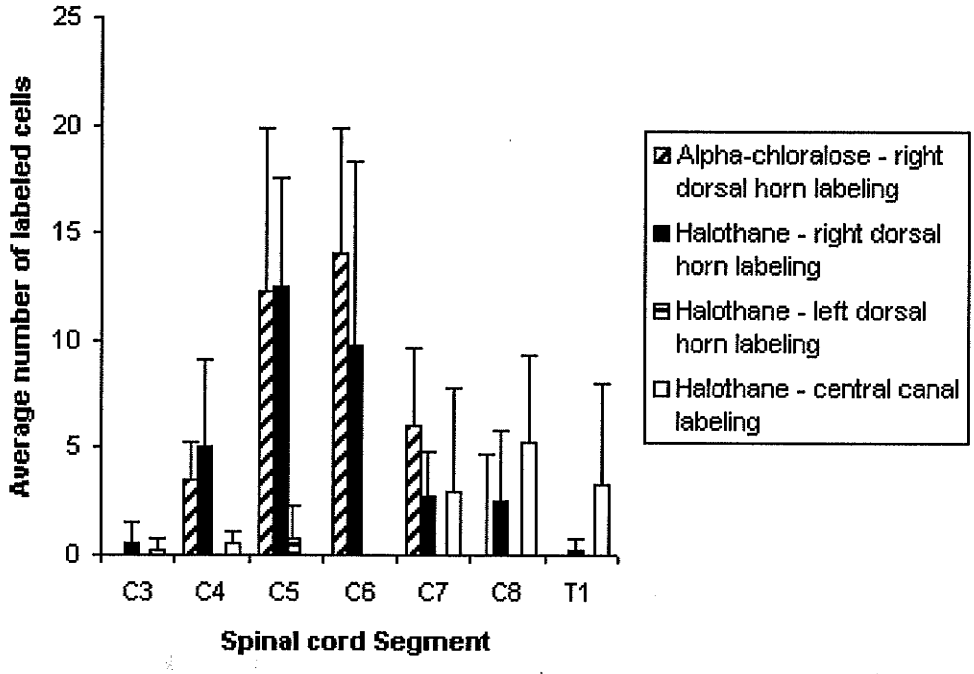

Figure 4. C-fos labeling observed in the cervical spinal cord of halothane (n=4) and alpha-chloralose (n=4) anesthetized rats following electrical stimulation of the right forepaw.

C-fos stained cells demonstrating immunoreactive nuclei appeared as round or oval structures. Labeled cells were clearly identified and distinguished from background. Figure 5 shows labeling in several segments from two rats; one anesthetized with alpha-chloralose (A) and one anesthetized with halothane (B). These results are from the same animals for which individual functional maps are shown in figure 3. Labeling in alpha chloralose animals was confined only to the ipsilateral dorsal horn and was observed only in the superficial layers (Figure 5 A-C). In halothane anesthetized animals, labeling was also observed in the contralateral dorsal horn and near the central canal of several sections (Figure 5 D-I). Labeling appeared to be more spread out in halothane anesthetized animal whereas in alpha-chloralose anesthetized animals labeling was observed in large clusters.

Individual labeled cells were observed in one of the four halothane anesthetized controls in the right dorsal horn of C3 and C7, and bilaterally in C4, C5, C6, and C8. There were also individual cells labeled near the central canal of one slice in C4, C6, C7 and C8. In most of the observed slices labeling was restricted to one or two cells, however, in one slice, five labeled cells were observed in the left dorsal horn of C8.

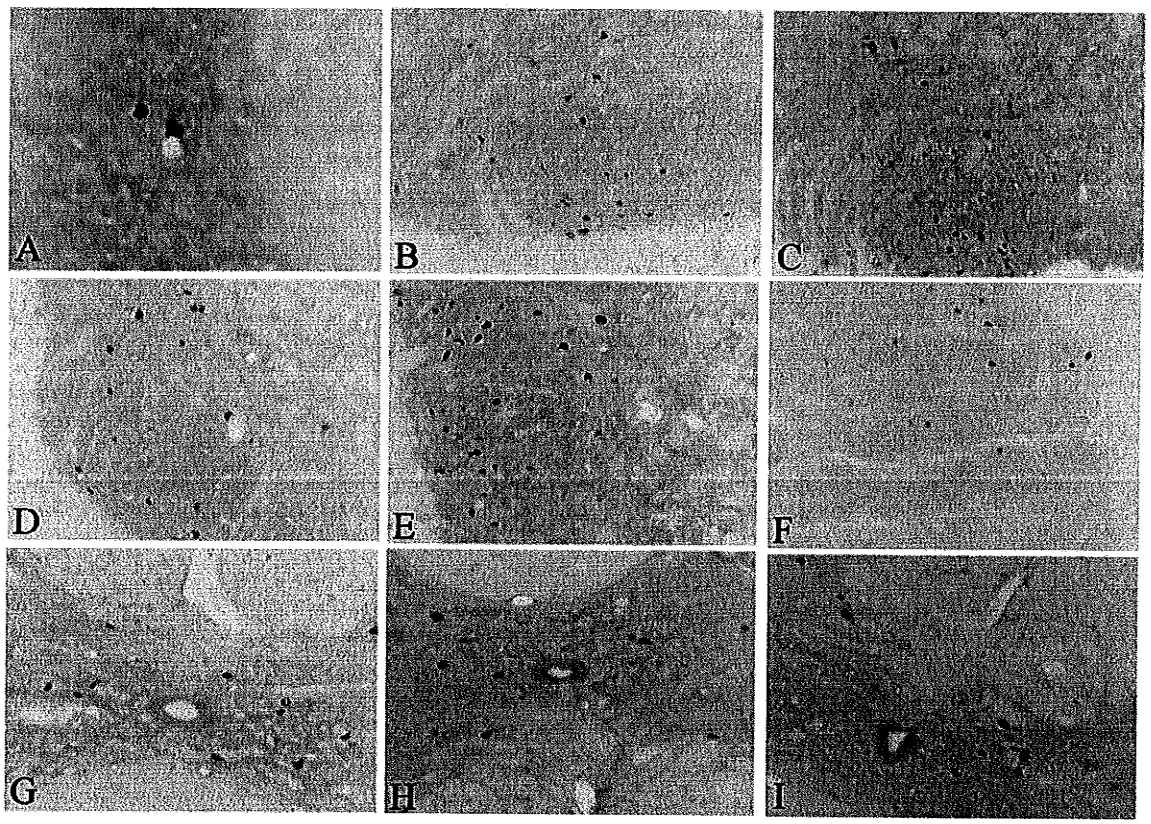

Figure 5 . C-fos labeling observed in the right dorsal horn of spinal cord segments A) C4, B) C5, and C) C6 in one alpha-chloralose anesthetized animal. C-fos labeling observed in the right dorsal horn of D) C4, E) C5, F) C6, and near the central canal of the spinal cord segments G) C7, H) C8, and I) T1 in one halothane anesthetized rat.

Discussion

The effect of type and depth of anesthesia has been a topic of great interest in animal brain fMRI. Depth and type of anesthesia can depress central nervous system metabolic activity and reduce cerebral blood flow. Activity detected with fMRI is dependent upon these factors. It is possible that inter-subject variability could be due to differences in level of anesthesia under alpha-chloralose; however, the arterial blood pressure and heart rate were closely monitored and maintained within normal parameters in order to establish stable levels of anesthesia. Austin et al. compared BOLD responses in the brains of alpha-chloralose and halothane anesthetized rats and found a gradual increase in BOLD response over a six hour period following transfer from halothane to alpha-chloralose anesthesia. Responses during halothane anesthesia were more stable than those during alpha-chloralose anesthesia (Austin et al. 2005). Similarly, results of the present study support these assertions, as indicated in Figure 2, with greater consistency in levels of activity following the paradigm under halothane compared to alpha-chloralose. However, due to the variability observed we are unable to confirm a depressed baseline in spinal fMRI activity with one anesthetic over the other. Average percentage signal change is higher in both anesthetic groups compared to brain fMRI studies, but are consistent with previous animal spinal fMRI studies performed at 7 T (Lawrence et al. 2004). In human spinal fMRI studies, larger percentage signal changes are observed in the spinal cord at 0.2 T(Li et al. 2005; Ng et al. 2006) and 1.5 T (Kornelsen and Stroman, 2004; Stroman et al. 2005) compared to those expected to be observed in the brain. Recently, one group has observed 3% signal changes in both the brain and spinal cord in the rat at 9T however, a single shot fast spin echo sequence with a much shorter echo time (3 ms) was employed (Majcher et al. 2006).

The exact mechanisms involved in general anesthesia are still a subject of needed research. Both inhalation and intravenous anesthetics affect synaptic transmission. Evidence has suggested that the physiological mechanisms of action are different for different anesthetics. Inhalation anesthetics cause hyperpolarization of neurons (Nicoll and Madison, 1982). They have been shown to inhibit excitatory synapses and enhance inhibitory synapses. It is likely that inhalation anesthetics work by pre- and post-synaptic actions (Evers and Crowder, 2001). The predominant action of intravenous anesthetics is at the synapse where they generally affect the postsynaptic response to neurotransmitters and enhance inhibitory neurotransmission (Evers and Crowder, 2001). The different mechanisms by which alpha-chloralose and halothane may act would likely cause some variability in the functional maps between the two groups due to differences in neural networks involved.

Similar areas of fMRI signal change in the cervical spinal cord can be detected using alpha-chloralose and halothane anesthesia during electrical stimulation of the rat forepaw. The electrical stimulation used was sufficient to be considered noxious. Activity was expected to be concentrated in lamina I and II of the ipsilateral dorsal horn. Noxious activity can produce a withdrawal reflex and therefore ventral horn activity was also anticipated. Afferent fibers from the rat forepaw terminate mainly between spinal cord segments C5 and C8; therefore, we expected fMRI activity in this region.

The greatest areas of overlapping active pixels between animals were in the C5 spinal cord segment in alpha-chloralose anesthetized animals (Figure 1A) and in C5 and C6 in halothane anesthetized animals (Figure 1 B). In both groups, consistent functional activity was observed in the right dorsal horn and left ventral horns of the spinal cord as well as around the central canal between C5 and C7. Large areas of activation were also

observed in C8 of the halothane anesthetized animals. Ipsilateral dorsal horn activity was anticipated due to the sensory input of the stimulus. Ipsilateral ventral horn activity was also expected since the stimulus administered can be considered noxious and may evoke a reflex response. It is possible that contralateral ventral horn activity could be due to a cross extension reflex. It is well known that noxious stimuli elicit a polysynaptic withdrawal reflex, however, the connections between interneurons and motoneurons in the ventral horn have not yet been identified. A toe twitch near the site of stimulation was observed in all of the animals, however, no movement of the contralateral limb was observed.

The average percentage signal change between rest and activation states was slightly less in the halothane-anesthetized rats (Figures 1C) despite similar physiological parameters observed during the experiments (Table 1). To determine whether this difference was significant we examined the standard deviation of the percentage signal changes in the two groups of animals. The resulting difference was found to not be significant between the two groups (Figure 1C). The average time course from each animal was also examined for differences in percentage signal change between animals. The peak signal changes within the alpha-chloralose group varied, however, all animals demonstrated time courses correlating ($p \leq 0.05$) with the stimulation paradigm (Figure 2A). The percentage signal changes between rest and activation states, in the halothane anesthetized animals, were similar with the exception of one animal (Figure 2B). While it is possible that a depressed baseline may account for greater activity in the alpha-chloralose animals, we are unable to confirm this finding. We suggest the greater percentage signal change observed in these animals is due to greater intersubject variability.

C-fos labeling was observed in the same spinal cord regions as the functional MRI activity in both alpha-chloralose and halothane anesthetized rats. In both experimental

groups the greatest amount of functional activation and the greatest amount of c-fos expression was observed in spinal cord segments C5 and C6 demonstrating good agreement between the functional data and the immunohistochemistry. C-fos labeling in the alpha-chloralose anesthetized animals were observed only on the ipsilateral side while labeling was widespread in halothane-anesthetized animals. This is consistent with the literature as several studies have found predominantly ipsilateral c-fos expression in the alpha-chloralose animal and bilateral labeling in the halothane anesthetized animal (Jinks et al. 2002; Menetrey et al. 1989). It is well known that anesthesia has some effect on the level and distribution of c-fos expression (Menetrey et al. 1989). Some difference in the patterns of expression observed between the two anesthetic groups in the present study can therefore be expected. Previous studies comparing four different concentrations of halothane anesthesia found no significant difference in the levels of expression in the rat lumbar spinal cord due to noxious mechanical stimulation of the hind paw (Jinks et al. 2002). Labeling on the contralateral side may be attributed to projections of primary afferents or second-order neurons (Fields et al. 1977; Giesler, Jr. et al. 1981). While there were some differences in the distribution of observed c-fos labeled cells within spinal cord segments, there was excellent agreement in the rostral-caudal direction between the anesthetic groups and with the functional activity observed by fMRI.

Small numbers of labeled cells were observed in one of the halothane anesthetized controls. There are always basal levels of c-fos expressed, but often these are low and not observed. In all control animals outside sources of stimulation were minimized (e.g. noise, light). We cannot overlook individual differences between rats or the possibility that the rat was under some stress (due to anesthetic induction, cannulation of the femoral artery). These factors may contribute to the immunoreactivity observed in the single rat. No

labeling was observed in the other three controls; therefore, the halothane anesthesia itself is likely not the cause of the c-fos expression.

Within the individual animals some correspondence was found between the areas of fMRI activity and segmental distribution of c-fos labeling (Figures 3 and 5). Small variations were observed between individual fMRI activity maps, as expected. The combined maps allow us to observe the areas of the spinal cord which are most often or repeatedly functionally active between scans and animals.

We observed good correspondence of functional activity determined by fMRI and neuronal activity determined by c-fos labeling in the rostro-caudal direction. The greatest spatial distribution of active pixels was observed in the C5 spinal cord segment in alpha-chloralose anesthetized animals and in the C6 spinal cord segment in the halothane anesthetized animals (Figure 1). The greatest number of c-fos positive cells were observed in the C5 and C6 spinal cord segments in both groups (Figure 4). Active pixels were observed in additional areas where c-fos labeling was not observed. Some difference between areas of c-fos and functional activity were anticipated as the scale of detection differs between the two methods, (e.g. a molecular pathway of gene expression in c-fos labeling versus a hemodynamic change in fMRI) and there are some limitations to the immunohistochemistry. In particular, not all neurons express the c-fos gene or do so selectively, only during a certain type, level or duration of stimulation (Dragunow and Faull, 1989). Furthermore, the immunohistochemistry identifies individual cells whereas the signal observed by fMRI is a hemodynamic response. Some signal may arise from draining veins resulting in areas of signal change further away from neuronal activity. This could contribute to the spread of functional activity in other areas of the spinal cord. Despite these limitations correspondence was observed in the segmental distribution of functional activity

and neuronal activity. Further investigations with other methods of detection of neuronal activity will elucidate the relationship between functional activity and neuronal activity in the spinal cord.

In conclusion, to our knowledge, this is the first study in which fMRI of the spinal cord has been performed to evaluate different anesthetics. Areas of signal change related to functional activity in the spinal cord can be observed during halothane anesthesia and yield similar results to that observed in alpha-chloralose anesthetized animals. Immunohistochemistry demonstrated areas of neuronal activity in agreement with the functional activity observed with spinal fMRI for both anesthetics. These findings suggest that the use of halothane as an anesthetic agent is feasible for chronic fMRI studies of the spinal cord. The results presented enable greater flexibility in experimental design and will facilitate future chronic studies.

CHAPTER 3: FUNCTIONAL MAGNETIC RESONANCE IMAGING OF THE CERVICAL SPINAL CORD IN THE ALPHA-CHLORALOSE AND HALOTHANE ANESTHETIZED RAT DURING NOXIOUS AND INNOCUOUS THERMAL STIMULATION OF THE FOREPAW

Introduction

Functional MRI is commonly used to observe areas of brain activity non-invasively. FMRI was implemented for use in the spinal cord and has several potential applications in clinic and in research. Establishing a comprehensive method for spinal cord fMRI (spinal fMRI) in animals is important for future directions. Previous spinal fMRI studies investigating noxious responses have examined activity elicited during electrical and chemical stimulation in animals (Lawrence et al. 2004; Lawrence et al., 2004b; Lilja et al. 2006; Majcher et al. 2006; Malisza and Stroman, 2002) and cold stimuli in humans(Stroman et al. 2002a). Comparison of the patterns of activity observed in an animal model during thermal stimulation at noxious and innocuous temperatures will aid in the understanding of the responses observed by spinal fMRI during painful stimulation and determine if spinal fMRI is capable of distinguishing between two intensities of stimulation.

Noxious and innocuous temperatures elicit different patterns of activity at the receptor site. The cutaneous receptors responding to heat stimuli have been divided into three categories: warming units (respond below 42.5°C), warming/noxious heat units (maximal response above 42.5°C), and noxious heat units (threshold between 42.5°C and 48°C) (Menetrey et al. 1979). Innocuous temperatures recruit Aδ fibres whereas noxious thermal temperatures result in the firing of both Aδ and C fibres. The three principle pathways mediating nociception in the rat are the spinothalamic, spinoreticular, and spinomesencephalic tracts. Collectively they have origins in laminae I, II, V-VIII, and X (Chaouch et al., 1983; Nahin and Micevych, 1986). Painful stimuli can also elicit a

withdrawal reflex leading to widespread activity. Withdrawal reflexes involve the whole limb; therefore, afferent information must extend over several spinal segments to stimulate several muscle groups. In addition, reflexes have crossed effects. As a flexor reflex is evoked on one side, extension occurs on the contralateral side. Therefore, fMRI is expected to reveal functional activity across several spinal cord segments an on both sides of the cord.

Antidromic stimulation of C-fibers was used to map the dermatomes of the rat limbs (Takahashi and Nakajima, 1996). Afferent fibers from the dorsal surface of the forepaw terminate between the seventh and eighth cervical spinal cord segments; however, afferents from various aspects of the forelimb terminate between the fifth cervical (C) and first thoracic (T) spinal cord segment (Takahashi and Nakajima, 1996). Previously, spinal fMRI revealed functional activity between the C3 and T1 spinal cord segments with the greatest number of active pixels observed in the C5 spinal cord segment during noxious electrical stimulation of the forepaw (Lawrence et al. 2004). Capsaicin has also been utilized in order to elicit painful stimulation observable by spinal fMRI between C5 and C8 (Malisza K.L. and Stroman, 2002). While these studies provided reproducible and consistent measures, there are a number of difficulties involved in the use of electrical stimulation and subcutaneous injection of capsaicin. The results of electrical stimulation are difficult to interpret as intense levels of stimulation can antidromically activate motor fibres. Capsaicin injection results in swelling at the injection site, mechanical allodynia and hyperalgesia. Investigation of the spinal fMRI maps obtained using different types of stimuli will assist in characterization of fMRI activity observed in the spinal cord. Thermal stimulation was used in several human spinal fMRI studies with cold temperatures at noxious and innocuous levels (Stroman et al. 2002b; Stroman et al. 2002a; Stroman et al. 2004; Stroman et al.

2005; Stroman and Krause, 2000; Stroman and Ryner, 2001). This is the first study to report spinal fMRI findings by thermal stimulation in an animal model.

The present study demonstrates that spinal FMRI can differentiate activity elicited by different intensities of thermal stimuli. Functional activity due to the two levels of stimulation was also observed under alpha-chloralose and halothane anesthesia in order to better understand the maps of activity obtained by spinal fMRI under different anaesthetic conditions. The use of halothane anesthesia would enable chronic studies. The presence of neuronal activity within the imaged region of the spinal cord was confirmed by labeling c-fos protein. C-fos is a known marker of neuronal activity and was used in a previous study with spinal fMRI during noxious electrical stimulation (Lawrence et al. 2004).

Methods

Specific pathogen-free Sprague-Dawley rats were obtained from Charles River, Canada, and acclimatized in the animal facility for a minimum of 7 days prior to use. Animals were treated according to the Canadian Council for Animal Care guidelines, and the protocol was reviewed and approved by local animal care committees.

Animal Preparation

Animals were anesthetized with either halothane (n=12) or isoflurane (n=12) (3-4% induction, 1.5-2% maintenance) in oxygen. Catheters (PE 50) containing heparinized saline were placed in the left femoral artery and vein. Bupivacaine (0.25%) was administered into the wound site prior to closure. Fluids and anesthetics were administered via the venous catheter. Animals anesthetized with isoflurane were transferred to alpha-chloralose (30 mg/ml, 80 mg/kg), administered intravenously over approximately 5 minutes. Isoflurane

was discontinued and anesthesia was maintained with additional doses of α-chloralose (40 mg/ml every 90 min). Animals were intubated and ventilated using a small animal ventilator (Columbus Instruments, Ohio, USA). The ventilation volume (3-4 ml) was adjusted to maintain the animal at normal arterial blood gases (pO_2 of 100-120 mmHg; pCO_2 of 35-45 mmHg) while keeping the ventilation rate constant (60/min).

In all animals, the rectal temperature was monitored and maintained at 37 ± 0.5 °C with a circulating water blanket and heating lamp. In the alpha-chloralose group, blood samples were collected from the arterial catheter to monitor blood gases. Heart rate and blood pressure were monitored continuously throughout the experiment. In the halothane group, expired O_2 and CO_2 levels were monitored using a pulse oximeter (Ohmeda) and maintained between 38–44% and 22–25% respectively. It was found that these levels corresponded to good pH, pO_2 and pCO_2 levels in normal physiological ranges. Physiological parameters were recorded every 10 to 15 minutes.

Functional Magnetic Resonance Imaging

FMRI experiments were performed using a 7 T horizontal bore magnet (Magnex, U.K) and 205/120 gradient insert (Bruker, Germany) with an Avance console and quadrature surface coil tuned to 300.0 MHz centered over the cervical spinal cord. The animal was placed supine over the surface coil and motion restricted by securing a water blanket over the animal.

A gradient echo sagittal scout image was acquired in order to position six, two mm thick transverse slices centered on the vertebrae and on the intervertebral discs between the C3 and C7 vertebrae. Based on known rat anatomy, these slices align with the C2/C3, C3/C4, C4/C5, C6, C7, and C8/T1 spinal cord segments (Hebel R and Stromberg, 1986).

Parameters were selected to achieve the highest quality image data with the shortest possible effective echo time. A multi-slice fast spin echo imaging sequence was used with acquisition triggered by the respiration (field of view = 3cm, 128 x 64, 2 shot, TE = 4.13, TE_{eff}= 49.0 ms, TR= 1800, RARE phase encoding).

A Medoc® TSA-II thermal sensory analyzer controlled from a personal computer was used to administer thermal stimulation with a small (5mm x 5mm) thermal pad, placed on the dorsal side of the right forepaw and secured with surgical tape. A series of 40 images were collected using an asymmetric paradigm of alternating rest (R) and thermal stimulation (S) conditions (10R-8S-6R-9S-7R). The temperature of the thermode during rest periods was ambient temperature (32°C). During stimulation periods, it was increased to either 48°C (n=12, 6 per anesthetic group) or 40°C (n=12, 6 per anesthetic group). In both groups the ramp time used to switch between rest and stimulation temperatures was as short as possible. The rate of temperature change was 6.5°C/s and 3°C/s for the noxious and innocuous groups, respectively. This was repeated for two hours, at which time c-fos expression was expected to be maximal, with a five minute rest period between experiments.

Immunohistochemistry

Following functional imaging, animals were given 0.5 ml of sodium pentobarbital (65 mg/kg i.p.) and then transcardially perfused at room temperature with a prefixative solution (150 mL consisting of 100 mL distilled water, 10 mL 9 % saline, 0.1 g sodium nitrite, and 10 μL of 10,000 i.u. Heparin), followed by 600 mL of 4% paraformaldehyde in 0.1 M phosphate buffer at pH 7.4. Spinal cords were removed and post-fixed for 24 hours in fixative. They were then transferred to 0.5 M phosphate buffered saline (PBS) containing

15 % sucrose with 500 μL 1 % sodium azide. The imaged region of spinal cord was identified (C3 to T1), isolated and stored in 15 % sucrose solution. Serial transverse sections were cut (20μm thick).

Prior to processing, slides were warmed to room temperature, washed for 1 hour in 0.1 M PBS and blocked with 3 % donkey serum for 1 hour. Primary incubations were carried out at room temperature for 24 hours. Slides were placed in Rabbit anti c-fos (Santa Cruz Biotechnology) in PBS (1:1000 dilution) with 1 % donkey serum and then washed for 20 minutes in 1% Triton in 0.1 M PBS and for 10 minutes in 0.1M PBS. Secondary incubations were carried out at room temperature for two hours in FITC Affinipure Donkey Anti Rabbit IgG (Can/Bio) in PBS (1:100 dilution) with 1 % donkey serum. Slides were then washed for 10 minutes in 1% Triton in 0.1 M PBS followed by 10 minutes in PBS, and 20 minutes in 50 mM Tris-HCl buffer.

To account for c-fos labeled activity due to surgical procedures, control experiments were performed in which alpha-chloralose (n=4) and halothane (n=4) anesthetized rats were monitored following surgery for the same duration as the experimental group without any stimulation prior to perfusion. The animals were then perfused and c-fos staining completed as described above.

A control slide was included in each batch of staining to confirm that the secondary antibody was not binding non-specifically. In control slides, 1% donkey serum in PBS was used instead of the diluted primary antibody and incubated in a different coplin jar to avoid any cross contamination of the primary antibody.

Stained sections were viewed with a Nikon Eclipse E600 microscope under a B-1E cube (excitation range of 470-490 nm) for FITC. C-fos activations were mapped by hand onto diagrams of the different spinal cord segments. The number of c-fos labeled cells were

counted in each region of the spinal cord in each slice and recorded. Only clearly distinguished cells with dark nucleoli were counted.

Data Analysis

Functional MRI data were analyzed for each animal by means of direct correlation to the paradigm using custom-made software developed in IDL (Interactive Data Language, Research Systems Inc. Boulder, Co). A model paradigm was defined for correlation of the signal intensity changes with stimulation using a correlation coefficient threshold, R, of 0.312 ($P \leq 0.05$).

Combined activity maps were created to observe areas with pixels that were active consistently across experiments and animal. Three individual activity maps were acquired from each animal in each experimental group resulting in the combination of a total of 18 functional maps per group. The individual maps were manually aligned with an anatomical reference image. The maps were then summed with each pixel being identified as active (1) or not active (0), and the result was smoothed within each slice over a 3 x 3 pixel region. The smoothing was applied to account for imperfect alignment of the individual activity maps and differences in anatomy between rats. The resulting combined activity map reflects the number of times a given voxel, or its immediate neighbours, was observed to be active across the repeated experiments. In order to display the combined results overlying an anatomical reference image, only pixels above a selected threshold are displayed as being active. A threshold of 10 was selected for all groups allowing for the direct comparison between fMRI maps. Therefore, active pixels in the combined map or its nearest neighbours, must appear active in at least of 10 of the 18 combined experiments. A colour scale was then applied to demonstrate the degree of consistency of the activity above the set

threshold, with red indicating the greatest amount of consistency, and decreasing in spectral order. Combined functional maps were overlaid on a reference anatomical image.

The time courses for all of the experiments overlaid in the combined maps were averaged in order to see the group response. The standard deviation between all experiments was calculated for each time point and then averaged to determine the mean variation between experiments.

Results

Functional Magnetic Resonance Imaging

Areas of signal change that were consistent between experiments were determined in the thresholded combined maps. During noxious thermal stimulation, alpha-chloralose anesthetized animals demonstrated the largest number of consistently active pixels in the C7 spinal cord segment (Figure 1A). Smaller amounts of activity were observed in the adjacent segments. Functional activity was present in the dorsal horn on the ipsilateral side between spinal cord segments C3/C4 and C8 and in the left dorsal horn between C6 and C8. Ventral horn activity was observed bilaterally in C3/C4, C7 and C8 and only contralaterally in C4/C5 and C6. The mean percentage signal change was 15 ± 4.5% above baseline (Figure 2). The frequency with which active pixels were observed across experiments is reported in Figure 4A. During noxious thermal stimulation active pixels were observed most frequently in the right dorsal horn of C7 (67% of experiments). Fifty percent of experiments showed activity in the right ventral horn in C6 and in the left ventral horn in C7. A representative single data set is shown in Figure 5A. Within a single slice, generally, one to three pixels appear active. Functional activity was mainly observed in the dorsal horns bilaterally and in the contralateral ventral horn.

The distribution of functional activity was more wide spread in alpha-chloralose animals that received innocuous thermal stimulation (Figure 1B). Consistent areas of functional activity were observed in the right dorsal horn between C2/C3 and C4/C5 and in the left dorsal horn at the C6 spinal cord segment. Bilateral activity was observed in the C7 and C8. Ventral horn activity was observed bilaterally at all levels of the spinal cord. The mean percentage signal change was 10 ± 3.6% above baseline (Figure 2). FMRI activity was most frequently observed in the right dorsal horn of C8 (56%, Figure 4B). Fifty percent of experiments demonstrated active pixels in the dorsal horns of C7 and in the ventral horns of C3/C4 on either side of the cord. Within an individual data set, active pixels were found to be located mainly in the ipsilateral dorsal and ventral horns (Figure 5B). Functional activity was also observed near the central canal at some levels.

In halothane anesthetized animals, functional activity was observed in the right dorsal horn or near the central canal in all slices during noxious heat stimulation (Figure 1C). Active pixels were observed in the left dorsal horn in the C2/C3 and C3/C4 spinal cord segments as well as between C6 and C8. Small areas of fMRI activity were observed in the ventral horn of all slices ipsilaterally and in the contralateral side in C2/C3 and C8. In several slices active pixels were located near the central canal. The mean percentage signal change was 20 ± 8.1% above baseline (Figure 3). FMRI activity was observed most frequently in the right ventral horn in spinal cord segments C4/C5 and C6 (50%, Figure 4C). Within an individual activity map, active pixels were observed between C3 and C8 (Figure 5C). FMRI activity was observed in the right dorsal horn in four slices, in the left dorsal horn in one slice and in the left ventral horn in another slice.

Halothane anesthetized animals demonstrated functional activity bilaterally in the dorsal horns between C3/C4 and C7 during the innocuous, 40°C stimulus (Figure 1D).

Bilateral fMRI activity was observed in the ventral horn between C2/C3 and C7. In the C2/C3 segment three distinct, consistent areas of activity were observed in the ipsilateral dorsal horn, ventral horn, and near the central canal. Ventral horn fMRI activity was observed bilaterally through the spinal cord segments, with the exception of C8, which shows only ipsilateral ventral horn activity. The mean percentage signal change was 15 ± 5.8 % above baseline (Figure 3). Active pixels were observed most frequently in the right dorsal horn in C6 and in the left ventral horn of C3/C4 (61%, Figure 4D). Fifty-six percent of experiments demonstrated functional activity in the left dorsal horn and right ventral horn in C6, and in the left dorsal horn in C3/C4. Fifty percent of experiments demonstrated activity in the ipsilateral dorsal and ventral horn of C7 and in the ipsilateral ventral horn of C3/C4. In an individual data set active pixels were observed between C3 and C8 (Figure 5D). Functional activity in the right ventral horn was observed across several segments from C4/C5 to C8. FMRI activity in the left ventral horn appeared from C3/C4 to C7. Right dorsal horn activity appeared in only two slices. Active pixels in the left dorsal horn appeared in three slices.

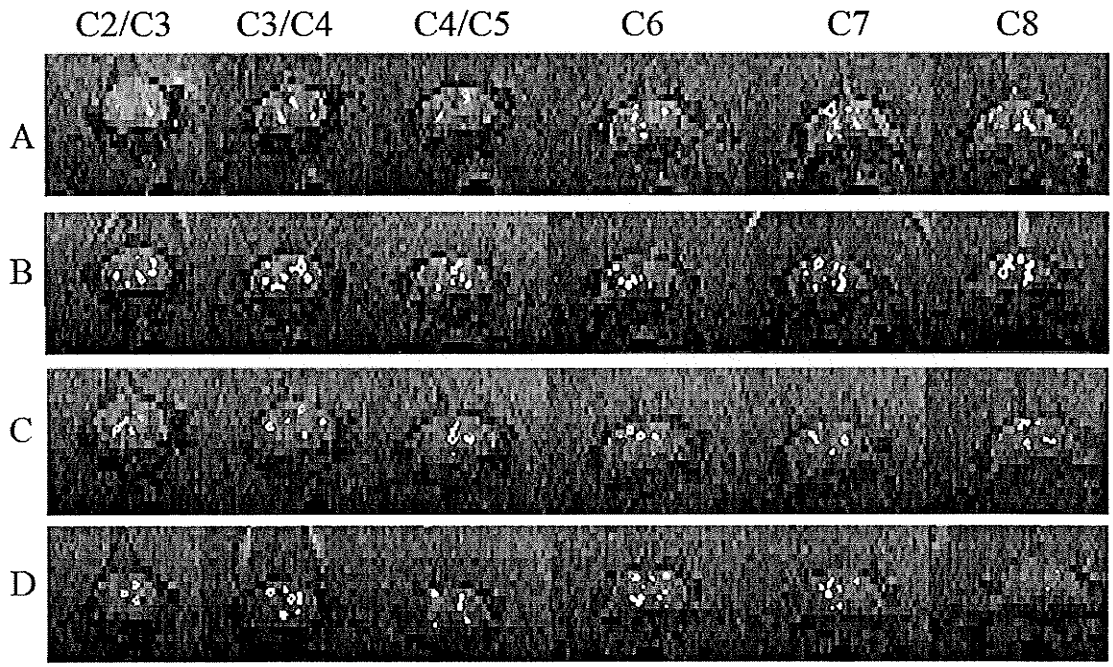

Figure 1. Combined functional activation maps with a threshold of 10 of alpha-chloralose anesthetized rats during thermal stimulation of the right forepaw at A) 48°C (n=6) and B) 40°C (n=6). Figures C and D show combined activity maps of halothane anesthetized rats during thermal stimulation of the right forepaw at 48°C (n=6) and 40°C (n=6), respectively. The images are oriented so that dorsal is up, ventral is down, left is on the left, and the right side is on the right. Red indicates areas of the most overlap followed by yellow and green. Labels indicated the approximate spinal cord segment the slice is positioned in.

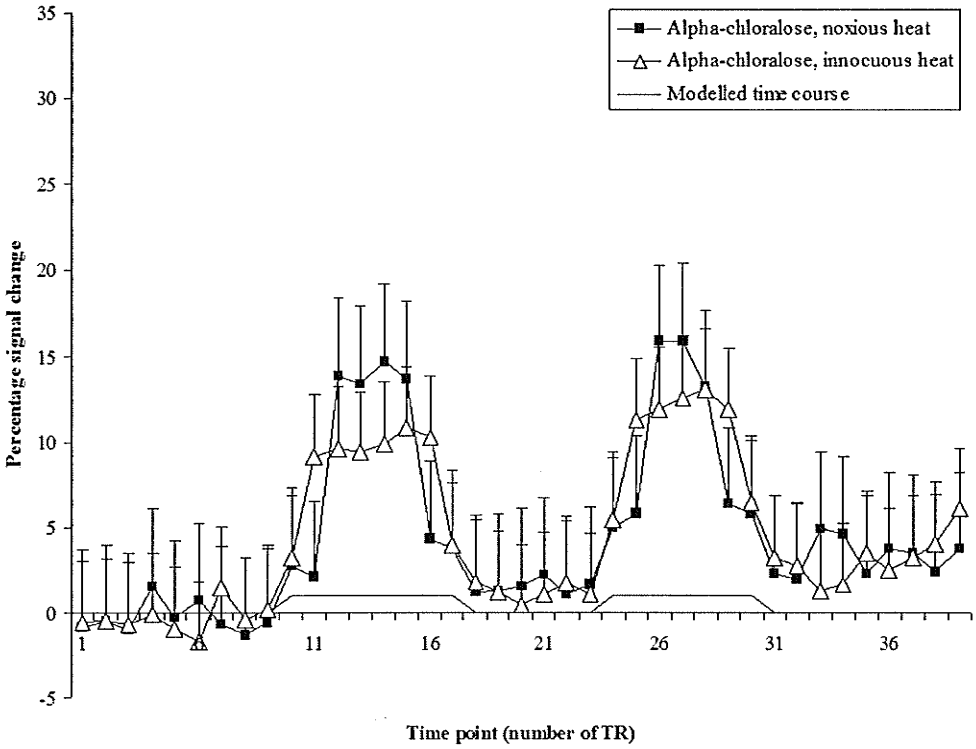

Figure 2. Average time courses of the combined activity maps of the alpha-chloralose anesthetized animals shown in figure 1 A and B. Error bars indicate the mean standard deviation.

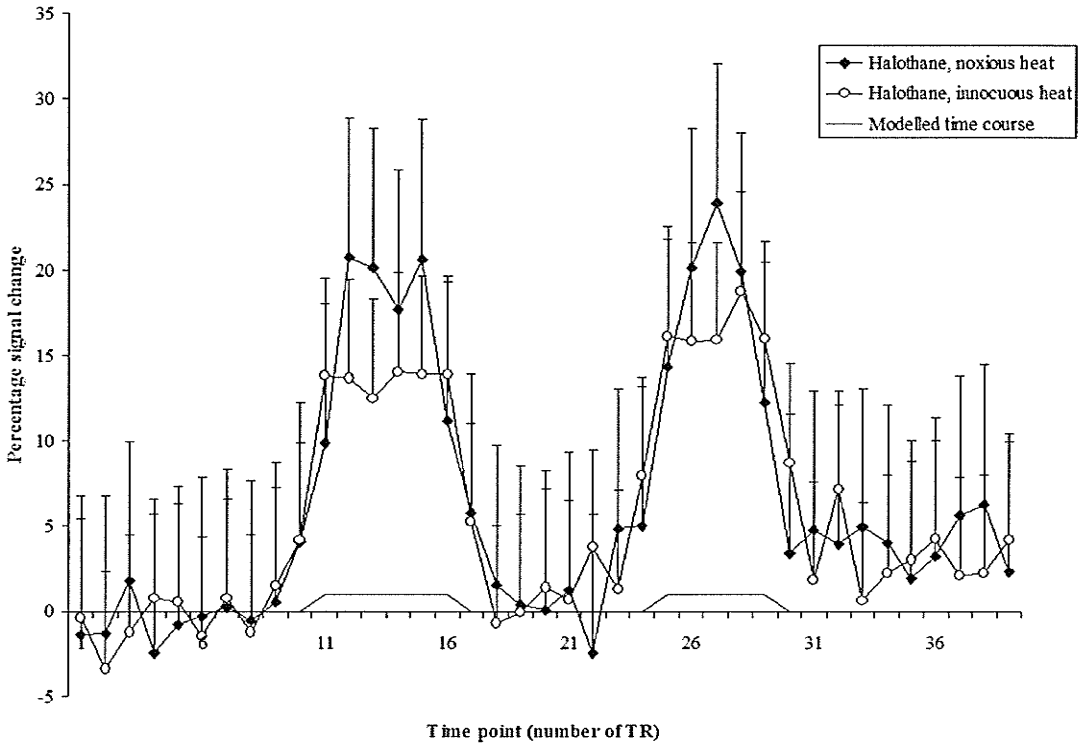

Figure 3. Average time courses of the combined activity maps of the halothane anesthetized animals shown in figure 1 C and D. Error bars indicate the mean standard deviation.

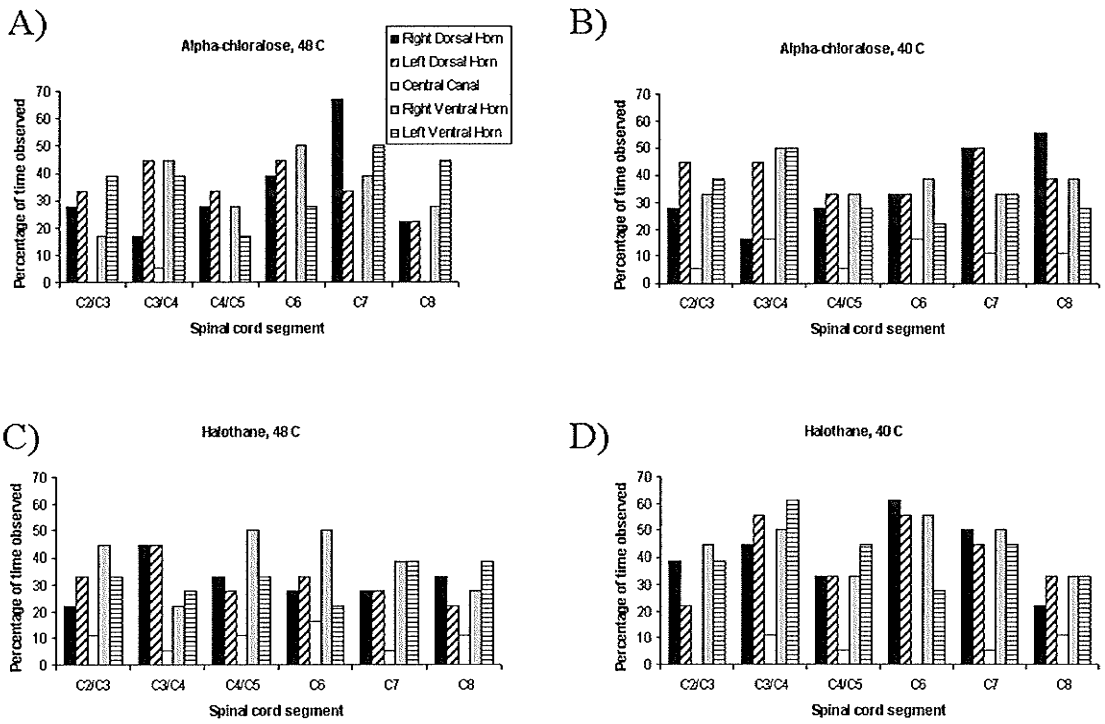

Figure 4. The frequency at which active pixels were observed within the different regions of the spinal cord across all experiments.

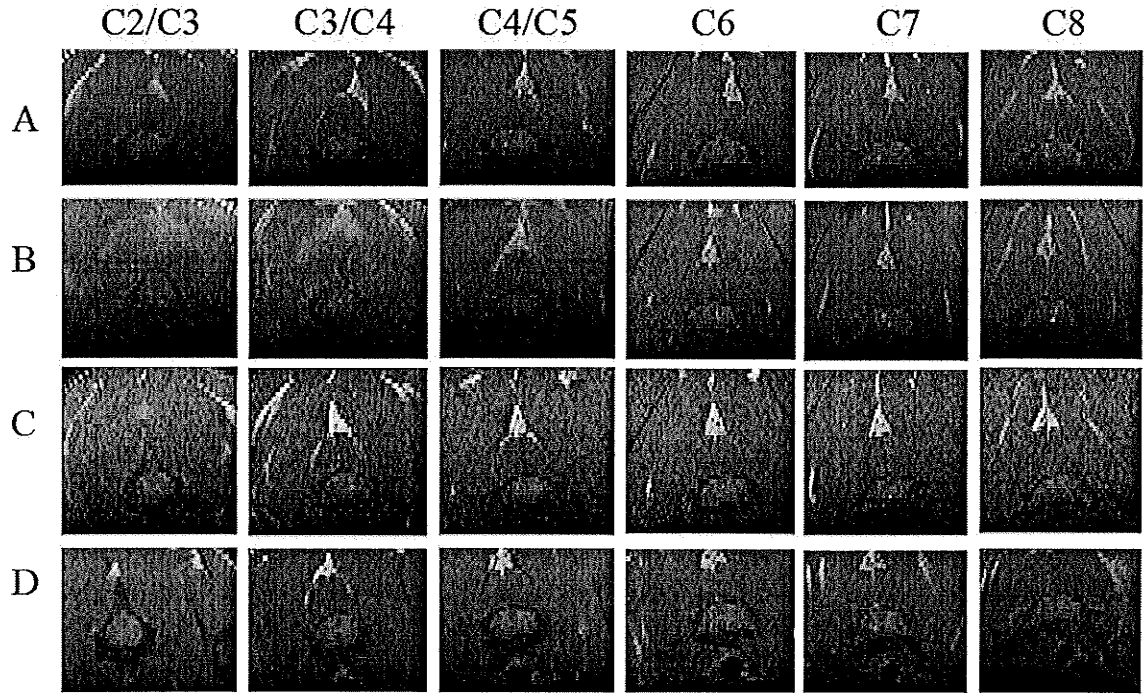

Figure 5. Single functional maps obtained during A) alpha-chloralose anesthesia and 48°C stimulation, B) alpha-chloralose anesthesia and 40°C, C) halothane anesthesia and 48°C, and D) halothane anesthesia and 40°C. Figures are in anatomical orientation with the dorsal side of the animal at the top of the image and left side of the animal on the left side of the image. Labels indicate the approximate level of the spinal cord the slices were positioned at.

Immunohistochemistry:

C-fos labeling was observed as brightly lit nuclei with a dark unstained nucleolus. All groups demonstrated labeling across several spinal cord segments and predominantly in the ipsilateral dorsal horn. The average numbers of counted cells observed in the right dorsal horn within a section from each level are shown in Figure 6. The spinal cord level in which the greatest labeling was observed was fairly consistent between experimental groups. The alpha-chloralose anesthetized group that received noxious stimulation exhibited peak activity in the C6 spinal cord segment while all other groups demonstrated peak activity in C5. In alpha-chloralose anesthetized animals, c-fos labeling was observed at all examined levels of the cord from the C3 to T1 spinal cord segments following noxious thermal stimulation. The group under the same anesthetic that received innocuous stimulation demonstrated neuronal activity from the C3 to the C6 spinal cord segments. During halothane anesthesia neuronal activity was observed between C3 and C7 during noxious stimulation and between C3 and T1 during innocuous thermal stimulation.

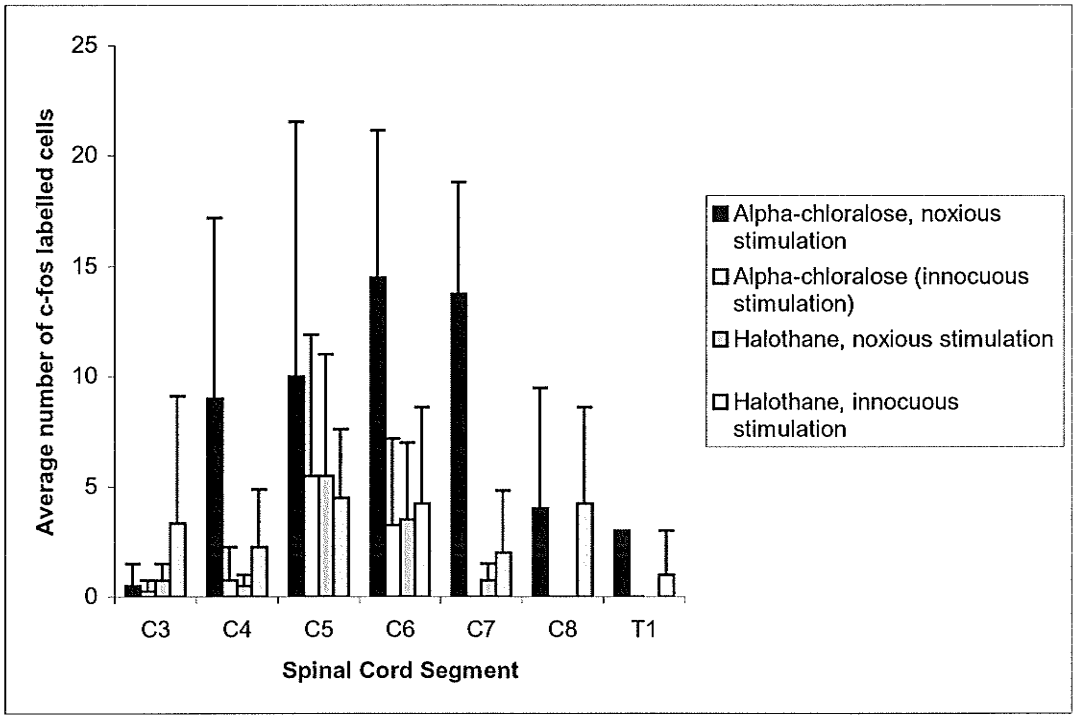

Figure 6. Average number of c-fos labeled cells observed in the right dorsal horn of a section from each spinal cord segment examined.

Less labeling was observed in halothane anesthetized animals in comparison to that observed in those anesthetized with alpha-chloralose. The pattern of labeling was also different. In the alpha-chloralose group, c-fos positive cells were clustered together in dense groups (Figure 7). In halothane anesthetized animals labeled cells were spread over a larger area. This is consistent with previous results (Lawrence et al., 2004b). Labeling in halothane anesthetized rats that received innocuous stimulation was very sparse and distributed broadly. In addition to the right dorsal horn labeling was also observed in other areas of the cord such as in the contralateral dorsal horn, lamina X (Figure 7D), and intermediate zone. C-fos labeled cells were observed in the right dorsal horn only in the alpha-chloralose anesthetized animals that received innocuous stimulation.

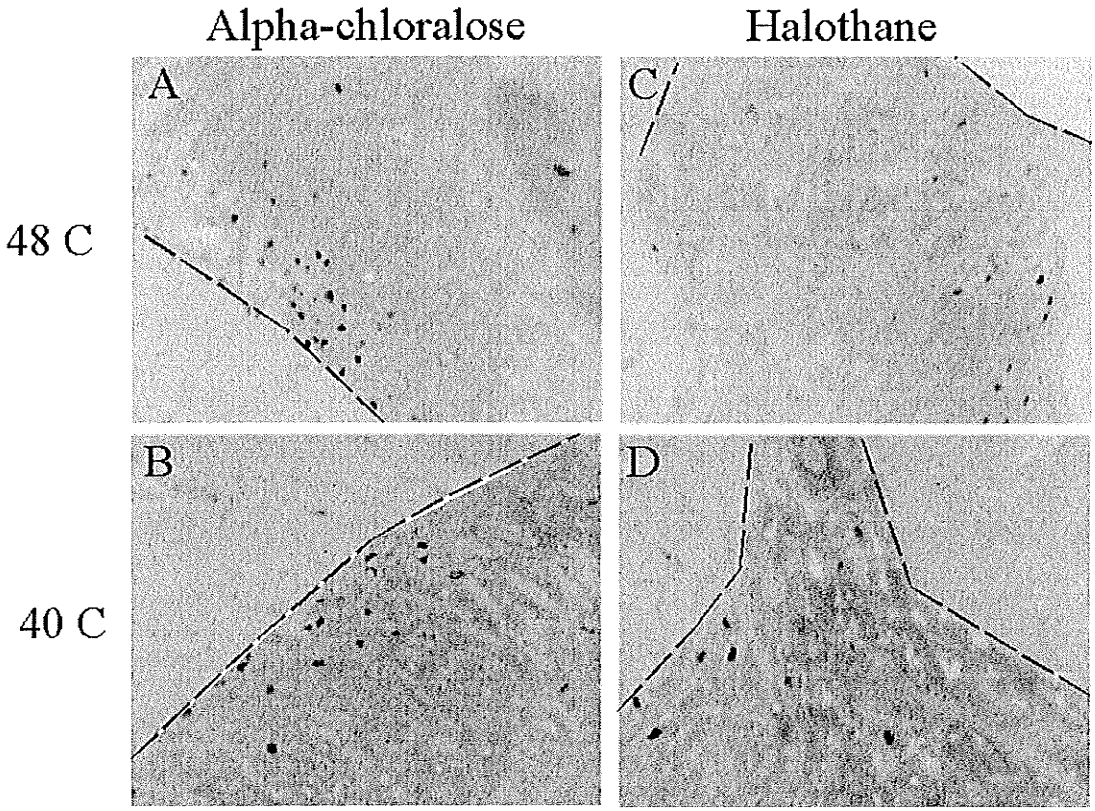

Figure 7. Examples of c-fos labeled cells observed (at 40x magnification) in alpha-chloralose anesthetized animals during A) noxious and B) innocuous thermal groups. The same stimuli were applied to animals anesthetized with halothane in C and D respectively. A-C show labeled cells observed in the right dorsal horns whereas D shows labeled cells observed near the central canal and in the right intermediate zone. Dashed lines indicate borders between gray and white matter. A, B, and C are oriented with the dorsal aspect at the top of the image. D is oriented with dorsal aspect towards the left side of the image.

Labeling was not observed on control slides in which the primary antibody was omitted. C-fos labeling was not observed in any of the alpha-chloralose anesthetized control animals and in three of the halothane anesthetized control animals. In one halothane anesthetized control ,individual labeled cells were observed sporadically in various areas of the spinal cord at several levels.

Discussion

The organization of pain processing at spinal and supraspinal levels is complicated and not yet fully understood. The three principle pathways mediating nociception in the rat are the spinothalamic, spinoreticular, and spinomesencephalic tracts. Collectively they have origins in laminae I, II, V-VIII, and X(Chaouch et al. 1983; Nahin and Micevych, 1986). anesthesia. The spinal cord is known to be an important site of action for anaesthetics(Collins et al. 1995; De Jong et al. 1968; Namiki et al. 1980). However, little is known about the mechanisms by which they work making interpretation between anaesthetic agents difficult.

Responses to noxious and innocuous stimuli could be clearly differentiated by examination of the time courses (Figures 2 and 3). Mean percentage signal changes were greater in the animals stimulated with noxious heat (48°C) regardless of the type of anesthesia. In a previous human spinal fMRI study, higher percentage signal changes were observed with noxious cold stimulation than with innocuous cold (Stroman et al. 2002a). The difference in percentage signal change can be attributed to varying encoding during innocuous and noxious thermal stimulation. Stimulus intensity is encoded by neuronal firing rate, duration and the number of neurons that fire; therefore, greater signal change during noxious stimulation was anticipated. The results show that the observed mean

percentage signal change can provide important information regarding neuronal activity and can be used to differentiate between activity elicited by noxious and innocuous stimuli.

Combined activation maps identified pixels that were repetitively active across experiments. Some areas of functional activity were consistent across thermal and anaesthetic groups. For example, areas of signal change were observed in the right dorsal horns at the C3 and C4 vertebra as well as bilaterally in the dorsal horn at the C6 vertebra in all four groups (Figure 1). These similarities in the patterns of active pixels were anticipated. The axons of afferent neurons carrying warm thermal information terminate mainly in lamina II, but some also terminate in lamina I of the spinal cord. These neurons respond to innocuous temperatures but become silenced at higher, noxious, temperatures (e.g. 48°C). Primary afferents carrying noxious information terminate mainly in laminae I, II, and V. Similar patterns in activity can therefore be expected as the terminations in the spinal cord are similar for the two levels of stimulation. Areas of signal change were also observed repeatedly in the contralateral ventral horn.

Within each group the frequency of activity in each zone was calculated (Figure 4). The locations of pixels were identified as being in the right or left, dorsal or ventral horn or being near the central canal. In general, physiological relevant areas had frequencies of activity greater than 50% in several areas of the cord. The highest frequency was observed in the alpha-chloralose anesthetized group that received noxious heat stimulation, where 67% of experiments demonstrated active pixels in the right dorsal horn of C7. The right dorsal horn was also the site of frequent functional activity in both groups that received innocuous thermal stimulation. In the alpha-chloralose group, 56% of experiments demonstrated fMRI activity in the right dorsal horn of C8. In the halothane anesthetized group, 61% of experiments showed active pixels in the right dorsal horn of C6. Mismatch

between these calculated frequencies and the overlap maps is not surprising as the techniques of identification are different. The overlay maps are manually aligned and thresholded in order to align the areas of the cord and spatially identify areas of interest. The manual counting and calculation of frequencies considers the areas of the spinal cord only generally as we currently cannot discern between laminae in the functional maps. Therefore, we can only separate the cord into quadrants with confidence, as well as include a zone near the central canal.

All animals demonstrated functional activity spread over the imaged region of the cord. Individual results from representative animals are shown in Figure 5. The thermal pad is approximately the size of the dorsal surface of the rat paw. Therefore, several dermatomes were being stimulated at once, evoking activity over several spinal cord segments. The spinal cord is an important site of integration and modulation of sensory information before it is sent in ascending tracts to the brain. There is a great amount of connectivity between lamina and spinal cord segments via interneurons. The areas of neuronal recruitment in the lumbar spinal cord during graded thermal stimulation of the hind paw have been observed with 2-deoxyglucose (2-DG)(Coghill et al. 1991). Metabolic recruitment was observed in all laminae on the ipsilateral side and in many laminae on the contralateral side during noxious stimulation. The rostral-caudal distribution varied between laminae; for example, activity in laminae V-VI was spread across 9 mm, whereas activity in laminae I-IV was restricted to approximately 3 mm (Coghill et al. 1991).

The present results confirm that fMRI activity in the spinal cord during noxious and innocuous stimulation can be observed with both halothane and alpha-chloralose anesthesia. The expected pattern of response, however, is complicated by the necessity of anesthesia. The spinal cord is known to be an important site of action for anaesthetics(Collins et al.

1995; De Jong et al. 1968; Namiki et al. 1980). Little is known about the mechanisms by which they work, making interpretation between anaesthetic agents difficult. It is known that anaesthetic actions in the spinal cord result in the loss or reduction of movement (Collins et al. 1995). Synaptic transmission is affected by anesthesia, however, different agents have differing physiological actions. Inhalation anaesthetics cause hyperpolarization of neurons and inhibit excitatory synapses and enhance inhibitory synapses (Nicoll and Madison, 1982). It is believed that the actions of inhalent anaesthetics are both pre- and post- synaptic, whereas, the predominant action of intravenous anaesthetics is to affect the postsynaptic response to neurotransmitters and enhance inhibitory neurotransmission (Evers and Crowder, 2001). Alpha-chloralose is commonly used for anesthesia during animal functional imaging studies as it was shown to best preserve the metabolic coupling between oxygen consumption and neuronal activity in the brain (Ueki et al. 1992). The use of alpha-chloralose limits experimental design as recovery of animals following anesthesia is difficult and the administration requires an invasive surgery. The use of an anesthetic agent which is non-invasive to administer and from which recovery is possible would allow chronic spinal fMRI studies to take place and would also reduce experimental animal numbers. Within brain fMRI studies, areas of signal change have appeared similar in location under alpha-chloralose and halothane anesthesia however, the spatial extent of activity under the former was more specific (Austin et al. 2005). Anesthetics are known to act on various sites of the central nervous system (Grasshoff et al. 2005). As a result, the effects on fMRI activity in the spinal cord cannot be assumed to be the same as in the brain. The mechanisms by which anesthetics work differ between agents (Grasshoff et al. 2005). Therefore, some variation in response between anesthetic groups are anticipated. In addition to actions on neuronal activity we must also considered any effects anesthetics may

have on the vasculature. Different anesthetics may also alter the physiological properties related to blood flow, blood pressure and oxygenation, altering the hemodynamic response and the BOLD signal. We have previously compared the areas of functional activity elicited by electrical stimulation in alpha-chloralose and halothane anesthetized rats (Lawrence et al., 2004b). The general distribution of activity between the two groups was similar with slight variations between the maps of activity (Lawrence et al., 2004b). This could be accounted for by the different actions of the anesthetic agents in the spinal cord, compared to the brain.

The average signal changes were slightly higher in halothane than in alpha-chloralose anesthetized animals (Figures 2 and 3). Clear baseline signal changes were observed in brain fMRI due to different types of anesthesia (Hyder et al. 2002). In the present study, the difference in signal change observed between anesthetic groups is not significant as they are within their standard deviations. Previously, we observed slightly higher percentage signal changes in alpha-chloralose anesthetized animals compared to those anesthetized with halothane during electrical stimulation of the forepaw (Lawrence et al., 2004b). It is important to bear in mind that anesthetic effects on fMRI activity in the spinal cord may differ from that expected in the brain.

The presence of neuronal activity in the imaged region of the spinal cord was verified by c-fos labeling. The alpha-chloralose anesthetized animals that received noxious thermal stimulation demonstrated the greatest amount of functional activity and c-fos labeling in the C6 and C7 spinal cord segments. In all four groups, c-fos labeling, like functional activity, was observed across several spinal cord segments. C-fos labeling was observed at all of the examined levels in the alpha-chloralose group that received noxious stimulation and in the halothane group that received innocuous stimulation. The other two

groups exhibited c-fos positive cells over fewer spinal cord segments. The pattern of labeling was observed to be different between groups; in alpha-chloralose animals, labeled cells were more densely packed (Figure 7). Some types of anaesthetics, such as ketamine and barbiturates, are known to alter c-fos expression and therefore may explain why differences are observed between animals under different modes of anesthesia(Dragunow and Faull, 1989). Despite these differences, across groups, the level in which maximal labeling was observed was similar. The alpha-chloralose group that received noxious stimulation demonstrated the greatest number of cells in C6 while the other three groups demonstrated the greatest amount of labeling in C5 (Figure 6).

C-fos is used primarily to label nociceptive neurons in the brain and spinal cord. Previous studies used graded thermal stimulation to evoke c-fos expression in the rat lumbar spinal cord (Dai et al. 2001). Studies investigating the expression of c-fos following noxious thermal stimulation have found labeling in the expected termination sites for C fibres (laminae I and II) and Aδ fibres (lamina I, II and V) (Hunt et al. 1987). Studies have also shown c-fos labeling following some types of innocuous stimulation (Jennings and Fitzgerald, 1996). C-fos is a useful neuronal marker, however, not all neurons express the c-fos gene and expression can be very specific to the stimulus type, duration, and intensity as well as the age of the animal (Dragunow and Faull, 1989). Other environmental factors and the condition of the animal (i.e. age, type of anesthesia) also cause differences in expression. Therefore, maps of c-fos expression will not identically match functional activation maps. Previously we have found correspondence in the rostral-caudal distribution of functional activity and c-fos labeling during electrical stimulation of the paw in alpha-chloralose anesthetized rats (Lawrence et al. 2004). This is consistent with present results. Other non-noxious stimulation such as brushing and hind limb manipulation produced c-fos

labeling in laminae II to IV(Hunt et al. 1987). The current observation of c-fos expression demonstrate that neuronal activity is not confined to one region of the spinal cord or to only one spinal cord segment; therefore, fMRI activity is also expected to be widespread. However, c-fos does not allow us to observe all neuronal activity that is occurring. C-fos identifies individual cells that are repetitively active. Spinal fMRI identifies regions in which there is an increased ratio of oxyhemoglobin to deoxyhemoglobin and increased extravascular water. Areas of signal change cannot be as specific as the labeling observed in the immunohistochemistry. Furthermore, contributions by draining veins can also account for additional areas of signal change not associated with neuronal activity. Further work is needed to distinguish these false positives from areas of signal change truly related to neuronal activity.

In conclusion the present study demonstrates that spinal fMRI can differentiate activity elicited by different intensities of thermal stimuli with both alpha-chloralose and halothane anesthesia. The latter findings enable chronic fMRI studies of the spinal cord in addition to enhancing the understanding of the impact of anesthetic agents on spinal fMRI under various stimulation conditions. Greater percentage signal change is observed with nociceptive stimuli compared to innocuous stimulation, and neuronal activity was confirmed by c-fos immunohistochemistry. This is the first fMRI study to use thermal stimulation to examine differences between noxious and innocuous pathways in the spinal cord in an animal model.

CHAPTER 4: COMPARISON OF FUNCTIONAL MAGNETIC RESONANCE IMAGING OF THE LUMBAR SPINAL CORD OF THE RAT WITH LOCAL FIELD POTENTIALS

Introduction

The previous chapters confirmed the presence of neuronal activity using immunohistochemistry within the imaged regions of the rat spinal cord. Correspondence between the numbers of c-fos labelled cells and fMRI was found in the rostral-caudal direction. C-fos could not be used to confirm all areas of activity as not all neurons express the gene, or do so selectively (Dragunow and Faull, 1989). Comparisons with other "gold-standards" are needed in order to reveal the relationship between activity identified by fMRI and neuronal activity in the spinal cord.

In this chapter, fMRI is used to identify areas of functional activity in the lumbar spinal cord of the rat during noxious electrical stimulation of the right hind paw. To further establish the relationship between functional activity observed by fMRI and neuronal activity in the spinal cord, areas of fMRI activity were compared with local field potentials. Local field potentials have previously been used to investigate the relationship between neural activity and BOLD signal changes in the visual cortex of the monkey brain (Logothetis et al. 2001). An emphasis will be placed on the comparisons between the two techniques within each animal rather than on group results. The first reason is that differences are anticipated between animals and we are primarily interest in how functional maps represent regions of neuronal activity. Secondly, landmarking the slice positioning is much more difficult in the lumbar spinal cord than it is in the cervical cord. The inter-subject differences in alignment between the spinal cord and the spine are much more apparent in the lumbar spinal cord. As a result, there are greater differences in the cross-sectional size of the spinal cord as the slices may not be positioned at exactly the same

spinal cord segment. Therefore, combined maps, as presented in the previous chapters, are not appropriate as the proper alignment between images cannot be made.

A recording electrode can detect extracellular changes in current related to neuronal activity. The size of the observed field potentials depends on the distance between the electrode and the area of activity, and the number of neurons in the population that are simultaneously recruited. Data from several columns of recordings, spanning the imaged region of the spinal cord, were collected to generally map the area of neuronal activity. Areas of functional activity were then correlated to the negative field potentials. This is the first comparison between spinal fMRI and electrophysiology. Logothesis and authors (2001) were able to record local field potentials and fMRI data simultaneously. Physical restrictions prevent the same experiment design from being performed in the spinal cord. Nevertheless, valuable information can be obtained by comparing that responses observed by each technique.

Methods

Male Sprague-Dawley rats were obtained from Charles River (Quebec) and acclimatized for a minimum of seven days in an environmentally controlled room. Animals were provided with water and food ad libitum. All procedures were approved by local animal care committees and were in accordance with the guidelines of the Canadian Council on Animal Care.

Functional MRI

Nine Sprague-Dawley rats were anesthetized with halothane (3-4% induction, oxygen/med. Air, 1-2% maintenance). Animals were ventilated and positioned supine on a quadrature surface coil. Sagittal scout and transverse fMRI images were collected using.

The same parameters were used as described in Chapter 3 of this thesis. Six, 2 mm thick slices were centred on the vertebra and intervertebral discs between T12 and L1. Three fMRI experiments were performed in each animal in which, electrical stimulation was delivered as described in Chapter 2, using 2 silver needle electrodes inserted subcutaneously in the dorsal surface of the hind paw. Expired pO_2 and pCO_2 were monitored with a pulse oximeter. Experiments were performed as quickly as possible and all animals were in the magnet for less than one hour. Following imaging, animals were recovered and rested for at least 48 hours before electrophysiology experiments.

Electrophysiology

During surgical preparation for electrophysiology, the animal was anesthetized with isoflurane (3-4% induction; oxygen/med. Air, 1-1.5L/min, 1-2% maintenance). An intraperitoneal injection of saline containing dextrose and atropine was delivered. Each animal was intubated and mechanically ventilated (small animal ventilator, Model #40-1002, Harvard Apparatus Canada, Saint-Laurent, PQ). Carbon dioxide levels were monitored with a CO_2 analyzer and maintained between 2.5-3.5%(CAPSTAR 100 model #50080, CWE Inc., Ardmore, PA, USA). The left carotid artery was cannulated in order to monitor mean arterial blood pressure and maintained above 80 mmHg (Pressure Monitor BP-1, World Precision Instruments, Sarasota FL, USA). During this period heart rate and oxygen saturation were monitored with a pulse oximeter (model #8500V, Nonin Medical Inc., MN, USA). Once the vertebrae were exposed and cleaned the animal was transferred to a sterotaxic frame. A heating blanket (Homeothermic Blanket Control Unit, Harvard Apparatus Canada, Saint-Laurent, PQ) was positioned under the rat to maintain a core body temperature of 37°C, monitored rectally. The head, thoracic vertebrae and lumber vertebrae

were immobilised with clamps. A laminectomy was performed from the T12 to L2 vertebrae in order to measure extra-cellular potentials in the imaged region of the spinal cord. Following laminectomy the dorsal roots were identified, when possible, to confirm the spinal cord segment from which recordings were made. In animals where the roots were not visible, confirmation of spinal cord segments from which the recordings were obtained were performed at the end of the experiment. The L4 nerve was observed at the rostral level of the T13 vertebra. Therefore, the L3 spinal cord segment was observed in alignment with the T12 vertebra.

Following surgical preparation, animals were transferred to halothane anesthesia (1-2%) and isoflurane was discontinued. Animals were monitored for approximately 45 minutes during which stimulation and recording electrodes were placed. The back incision was filled with mineral oil and dura mater covering the incised spinal cord.

Two silver needle stimulating electrodes were placed in the dorsal skin of the right hind paw, as in the fMRI experiments. The same strength of electrical stimulation was applied during recordings as in the previous fMRI experiments of the same animals. Extracellular potentials were measured using 2 MΩ tungsten electrodes (World Precision Instruments, USA). Recordings were acquired, first during rest and then during stimulation, every 150 μm to a depth of 1800 μm at several sites spanning the spinal cord segments L3 to L5 corresponding to the T12 to L1 vertebrae. The recording electrode was positioned approximately 0.05-0.08 mm laterally from the midline on either side. In some cases, the electrode positioning had to be adjusted in order to avoid puncturing blood vessels. A minimum of 50 traces were recorded at each location. Animals were euthanized with a lethal dose of KCl at the completion of all recordings. The region of spinal cord examined was removed and fixed in 4% paraformaldehyde. The L3-L5 spinal cord segments were

sectioned (20 μm thick) and collected onto 6 slices. Slides were stained with cresyl violet and viewed to observe the pathway of the recording electrodes.

Data Analysis

Functional MRI data were analyzed by a direct correlation to the stimulation paradigm ($p \leq 0.05$) using custom made software written in MatLab (Mathworks, USA). To determine the general pattern of activity across the group, the number of times a pixel appears active in each area of the cord (right and left, dorsal and ventral horn, and near the central canal) were counted. The percentage of experiments in which activity appears in each of the five areas was recorded. The individual fMRI activity maps were summed for each animal to produce a combined map of total functional activity. The colour spectrum applied to active pixels represents the correlation to the paradigm with red indicating pixels that are most correlated to the time course. Combined activity maps as presented in the previous chapters could not be created, as the anatomical variability between subjects was too great and normalization of the MRI images of the rat spinal cord across subjects into a standard space is not possible. The time course of the signal change was found for the right and left sides of the spinal cord across all six slices for each animal and then averaged.

Extra-cellular potentials were analyzed using in-house software (Spinal Cord Research Centre, Department of Physiology, University of Manitoba) run on a Pentium PC under Linux Redhat operating system. A minimum of 50 traces were collected and averaged to observe the mean response. The delay between stimulation and response, peak response (mV), time to peak, and area of the potential for the averaged response was measured for each individual recording site. The responses for each animal were then

calculated as a percentage of that animal's maximal response. The time integral of the amplitude of response was considered for this normalization.

To determine the statistical correspondence between spinal fMRI and electrophysiology the distance between the recordings sites where the local field potentials were observed, and location of the greatest fMRI activity, taking into consider both degree and consistency between fMRI experiments, in each region of the spinal cord were correlated. For each animal, the activity observed within the three functional experiments was summed onto one map. On each summed activity map the region of most intense activity was identified. In general these were the red pixels but green pixels were also considered if red pixels were absent. The approximate locations of the electrophysiological recordings on the fMRI activity maps were calculated based on measurements of the anatomy taken from the same MR image. The distance from each calculated recording site to the identified region of fMRI activity was measured. These values were correlated with the values of the areas of the local field potential responses.

Results

The combined activity from the three fMRI experiments and local field potentials observed in one animal are shown in Figure 1. Active pixels were observed along the surface of the ventral median fissure in all slices except the first. It should be noted that signal from pixels near the edge of the cord along the dorsal sulcus or the ventral median fissure are likely contributions from blood vessels as these are found in the same location as the median dorsal and ventral spinal arteries. It is important to exclude these regions when selecting the most consistent regions of fMRI activity for the correlation analysis. Functional activity was observed mainly in areas of negative local field potentials. In some

cases fMRI activity was also present in areas of positive field potentials. At the level of the T12 disc (slice 1) functional activity was observed in the ipsilateral dorsal and ventral horns. Negative field potentials were observed at depths from 600 μm and 1500 μm on the ipsilateral side. Functional activity was also observed in the contralateral ventral horn; however, extracellular recordings were not measured at this level in this animal.

At the T12/T13 level (slice 2), functional activity was observed bilaterally in the dorsal and ventral horns. Small negative local field potentials were observed on the ipsilateral side (Figure 1). Recordings on the contralateral side were not measured at this level.

Both techniques found the greatest amount of activity in slices 3 and 4 at the T13 vertebra and T13/L1 disc, respectively (Figure 1). Functional activity maps also showed clusters of active pixels within the slices placed at the T12/13 and L1/L2 discs. Functional activity was observed bilaterally in both slices. Functional activity at the level of the T13 vertebra was found to be more in the ventral horns; whereas, activity at the T13/L1 disc was spread over the dorsal and ventral horns. Negative field potentials were observed from 150 μm to 90 μm from the dorsal surface of the cord. Small negative local field potentials were also observed on the contralateral side at the T13 vertebra and T13/L1 disc. There was little fMRI activity in the right dorsal horn at the L1 vertebra although negative local field potentials were present. Functional activity was observed in the ipsilateral ventral horn. Negative field potentials on the same side were observed from 150 μm to 1200 μm. Areas of functional activity were observed across the contralateral side from 150 μm to 1050 μm. In the last slice, at the L1/L2 disc, functional activity was observed medially in the ipsilateral dorsal and ventral horns and spread across the contralateral side. Negative field

potentials were observed in the ipsilateral side from 150 μm to 600 μm from the dorsal surface of the spinal cord.

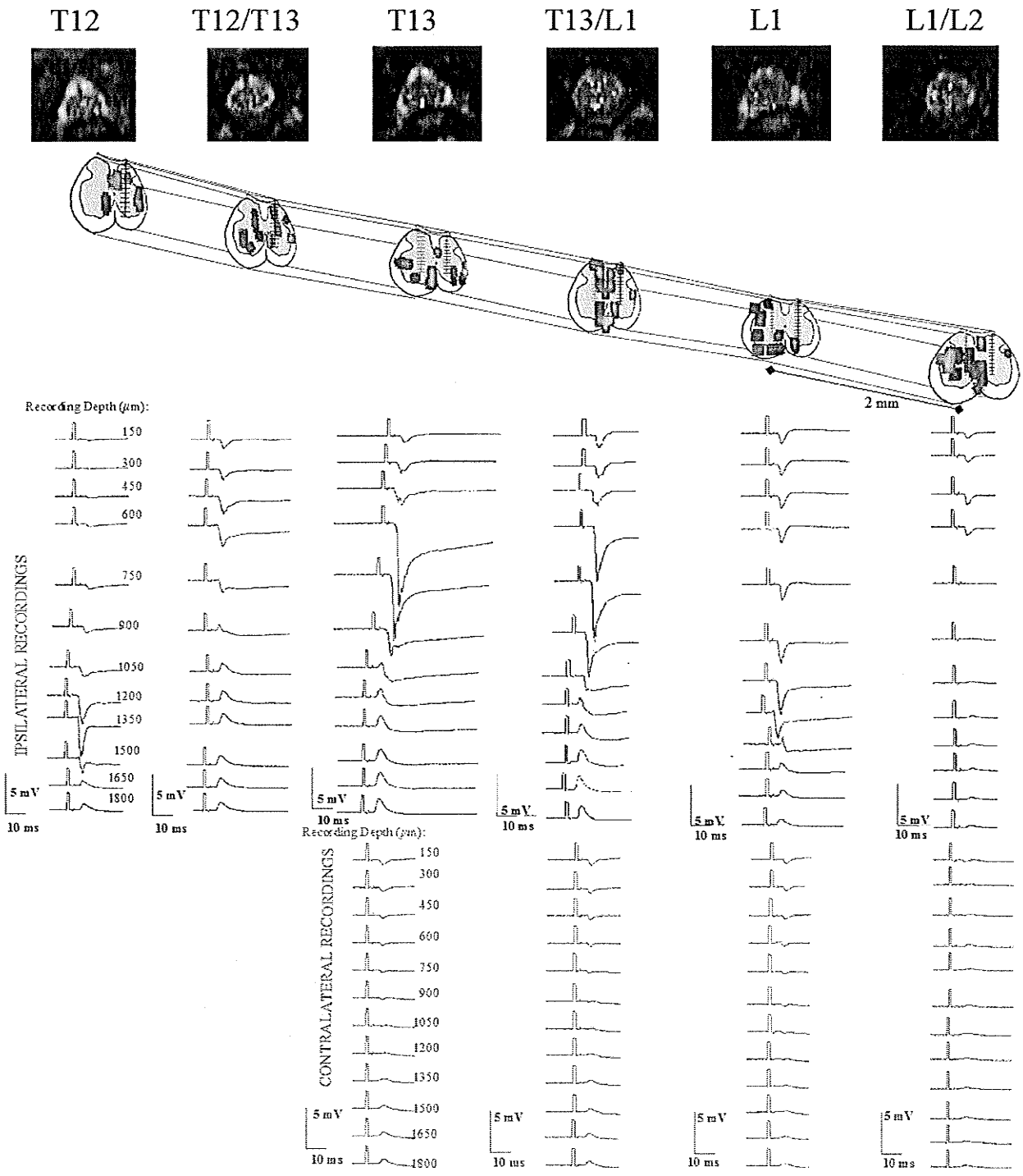

Figure 1. Functional MRI and electrophysiology data from Animal 1. Functional maps show the total activity observed in three fMRI experiments. The images are oriented with dorsal up, ventral down, left side of the animal is on the left side of the image, and the right side of the animal is on the right side of the image.

Similar individual comparisons between fMRI and electrophysiology for each subject are shown in Appendix A. Correlation coefficients were calculated between areas of fMRI activity and the distance to the recording sites of the local field potentials. Correlation coefficients (R) indicated by the arrows and corresponding values in Figures 1-9, Appendix A were between -0.971 and 1. The greatest correlations were observed between T13 and L1 vertebrae in all subjects expect one in which maximal correlation was observed at the L1/L2 disc. Four animals also demonstrated areas in which acceptable correlation was found more rostrally at the T12 vertebra and at the T12/T13 disc.

A 20 μm thick section taken at the L4 spinal cord segment demonstrating the pathway of the recording electrode on the ipsilateral side is shown in Figure 2. This pathway was measured at 1000 μm from the dorsal surface of the cord.

Figure 2. Electrode pathway observed at 20x magnification in one section taken from the L4 spinal cord segment of one animal. Depth of the pathway was measured to be 1000μm.

FMRI detected areas of activity across all 6 slices in all nine animals. The first of three individual functional maps obtained from each animal is shown in Figure 3. Maps showing the total activity in all 3 experiments for each animal are shown in the Appendix 1. Some patterns between individual scans and animals can be observed despite variations in the location of active pixels. Most animals exhibit the peak number of pixels between the slices positioned at the T13 to L1 vertebrae. The L4 spinal cord was observed to be in alignment with the T13 vertebra in all animals.

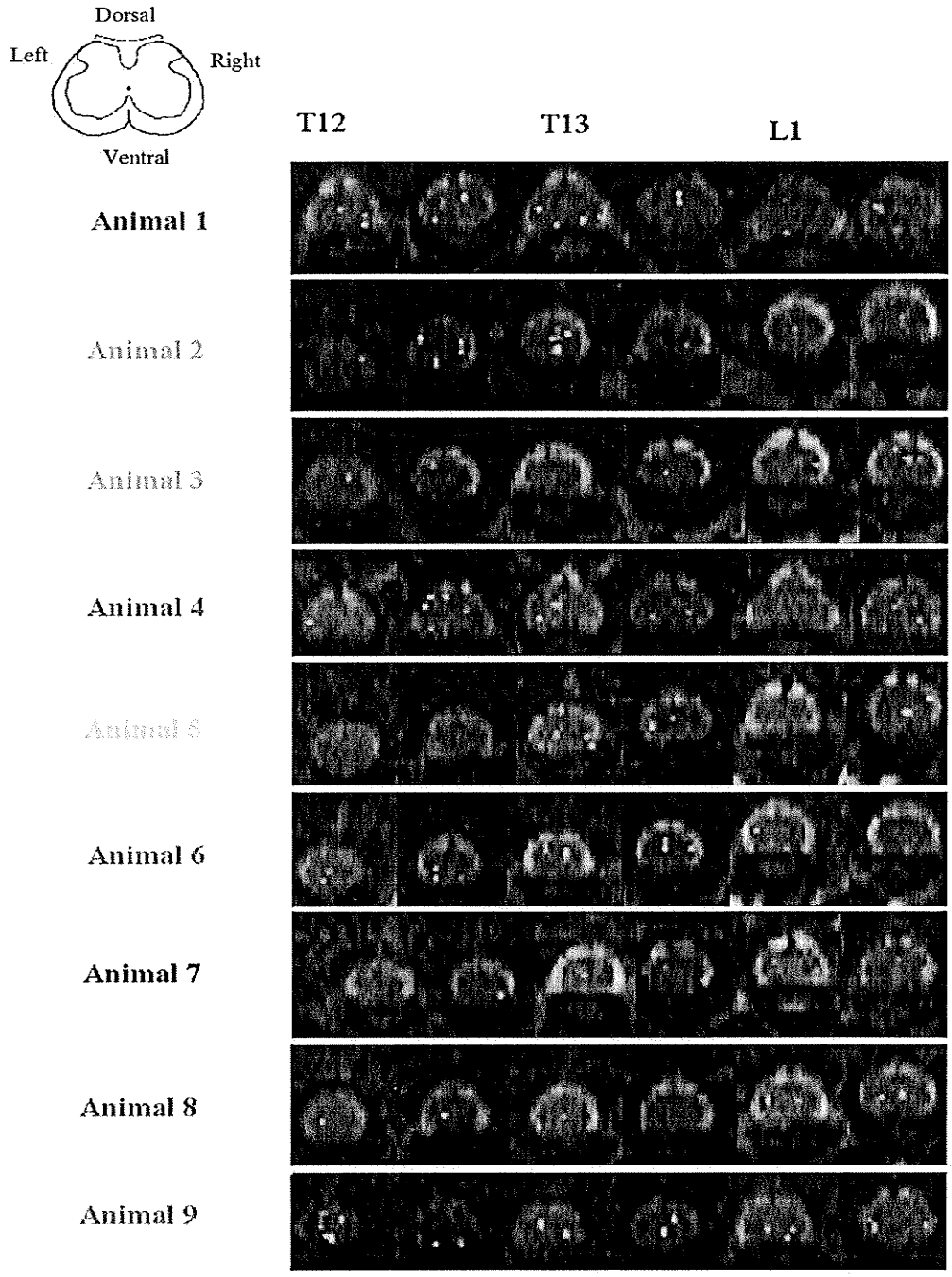

Figure 3. A representative fMRI experiment from each of the nine animals. Three experiments were completed in each animal. Here, the first of those three is shown.

The number of active pixels observed in different regions of the cord (right and left, dorsal and ventral horns, near the central canal) of all experiments (n=27 from 9 animals), were counted and the frequencies reported as a percentage in Figure 4. Within the first slice (at the T12 vertebra) four of the nine animals demonstrated fMRI activity in the right dorsal horn and contralateral ventral horn. Functional activity in the latter area was observed in 52% of all experiments. All animals showed fMRI activity in the contralateral ventral horn at the T12/T13 disc (slice 2) in at least one experiment. In the same slice, four of the nine animals showed functional activity in the left dorsal horn and right ventral horn. The right ventral horn activity was observed in 56% of all experiments. In the third slice, positioned at the T13 vertebra, fMRI activity was frequently observed in the right ventral horn (63%). At the level of the T13/L1 disc (slice 4) active pixels were observed most frequently (48%) in the right dorsal horn. Seventy percent of experiments showed fMRI activity in the right ventral horn at the L1 vertebrae (slice 5). Functional activity was observed across scans on the contralateral side in the ventral horn (48%) and dorsal horn (56%). In the last slice examined, between L1 and L2, four animals demonstrated active pixels in the right ventral horn and three animals showed active pixels in the left and right dorsal horns. Active pixels were observed in the contralateral dorsal horn in 59% of all experiments.

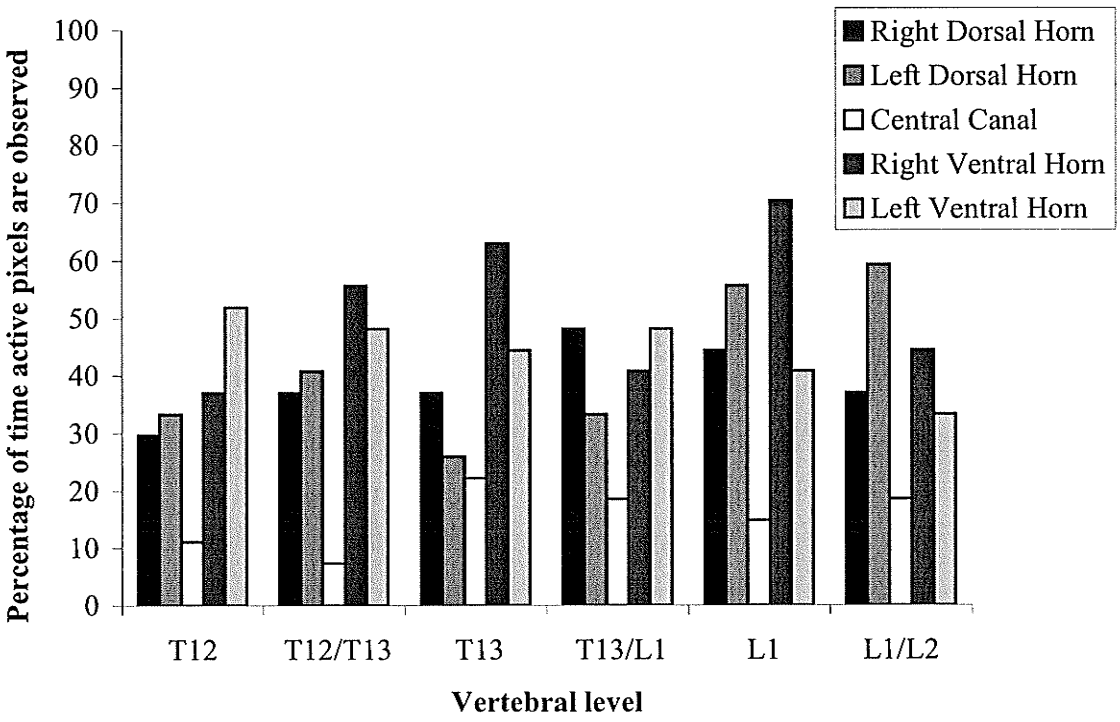

Figure 4. Percentage of the time active pixels were observed in each zone (n=27 experiments from 9 animals).

The group average time course observed on either side of the spinal cord is shown in Figure 5. Within the individuals, six of nine animals showed slightly higher percentage signal change on the ipsilateral side of stimulation. Three of the animals showed no difference or slightly higher percentage signal change on the contralateral side. In the group average, the highest percentage signal change observed on the ipsilateral side was 18% while on the contralateral side it was 14%. This is with the deviation between animals and so does not appear to be statistically significant, however, a more thorough analysis is needed to exclude areas of signal change related to noise and draining veins.

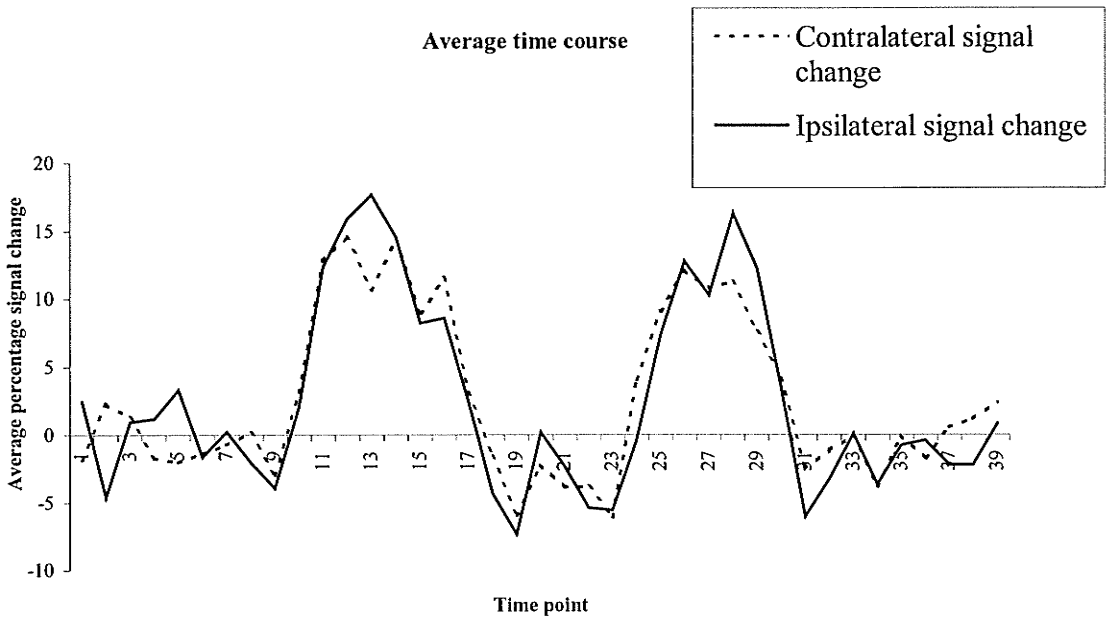

Figure 5. Average time courses from nine animals observed on each side of the spinal cord during right hind paw stimulation.

Negative field potentials indicating neuronal activity were observed across the 6 slices bilaterally. The responses observed by electrophysiology are shown in Figures 6 to 11. The values were normalized for comparison between animals so that the responses at each location are expressed as a percentage of the animal's own maximal response. As with fMRI, variation in the location of the peak activity was observed between animals. Five of the subjects showed the largest negative field potentials in the recording taken at the level of the rostral part of the T13 vertebra (Figure 8). This level corresponds with the third slice obtained during imaging. Correlation coefficients in four of these animals at these levels were found to be R=0.54 (Appendix A, Figure 1), R=0.67 (Appendix A, Figure 2), R=0.70 (Appendix A, Figure 4), and R=0.88 (Appendix A, Figure 5). In one animal negative local field potentials were not observed and so a statistical comparison

could not be made (Appendix A, Figure 7). In two animals ipsilateral activity was found to be poorly, or negatively correlated as they correlation coefficients were R=0.484 (Appendix A, Figure 6) and R= -0.50 (Appendix A, Figure 3). In one animal activity on the contralateral side was negatively correlated (Appendix A, Figure 8). In one animal the calculated correlation coefficients were R= -0.97 for activity on the contralateral side and R= -0.467 on the ipsilateral side (Appendix A, Figure 9). The same animal demonstrated better correspondence between fMRI and electrophysiology at the level of the T13/L1 disc (R=0.53, Appendix A, Figure 9). Animal 3 showed the greatest negative potential in the caudal half of the same vertebra. Within the same animal, reasonable correlation was found in the adjacent slice at the L1 vertebra (R= 0.76, Appendix A, Figure 3). Animal 8 demonstrated peak activity at the level of the rostral portion of the T12 vertebra (Figure 6). Correspondence was observed between the two techniques in the same animal at the T12/13 disc (R= 0.51, Appendix A, Figure 8). Maximal field potentials were observed in the rostral and caudal portions of the L1 vertebra in Animals 7 and 6 respectively (Figures 10 and 11). Both animals showed fair to good correlation between fMRI and electrophysiology in the adjacent slices at either the L1/L2 disc or the T13/L1 disc (R=0.88, R=0.78, Appendix A, Figures 6 and 7 respectively). The depth at which peak activity was observed varied between 300 μm and 1200 μm. All animals demonstrated smaller sized potentials on the contralateral side from 150μm and as deep as 1500 μm in one animal.

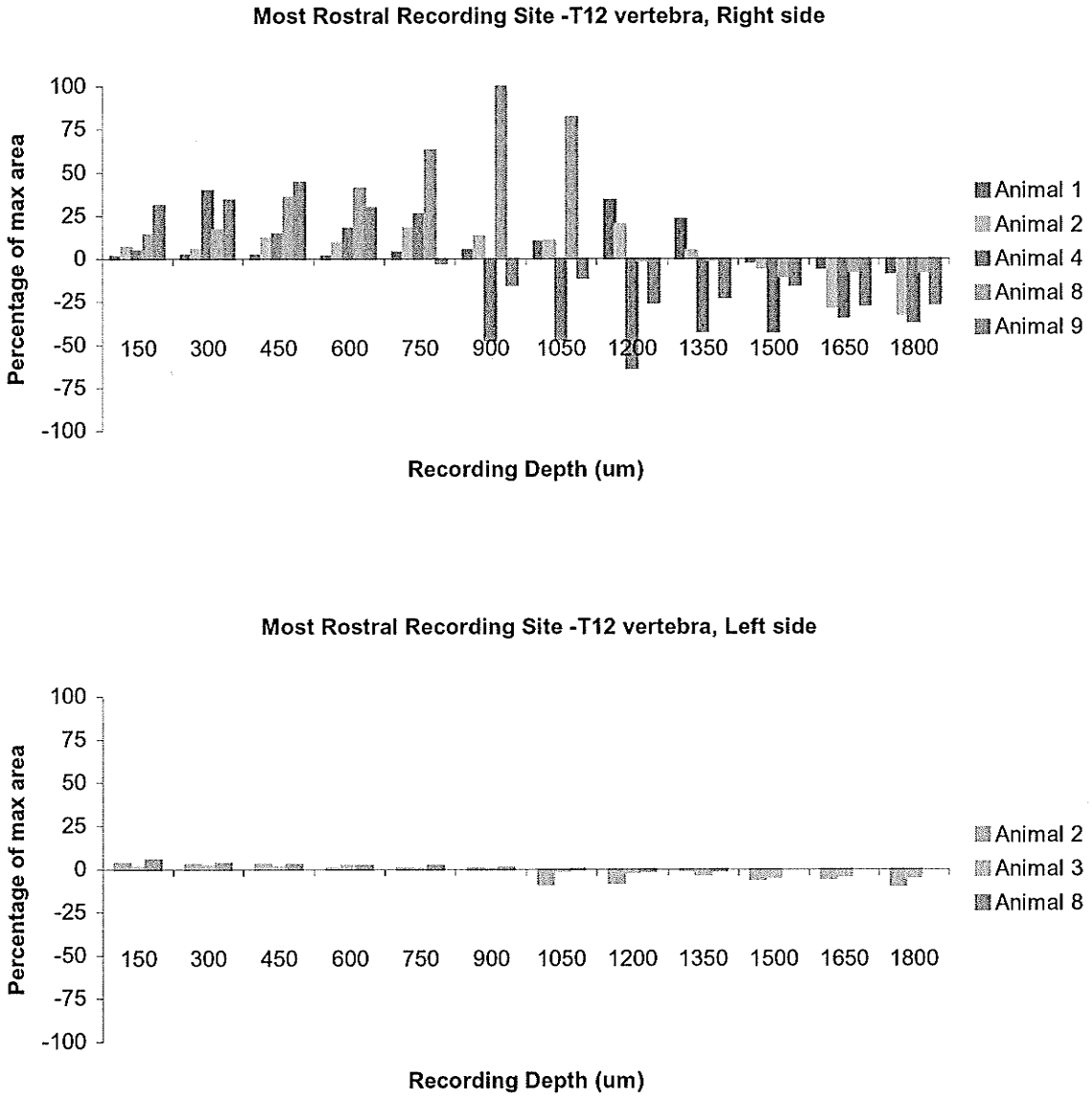

Figure 6. Normalized responses measured in the rostral end of the T12 vertebra (L3 spinal cord segment) on the ipsilateral (top) and contralateral side (bottom) of stimulation. This region corresponds with the first slice acquired during fMRI.

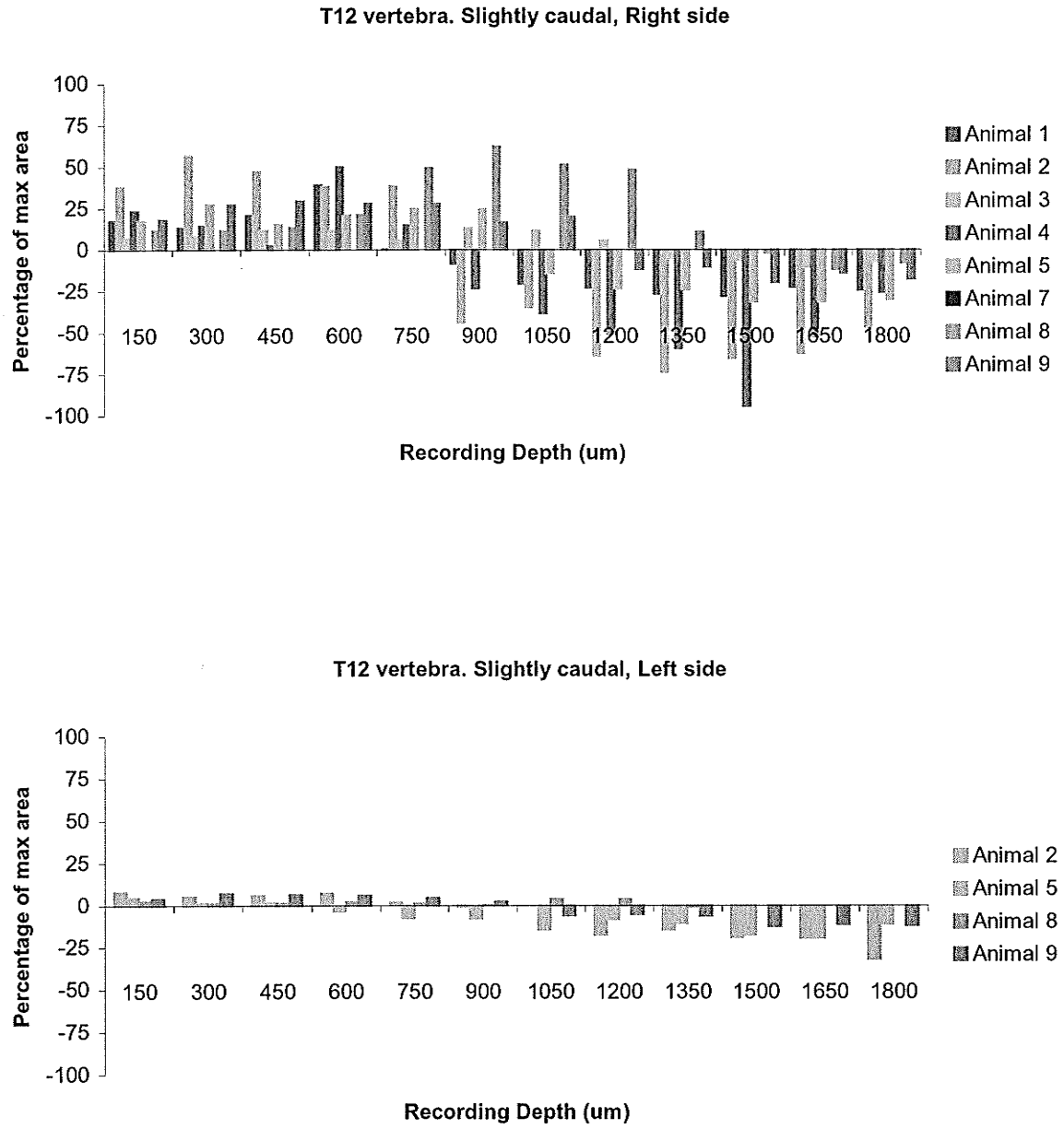

Figure 7. Normalized responses measured in the caudal end of the T12 vertebra (near the juncture of the L3 and L4 spinal cord segments) on the ipsilateral (top) and contralateral side (bottom) of stimulation. This region corresponds with the second slice acquired during fMRI.

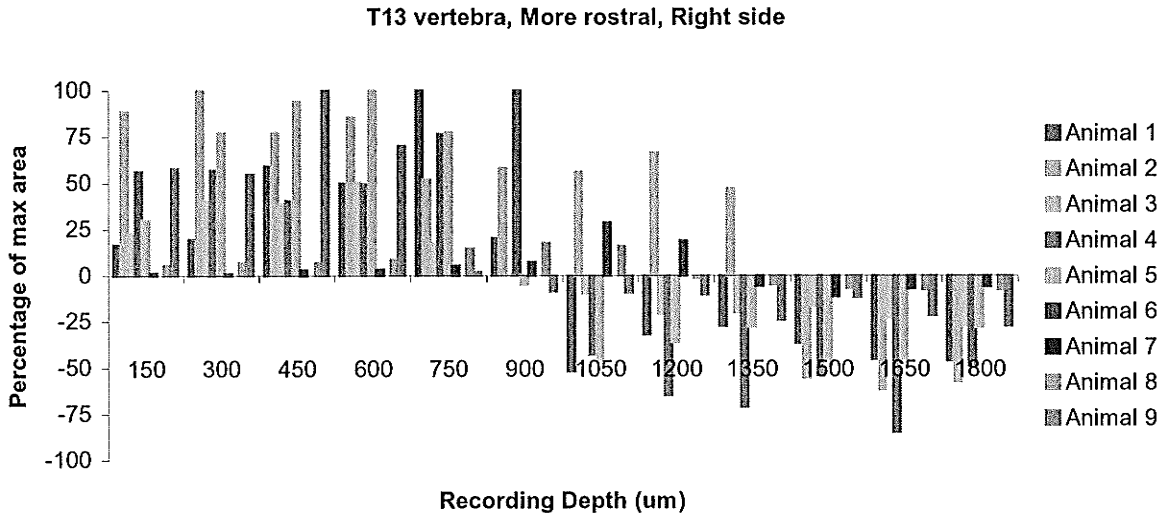

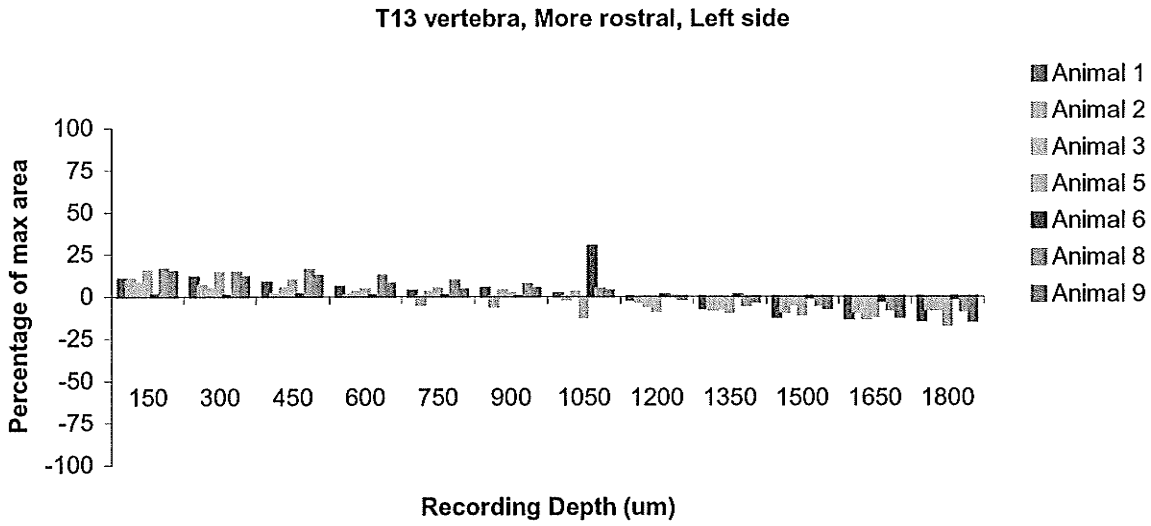

Figure 8. Normalized responses measured in the rostral end of the T13 vertebra (L4 spinal cord segment) on the ipsilateral (top) and contralateral side (bottom) of stimulation. This region corresponds with the third slice acquired during fMRI.

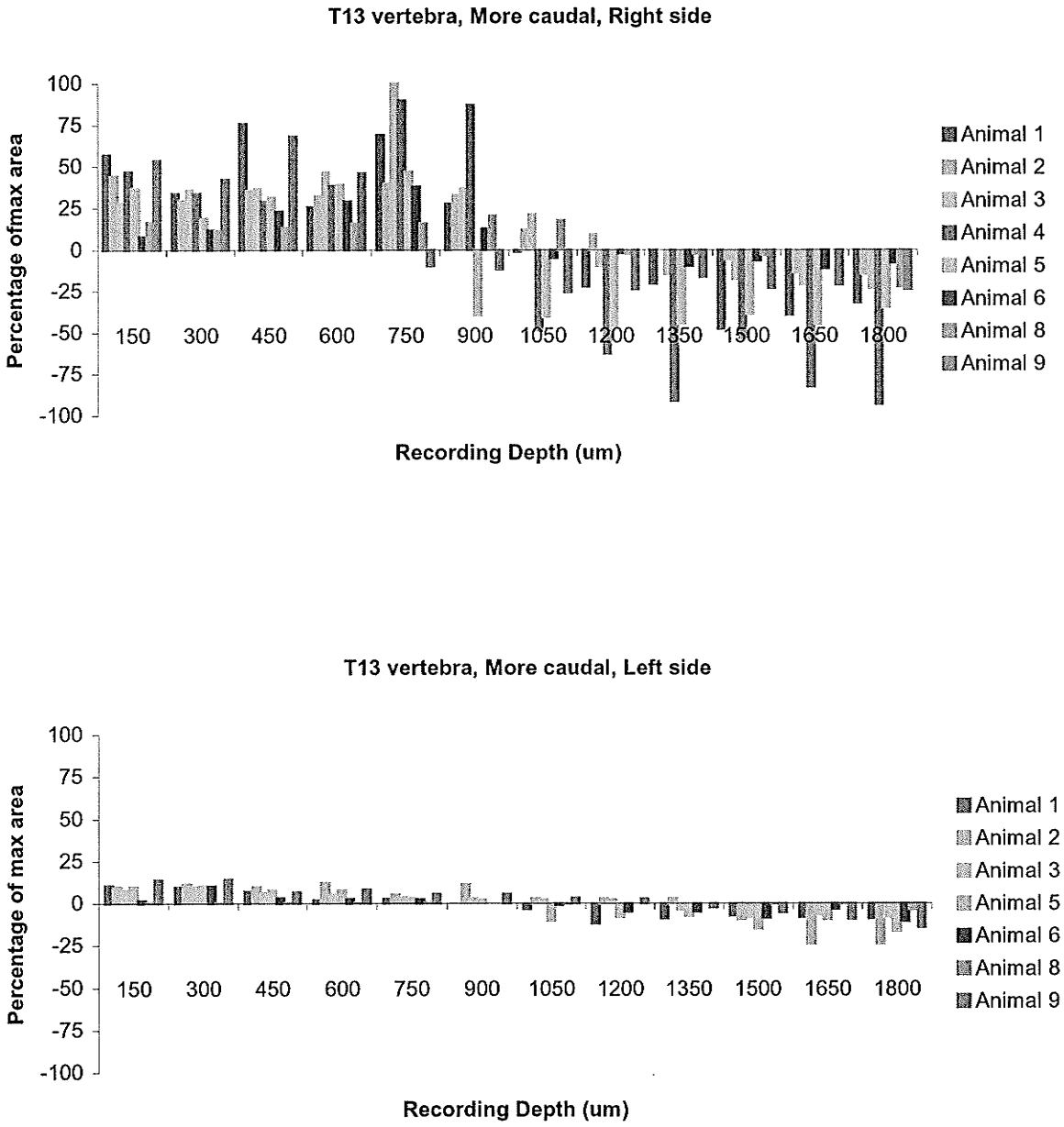

Figure 9. Normalized responses measured in the caudal end of the T13 vertebra (near the juncture of the L4 and L5 spinal cord segment) on the ipsilateral (top) and contralateral side (bottom) of stimulation. This region corresponds with the fourth slice acquired during fMRI.

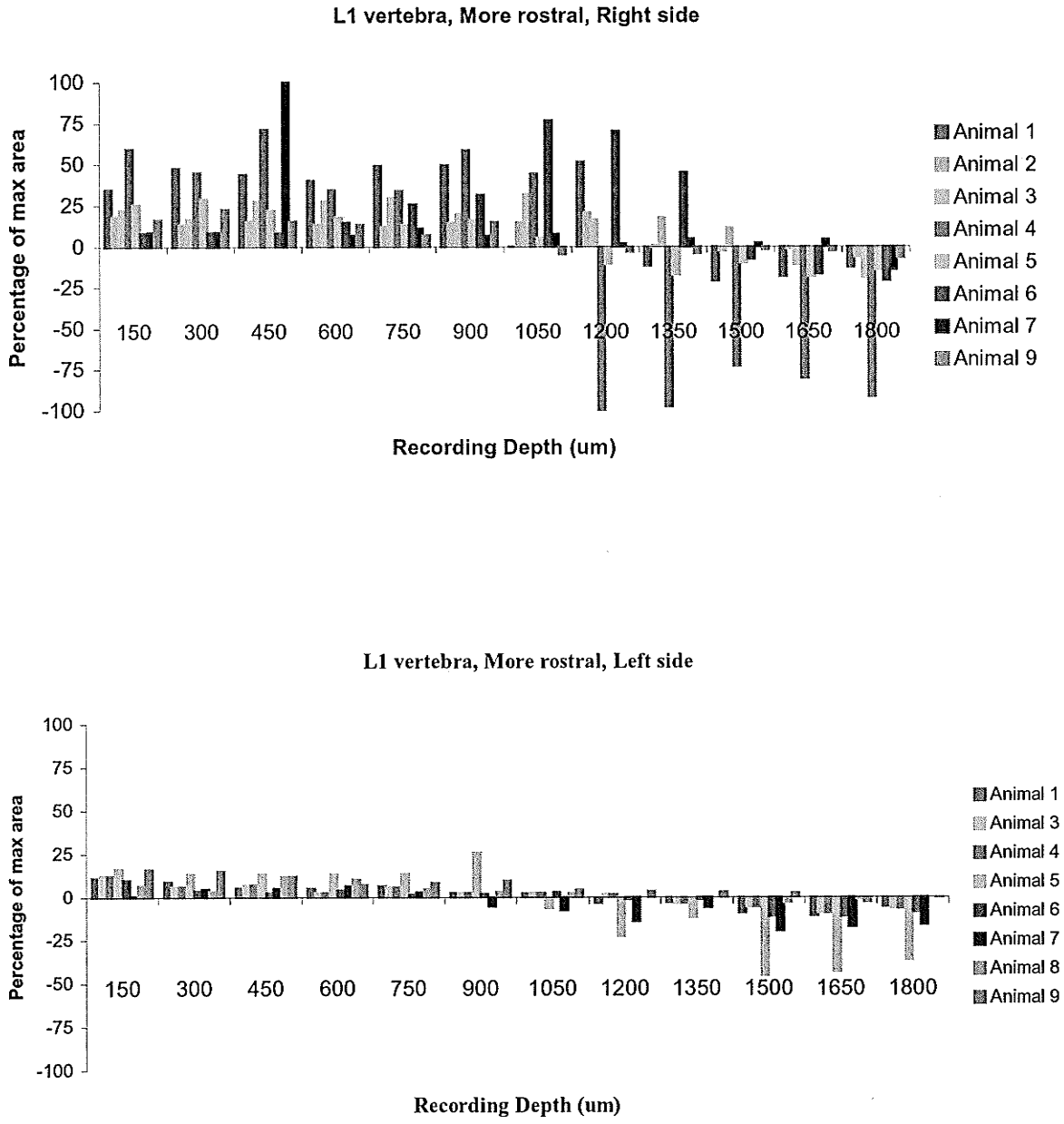

Figure 10. Normalized responses measured in the rostral end of the L1 vertebra (L5 spinal cord segment) on the ipsilateral (top) and contralateral side (bottom) of stimulation. This region corresponds with the fifth slice acquired during fMRI.

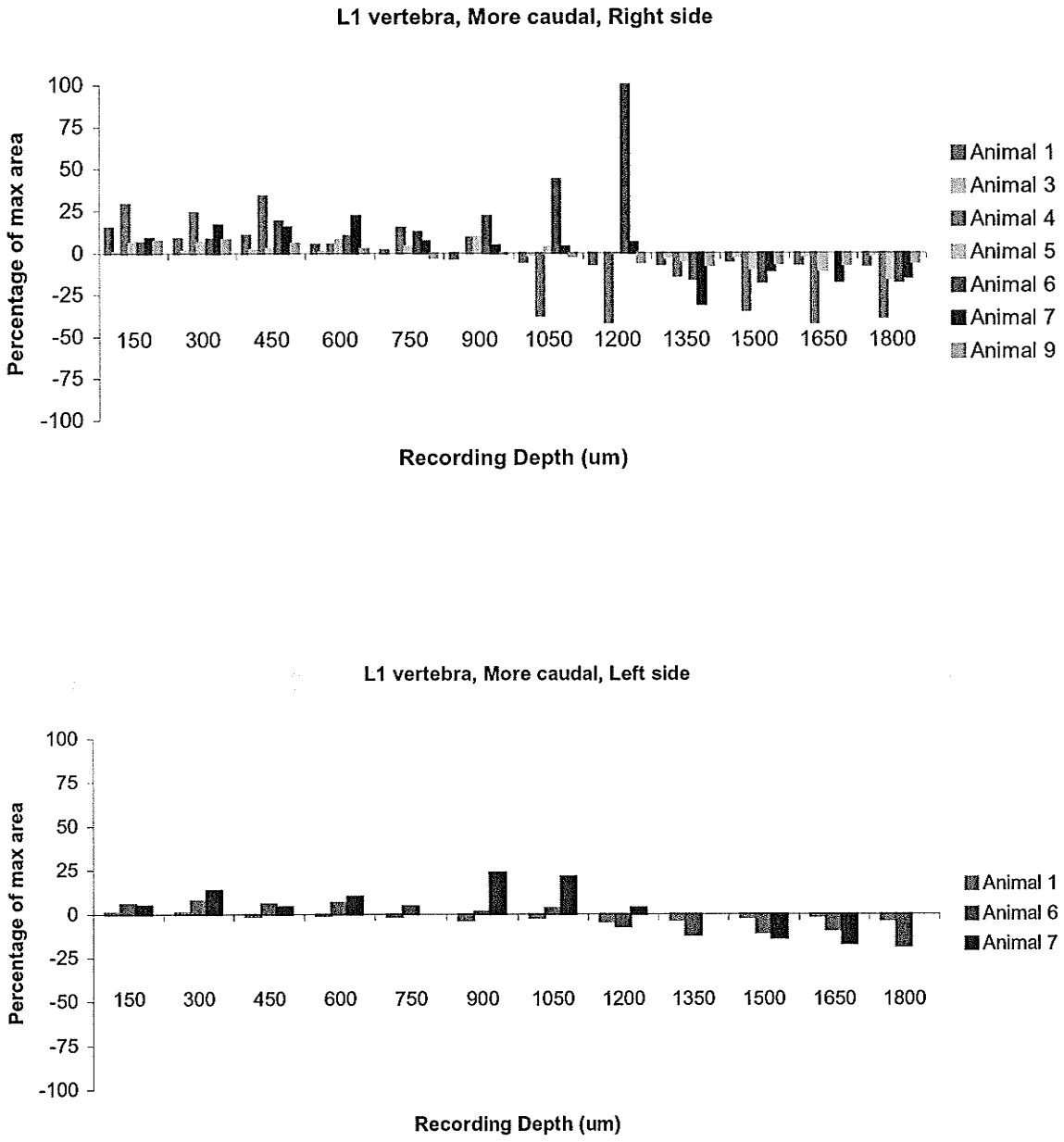

Figure 11. Normalized responses measured in the caudal end of the L1 vertebra (near the juncture of the L5 and L6 spinal cord segments) on the ipsilateral (top) and contralateral side (bottom) of stimulation. This region corresponds with the sixth slice acquired during fMRI.

Discussion

Spinal fMRI and electrophysiology identified areas of activity in all of the imaged levels of the spinal cord. This was expected as the stimulus was administered to a broad general area, encompassing several dermatomes of the hind paw and was of a noxious intensity. Previously, functional activity and c-fos labelling was observed over several segments of the lumbar cord during the same stimulus (Lawrence et al. 2004). Neuronal activity was found to peak in the L4 spinal cord segment, which is in alignment with the T13 vertebra (Lawrence et al. 2004). In the present study, most animals exhibited the greatest negative field potentials at the T13 vertebra. FMRI showed the most active pixels at the level of the T13 vertebra and T13/L1 disc. Therefore in most cases, the rostral-caudal distribution of neuronal activity detected by the two techniques was similar.

C-fos labelling could not account for all areas of neuronal activity within slices due to the specificity of expression (Hunt et al. 1987). Previous animal spinal fMRI studies have observed functional activity on both sides of the cord and in both the dorsal and ventral horns (Lawrence et al. 2004; Lawrence et al., 2004b). In the present study, negative local field potentials were observed bilaterally and as far as 1650 μm from the dorsal surface on the ipsilateral side of the spinal cord (Figure 6-11). Greater areas of neuronal activity were detected than found using c-fos alone in the previous chapters.

Variation within individual fMRI scans is expected. Within brain fMRI small variations between the locations of active voxels are observed between scans, imaging sessions, and subjects. The variations become more apparent in spinal fMRI as the cross-sectional area of neural tissue is much smaller. The frequency with which pixels in

different areas of the spinal cord were found to be active were calculated. Some areas of cord demonstrated active pixels in up to 70% of experiments (Figure 4). Previous chapters presented thresholded combined activity maps in order to identify areas of fMRI activity that were consistent between experiments and animals. The optimal threshold for these maps is often slightly over 50%. Therefore we are mainly interested in areas which show fMRI activity in over 50% of all experiments. Combined activity maps require several fMRI experiments to be repeated. In the present work, fMRI experiments were repeated only three times in order to minimize the length of time the animal was under anesthesia. If time was not a restriction, increasing the number of experiments would increase confidence in areas that are observed to be active.

Combined activation maps also rely on aligning the anatomy of different animals. Within human brain fMRI, normalization of data from multiple subjects is possible by conforming the anatomy into a standard space such as that described by Talairach (Talairach and Tournoux, 1998) or the Montreal Neurological Institute (MNI) (Collins et al., 1994). Standard space currently do not exist for the spinal cord making normalization difficult. Only recently was a technique developed which allows normalization of the cervical spinal cord (Stroman and Cahill, 2006). Previous combined activity maps of animal spinal cord data are created by a rigid alignment of the data. In the two previous chapters, data were collected from the cervical spinal cord and there was little variation observed in the cross sectional size of the spinal cord. In the present chapter, greater variability in the dimensions of the spinal cord can be observed across subjects and is apparent in Figure 3 especially within the first two slices. In the current study it is not

possible to create overlay maps due to the variability between animals in the alignment of the spinal cord segments to the vertebrae.

A visual examination of the spatial distribution of active pixels and negative local field potentials does not reveal a clear correlation within the cross-sections of the spinal cord. In several areas mismatch was observed. In the presented results there were 13 sites in which functional activity was absent while local field potentials were observed. This raises issues regarding the sensitivity of spinal fMRI. The minimal metabolic demand required in order to evoke an observable response by fMRI in the spinal cord has not been investigated. Such studies would perhaps explain some of the variability observed.

There were two sites in which functional activity was observed while no local field potentials were observed. In some areas functional activity was observed within areas of negative field potentials, however the locations of the two techniques were poorly correlated or not correlated at all. Active pixels that relate closely to neuronal activity are expected to occur within the gray matter as this is the location of metabolism related to neuronal activity. Some regions of functional activity may also be false positives. A cluster analysis may be useful to separate active pixels related to noise based on the time courses of signal change (Baumgarter, 1998).

Another consideration is the state of the animal. During fMRI the animal is anesthetized for a total of one hour. Electrophysiological recordings often did not start until five hours after the initial anesthestic induction due to the time for surgical preparation. Blood pressure, heart rate and oxygen saturation were monitored. The surgical procedure can cause rapid decreases in blood pressure and is physically stressful

on the animal. As a result the animal may be in a fragile state by the end of the surgical procedure.

Analysis of the percentage signal change on each side of the cord is also important. Negative field potentials were larger on the ipsilateral side of the spinal cord. Therefore it can be hypothesized that there is also a larger metabolic demand resulting in a change in blood oxygenation at the level of the stimulation. If the metabolic demand is related to the percentage signal change observed by fMRI, then we may expect an increase in percentage signal change on the side ipsilateral to the stimulation. Analysis of the laterality of the percentage signal change did not produce a clear distinction. In six of the nine animals the percentage signal change was slightly higher on the ipsilateral side. In the group average this difference is only 4%. The difference in the hemodynamic response on each side of the cord is too small to detect a clear difference. Further analysis is needed in order to eliminate signal contributions from pixels near large blood vessels. Perhaps then differences in the laterality of signal change will be observed.

The positioning of the fMRI slices and recording sites were taken carefully in order to best match the locations. During functional imaging a sagittal image was used in order to centre axial slices on the vertebral bodies and intervertebral discs. Therefore, the position in the spinal cord can only be estimated in relation to the spine. In some cases a slight bend in the recording electrode was noted, which could also affect the actual recording depth at which local field potentials were observed. The only way in which the recording electrode could be guaranteed to be positioned in the exact area of functional activity is to perform both techniques simultaneously as previously reported for the monkey brain (Logothetis et al. 2001). With spinal cord imaging this is not possible due

to animal positioning within the magnet and the way in which electrodes need to be moved in this type of experiment.

The nature of the fMRI signal must be taken into consideration. While fMRI has better spatial resolution than other neuroimaging techniques such as MEG, and PET, the signal is an indirect measure of neuronal activity. The relationship between neuronal activity and the BOLD response is not linear. Therefore the two techniques cannot expect to be perfectly in correlation as other influences also play a role. Large draining veins can also contribute to the signal. Within the brain, the region of neural tissue that received an increased blood supply is larger than the region in which neuronal activity is occurring. This response was likened to "watering a whole garden for the sake of one thirsty flower" (Malonek and Grinvald, 1996). Likewise, it can be anticipated that the region of increased blood flow is larger than the area in which neuronal activity is observed. This may account for the large spatial spread of active pixels. Another consideration is the neurovascular-coupling that the fMRI signal is dependent on. The relationship is not fully understood in the brain (Logothetis and Wandell, 2004) and it is not known if the response in the spinal cord is the same. A complication within animal studies is the necessity of anesthesia. Anesthetics can also affect the vascular reactivity and therefore influence the signal. Halothane anesthesia was used in the present work as recovery of the animal was needed to transfer the animal to the lab in which electrophysiology was performed.

Variation was also observed within the electrophysiological recordings. While the majority of animals showed the greatest response at the level of the T13 vertebra, some animals showed the greatest local field potentials slightly more rostrally or caudally

(Figures 6,8,10,11). The depth of the peak local field potential also varied between 300 μm and 900 μm. Areas of functional activity that correlated with negative fields potentials were also found in the rostral levels observed at the T12 vertebra and T12/T13 disc (Figures 1,2,8,9 in Appendix A) and in the most caudal level examined at the L1/L2 disc (Figure 7 in Appendix A) in some animals.

This is the first comparison of activity observed non-invasively by fMRI with electrophysiology. The spatial distribution of functional activity in the rostral-caudal direction as well as within the cross-sections, were compared to the areas of local field potentials. This study reveals that segmentally, the peak region of fMRI activity and local field potentials were the same in three animals (Figures 2, 5, and 7 in Appendix A), within adjacent segments in three animals (Figures 1, 3, and 4 in Appendix A) and within two segments in one animal (Figure 9 in Appendix 1). This suggests that some information may be gained from the spatial comparison of activity.

The relationship between fMRI activity and neuronal activity is not simple. The rostral-caudal distribution of negative local field potentials and active pixels were similar and electrophysiology was able to confirm neuronal activity was present on the contralateral side and in deeper levels of the spinal cord. Within cross-sections a direct overlap between the techniques is limited. The results of this study suggest that general commonalities exist between the segmental distribution of activity, however, a direct link between an active pixel and negative field potentials cannot be made. Further analysis of other attributes of the fMRI signal, such as percentage signal change, are needed to reveal more information about the relationship between the response observed by fMRI and local field potentials.

CHAPTER 5: GENERAL DISCUSSION

Overview of Results

The work presented in Chapters 2 and 3 describe a chronic experimental model of animal spinal fMRI. It is essential to note that without this preliminary work the subsequent chronic studies would not be possible. Previously, alpha-chloralose was used during animal functional MRI studies of the brain and spinal cord. Recovery of animals from alpha-chloralose anaesthesia is not feasible, limiting experimental design.

Areas of functional activity were similar between alpha-chloralose and halothane anaesthetized animals. A rostral-caudal correspondence between fMRI activity and c-fos labelling was observed. Functional activity was spread over several areas within slices of the spinal cord, whereas c-fos expression was more restricted spatially. The patterns of c-fos labelling were consistent with those reported in the literature (Jinks et al. 2002; Menetrey et al. 1989). The use of c-fos labelling confirmed the spinal cord segments in which neuronal activity was occurring. A comparison within sections of the spinal cord cannot be made between c-fos and fMRI as they are measuring two different, but related responses. The immunohistochemistry reports individual cells that express a certain molecular pathway upon repetitive stimulation. Expression of c-fos protein is specific, therefore it cannot account for all neuronal activity. FMRI is an indirect measure based on a hemodynamic response to an increased metabolic demand. Therefore, the response observed by fMRI is expected to be more widespread as it will respond to changes in blood oxygenation, blood flow and related metabolic changes. Furthermore, a vascular response is being observed. The region of vasodilation is expected to be larger than the area of neuronal activity.

The experiments in Chapter 3 also add to the growing body of literature in spinal fMRI and help characterize the fMRI response observed in the spinal cord. Greater percentage signal change was observed during noxious thermal stimulation regardless of the type of anaesthesia used. These results confirm observations made previously in a human study with cold stimuli (Stroman et al. 2002). Again, fMRI activity was observed with both alpha-chloralose and halothane anaesthesia using both noxious and innocuous thermal stimuli. These results examined if spinal fMRI could map changes in activity elicited by slightly different stimuli in an animal model. The activity elicited by the two intensities of stimulation could only be differentiated by differences in the percentage signal change. The results of this chapter emphasize the valuable information that can be obtained from the time course of signal change. C-fos confirmed the presence of neuronal activity across multiple spinal cord segments. As in the previous chapter, a one-to-one correspondence between c-fos and fMRI was not made due to the specific expression of c-fos protein.

Chapter 4 presents a comparison between areas of fMRI activity and areas of local field potentials. Electrophysiology confirmed neuronal activity was present in deeper lamina of the cord than observed previously by c-fos. The presence of neuronal activity on the contralateral side was also demonstrated by electrophysiological recordings. Again, the results demonstrate a rostral-caudal distribution of activity that can be observed with spinal fMRI. Conclusions about the relationship between the location of active pixels and negative local field potentials cannot be made. There is very limited correlation between specific regions of fMRI activity and neuronal activity detected by electrophysiology. This suggests that the two measures are examining different processes associated with the same stimulus. Local field potentials are extracellular changes in current whereas fMRI detects hemodynamic changes related to changes in metabolism. Further investigations into other

aspects of the fMRI signal, such as the distribution of signal intensities may provide additional information regarding the nature of the discrepancies between the fMRI and electrophysiological measures. The comparison we can make is also affected by the fact that the fMRI and electrophysiology recordings were taken on different days and the state of animal would be slightly different due to the nature of the experiments. The necessity of recovery meant that fMRI experiments were performed as quickly as possible, therefore, the animal was anaesthetized for a maximum of one hour. Electrophysiology experiments were performed after a long surgical preparation that lasts several hours. Therefore, the physiological state of the animal due to the length of anaesthesia and stress due to surgery could influence the results obtained by each method. A solution for these confounds is to perform both measurements simultaneously. This was not physically possible for these studies.

The implications of the results of this work demonstrate that we can obtain valuable information about spinal function using fMRI. Differences in function between normal healthy human subjects and those with spinal cord injury were observed with spinal fMRI (Stroman et al. 2004). The technique was also used to observe decreasing areas of sensory input into the rat spinal cord following graded peripheral nerve injury (Majcher et al., 2006b). Recently, within the rat spinal cord and brainstem, the altered patterns of activity during innocuous and noxious electrical stimulation as well as following the administration of morphine were observed with fMRI (Lilja et al. 2006). Collectively, these studies and the results presented here suggest that some information about spinal cord activity can be obtained using fMRI. The results discussed within this thesis demonstrate that fMRI can detect approximately the level of the spinal cord in which neuronal activity is greatest and reveal information about the rostral-caudal distribution. The advantage of this technique is

that it is entirely non-invasive. The main disadvantage is that within the sections of the cord there are regions in which there appears to be little or no correspondence between the locations of active pixels and the sites of neuronal activity. The contributions of false positive and false negative signal changes may account for some of these discrepancies.

False positives could result from physiological noise, and certain aspects of the imaging itself. Motion is one of the greatest difficulties in spinal fMRI and comes in several forms: the movement of the spinal cord, the flow of CSF, which is related to the cardiac cycle, and motion due to respiration. In all of the performed experiments presented respiration gating was used during acquisition of the fMRI data. Furthermore, an asymmetric stimulation paradigm was used. Physiological contributions tend to occur rhythmically and therefore will be less likely to appear in the analysed data in which a correlation to the paradigm is performed. The limitations of the imaging technique may also contribute to false positives. In addition, due to limitation in the instrumentation, the data presented are complicated in that there are two contrast mechanisms that contribute to the signal observed by fMRI, BOLD and SEEP. All of the fMRI data were collected with a spin-echo sequence, however, the effective echo time that was employed and high field strength result in a significant contribution from the BOLD effect. As a result, there are contributions to the signal by draining veins, resulting in significant activity appearing in the blood vessels confounding the data. At a lower field strength and with very short echo times contributions from BOLD could be eliminated and the arising signal would be only SEEP (Stroman et al., 2003). The result would be signal restricted to the capillary level and would be more specific to areas of neuronal activity (Stroman et al., 2005b).

The current sensitivity of fMRI may result in false negatives. It is not known what quantity of neuronal activity is required in order to elicit a response observable by fMRI.

Other factors that influence the response observed by fMRI must also be considered. The SEEP contrast mechanism arises from an increase in extravascular water and glial cell swelling (Stroman et al., 2003). Local volume changes in the extracellular space were observed in relation to neuronal activity due to water uptake by glia (Amiry-Moghaddam and Ottersen, 2003; Sykova, 1987; Sykova et al., 2003; Svoboda and Sykova, 1991). Recently the contribution of glial cells to the response observed by fMRI has received more attention (Raichle and Mintun, 2006). As we learn more about the mechanisms that give rise to the signal, we may also discover methods in optimizing the sensitivity of the fMRI.

Challenges in spinal fMRI

Functional MRI was only recently applied to the spinal cord (Malisza and Stroman, 2001; Stroman et al. 1999; Stroman and Ryner, 2001). As a new and emerging technique it has many challenges to overcome including several limitations. This section examines areas of limitation that must be considered and reviews recent advances addressing these issues. An important consideration is that much of the existing work focuses on improvements to human spinal cord imaging. Animal imaging share these limitations and also present additional challenges. Substantial limitations include animal care, instrumental issues at higher field, and imaging a much smaller spinal cord in the rat compared to human.

Spatial resolution

Spatial resolution is a common issue within neuroimaging techniques. In the present animal studies, the smallest voxel size obtainable was 0.2 x. 0.4 x 2.0 mm. Better resolution is always desirable, especially within small animal studies. The lumbar spinal cord segments of the rat are approximately 3 mm wide and 2 mm in the dorsal ventral plane.

Each imaged slice of spinal cord will contain approximately 70 voxels. Given that the gray matter, where neuronal activity related signal changes are expected, is only a small portion of the spinal cord, there are only a few voxels spanning the cord from which to report the presence of activity. Despite these limitations we have obtained moderately consistent results.

The first human spinal fMRI studies used transverse slices, such as employed within this work (Stroman et al. 1999). The main advantage is that any motion would be through the slice. As a result one would hope that voxels containing gray matter would stay within gray matter. The use of transverse slices limits the number of spinal cord segments that can be imaged in one experiment as increasing the number of slices results in longer scanning times. The limitation of only being able to image a small region of the cord is that activity is observed across all slices with the types of stimulation or task that are generally employed during fMRI studies. In order to observe the rostral and caudal borders of an evoked area of activity, several sequential experiments would be required to observe a larger area of the cord. More recently, a method using sagittal slices was developed in human spinal fMRI studies which allows a much larger region of the spinal cord to be imaged simultaneously (Stroman et al. 2005a). Acquisition of sagittal slices was attempted within the rat spinal cord, however, the technique requires extremely thin slices which could not be obtained with the present imaging system. Using the 7 Tesla system the thinnest slice obtainable was 1.8 mm; this is unacceptable for a rat spinal cord that is approximately 3 mm wide at the lumbar enlargement. In this scenario, only 2 slices could be obtained across the spinal cord. Within human studies there are usually 8 sagittal slices obtained across the spinal cord (Stroman et al. 2005a).

Variability

The most common criticism of the spinal cord functional maps obtained is the observed variability in active pixels between scans and between subjects. FMRI is a technique of considerable variability. Some variability is observed in brain fMRI not only between subjects, but between scans within the same subject (Lund et al. 2005; McGonigle et al. 2000; Smith et al. 2005; Thomason et al. 2006). Naturally, the variability is more apparent within a very small area of neural tissue. Therefore, multiple data sets are needed in order to establish areas that are repetitively active. The consistency in activity demonstrated by the overlay maps throughout these studies is very high. Combined activation maps, such as used in parts one and two, were very useful for identifying the active regions of the spinal cord.

Variability in fMRI activity can arise from physiological noise. Throughout the experiments described, noise from respiration was minimized by gating the acquisition to the respiration cycle. Preprocessing can also remove motion by registering the data sets. This was performed in several data sets, however, no corrections were identified by the software presumably since motion was so well restricted in the anaesthetized animals and respiratory gating was employed in the acquisition. Recently it was shown that monitoring the peripheral pulse is helpful in removing motion related to the cardiac cycle in human spinal fMRI studies (Stroman, 2006). Contributions from cardiac motion in rats may be less due to the high frequency of the heart rate. Therefore, motion related to the cardiac cycle in rats may not be identified during preprocessing of the data prior to analysis. The design of the stimulation paradigm is also important in reducing contributions from physiological noise. Physiological motion such as that related to the cardiac and respiratory cycles occur rhythmically. The experiments employed asymmetric periods of rest and stimulation. As a

result during correlation analysis a more characteristic response can be identified, with much less physiological noise superimposed then if acquired using a symmetric paradigm.

Advances in preprocessing and data analysis are greatly needed in spinal fMRI. Within brain fMRI, the use of standard brain spaces such as that described by Talairach (Talairach and Tournoux, 1998) or by the Montreal Neurological Institute (MNI) (Collins et al. 1994) allow normalization of fMRI data sets. Normalization is needed in order to effectively make comparisons between subjects and perform group analyses. A standard space does not exist in the spinal cord. Furthermore, fewer distinctive anatomical landmarks exist in the spinal cord in comparison to the brain. Commonly, a line drawn through the anterior and posterior commissures is used to align brain images. Alignment of spinal cord images within chapters 2 and 3 were performed by manually aligning the edges of the spinal cord and the gray matter where visible. This is described as a rigid body alignment as the size of the cord cannot be adjusted to account for individual differences. Rigid body alignment of the spinal cords is sufficient for studies in which the subject is anaesthetized and therefore motion restricted, such as the animal work presented here. Within human studies where motion is more problematic, better methods are desired. A process in which the cord can be normalized has recently been developed (Stroman and Cahill, 2006). This is a great improvement for group analysis as more detailed adjustments in the position of the spinal cord are possible.

Recommendations

Improvements could be made in order to obtain more reliable results and better image quality. While there has been dramatic improvement in the data obtained over the last five years, better signal to noise may be attainable at higher field strength. Majcher et

al. have obtained excellent results using very short echo times at 9 Tesla to image the rat spinal cord (Majcher et al., 2006a; Majcher et al. 2006b). The parameters for these studies were significantly different from what is possible on the 7T system used here.

The use of longer blocks of rest and stimulation, as well as more repetitions of alternating blocks would allow greater statistical significance in the fMRI analysis. Recently two studies showed that larger data sets allow identification of active areas in rat spinal cord with greater statistical significance (Lilja et al. 2006; Majcher et al. 2006a). Such large data sets also greatly increase the acquisition time.

Future Directions

The results presented open the door to several possibilities for future animal work. In particular, halothane anaesthesia can be used during animal spinal fMRI. This is an extremely important finding as it enables chronic studies. Alpha-chloralose is most commonly used during animal fMRI studies, however, recovery of the animal at the end of the study is not feasible. Not only does a chronic model decrease the numbers of animals required for studies, but it reduces intersubject variability. A chronic model will enable longitudinal studies to be performed. This is extremely valuable in animal models of spinal cord injury and intervention.

This work has implications for human spinal fMRI studies as often interventions must be investigated first within animals. Development of spinal fMRI animal models is not only important for studying spinal cord injury and interventions, but in investigations of neurodegenerative diseases such as multiple sclerosis and in disorders such as chronic pain.

I have used two techniques in order to compare fMRI activity in the spinal cord with neuronal activity. Other methods could also be employed in order to further understand the

relationship between the two and possibly account for some areas in which the two techniques did not correspond. The use of 2-deoxyglucose labelling can identify areas of increased glucose utilization and confirm areas of neuronal activity. A comparison with spinal fMRI would be interesting and could be used to confirm the findings that were presented in the previous chapters.

Concluding Remarks

Functional MRI was employed for assessment of spinal cord function only within the last few years. Several advances were presented here. In Chapter 2, a chronic model for animal spinal fMRI was described. In Chapter 3, responses to noxious and innocuous heat stimulation were observed by spinal fMRI and could be differentiated based on the percentage signal change. In both chapters the use of c-fos confirmed the presence of neuronal activity within the imaged region of the spinal cord. In Chapter 4, a comparison with local field potentials demonstrates that fMRI may be used to observe the rostral-caudal distribution of neuronal activity. To date, no other groups have investigated the patterns of neuronal activity that lead to the hemodynamic response observed by fMRI in the spinal cord. The spatial distribution of active pixels and negative local field potentials revealed overlap in some areas, however, there was either no or limited correlation in others.

The final results presented here suggest that some information regarding spinal cord function can be obtained using fMRI. The detail of that information is limited by the sensitivity and specificity of the technique. The comparison made between spinal fMRI and electrophysiology suggest that at this point, with the methods used, the technique cannot obtain detailed information within the cross-sections of the spinal cord that detect all areas of neuronal activity using only a few activity maps. Further analysis is needed regarding the

laterality of the distribution of activity. Additional information can be obtained by comparing other aspects of fMRI, such as the percentage signal change, to the electrophysiology. Further investigation is also needed to evaluate the different physiological contributions to the response observed by spinal fMRI. The maps presented here show areas of signal change that extend beyond the areas of neuronal activity. The identification of signals arising from larger blood vessels as well as from physiological noise would aid in our understanding of the impact of contributions from sources other than neuronal activity have on the fMRI response observed in the spinal cord. As a result this would also eliminate some of the variability that is currently observed.

Spinal fMRI is a young technique and there is much work to be done to improve the methods in imaging, analysis, and assessment. The techniques used in human spinal fMRI have advanced much more rapidly than in the rat in the last few years. Further technical work is needed to apply the imaging strategies to animal spinal fMRI as these advances may improve the detail of information that can be gained. A logical extension of the work presented in this thesis would be to investigate the response observed by spinal fMRI in the same animal, in the same physiological state as during electrophysiological measurements and ideally, recordings would be taken simultaneously during imaging.

In conclusion, we have shown that the responses observed by spinal fMRI are influenced by neuronal activity, however, other factors also affect the signal and require further investigation to establish more reliable maps of activity. The application of fMRI to the spinal cord has rapidly advanced since it was first implemented. Spinal fMRI is a promising tool for the non-invasive assessment of spinal cord function.

REFERENCES

Amiry-Moghaddam,M.,.Ottersen,O.P., 2003. The molecular basis of water transport in the brain. Nat.Rev.Neurosci. 4, 991 - 1001.

Attwell, D., Iadecola, C., 2002. The neural basis of functional brain imaging signals. Trends in Neurosci. 25, 621 – 625.

Austin,V.C., Blamire,A.M., Allers,K.A., Sharp,T., Styles,P., Matthews,P.M., Sibson,N.R., 2005. Confounding effects of anesthesia on functional activation in rodent brain: a study of halothane and alpha-chloralose anesthesia. Neuroimage. 24, 92 - 100.

Baker,M.L.,.Giesler,G.J., Jr., 1984. Anatomical studies of the spinocervical tract of the rat. Somatosens.Res. 2, 1 - 18.

Baumgartner R, Windischberger C, Moser E. Quantification in functional magnetic resonance imaging: fuzzy clustering vs. correlation analysis. Magn Reson. Imaging 1998;16:115-125.

Brooks, J., Robson, M., Schweinhardt, P., Wise, R., and Tracey, I., 2004. Functional magnetic resonance imaging (fMRI) of the spinal cord: a methodological study. American Pain Society 23rd Annual Meeting. 667.

Brown, A.G., Brown P.B., Fyffe, R.E.W., Pubols, L., 1983. Effects of dorsal root section on spinocervical tract neurones in the cat. J. Physiol. 337, 589 – 608.

Bullitt,E.,1991. Somatotopy of spinal nociceptive processing. J.Comp Neurol. 312, 279 - 290.

Buzsaki,G.,1931. Theta oscillations in the hippocampus. Neuron. 33, 325 - 40.

Buzsaki,G.,.Gage,F.H.,1988. Mechanisms of action of neural grafts in the limbic system. Can.J.Neurol.Sci. 15, 99 - 105.

Chaouch,A., Menetrey,D., Binder,D., Besson,J.M.,1983. Neurons at the origin of the medial component of the bulbopontine spinoreticular tract in the rat: an anatomical study using horseradish peroxidase retrograde transport. J.Comp Neurol. 214, 309 - 320.

Chiasson,B.J., Hong,M.G., Robertson,H.A.,1997. Putative roles for the inducible transcription factor c-fos in the central nervous system: studies with antisense oligonucleotides. Neurochem.Int. 31, 459 - 475.

Christensen,B.N.,.Perl,E.R.,1970. Spinal neurons specifically excited by noxious or thermal stimuli: marginal zone of the dorsal horn. J.Neurophysiol. 33, 293 - 307.

Coghill,R.C., Price,D.D., Hayes,R.L., Mayer,D.J.,1991. Spatial distribution of nociceptive processing in the rat spinal cord. J.Neurophysiol. 65, 133 - 140.

Collins,D.L., Neelin,P., Peters,T.M., Evans,A.C., 1994. Automatic 3D intersubject registration of MR volumetric data in standardized Talairach space. J.Comput.Assist.Tomogr. 18, 192 - 205.

Collins,J.G., Kendig,J.J., Mason,P.,1995. Anesthetic actions within the spinal cord: contributions to the state of general anesthesia. Trends Neurosci. 18, 549 - 553.

Craig,A.D.,.Kniffki,K.D.,1985. Spinothalamic lumbosacral lamina I cells responsive to skin and muscle stimulation in the cat. J.Physiol. 365, 197 - 221.

Curran,T.,.Teich,N.M.,1982. Identification of a 39,000-dalton protein in cells transformed by the FBJ murine osteosarcoma virus. Virology. 116, 221 - 235.

Dai,Y., Iwata,K., Kondo,E., Morimoto,T., Noguchi,K.,2001. A selective increase in Fos expression in spinal dorsal horn neurons following graded thermal stimulation in rats with experimental mononeuropathy. Pain. 90, 287 - 296.

De Jong,R.H., Robles,R., Corbin,R.W., Nace,R.A.,1968. Effect of inhalation anesthetics on monosynaptic and plysynpatic transmission in the spinal cord. J.Pharmacol.Exp.Ther. 162, 326 - 330.

Dragunow,M.,.Faull,R.,1989. The use of c-fos as a metabolic marker in neuronal pathway tracing. J.Neurosci.Methods. 29, 261 - 265.

Dudley,R.E., Nelson,S.R., Samson,F.,1982. Influence of chloralose on brain regional glucose utilization. Brain Res. 233, 173 - 180.

Edgley, S.A., Jankowska, E., 1987. Field potentials generated by group II muscle afferents in the middle lumbar segments of the spinal cord. J Physiol. (London) 385: 393-413.

Evers,A.S.,.Crowder,C.M.,2001. General Anesthetics. 10, 340.

Fields,H.L., Clanton,C.H., Anderson,S.D.,1977. Somatosensory properties of spinoreticular neurons in the cat. Brain Res. 120, 49 - 66.

Fitzgerald, M. Alterations in the ipsi- and contralateral afferent inputs of dorsal horn cells produced by capsaicin treatment of one sciatic nerve in the rat. Brain Res. 248, 97 - 107.

Fromm,G.H.,.Bond,H.W.,1967. The relationship between neuron activity and cortical steady potentials. Electroencephalogr.Clin.Neurophysiol. 22, 159 - 166.

Fujita,H., Meyer,E., Reutens,D.C., Kuwabara,H., Evans,A.C., Gjedde,A.,1997. Cerebral [15O] water clearance in humans determined by positron emission tomography: II. Vascular responses to vibrotactile stimulation. J.Cereb.Blood Flow Metab. 17, 73 - 79.

Giesler,G.J., Jr., Yezierski,R.P., Gerhart,K.D., Willis,W.D.,1981. Spinothalamic tract neurons that project to medial and/or lateral thalamic nuclei: evidence for a physiologically novel population of spinal cord neurons. J.Neurophysiol. 46, 1285 - 1308.

Giovannelli,L., Casamenti,F., Pepeu,G.,1998. C-fos expression in the rat nucleus basalis upon excitotoxic lesion with quisqualic acid: a study in adult and aged animals. J.Neural Transm. 105, 935 - 948.

Goehler,L.E., Gaykema,R.P., Hammack,S.E., Maier,S.F., Watkins,L.R.,1998. Interleukin-1 induces c-Fos immunoreactivity in primary afferent neurons of the vagus nerve. Brain Res. 804, 306 - 310.

Grasshoff,C., Rudolph,U., Antkowiak,B.,2005. Molecular and systemic mechanisms of general anaesthesia: the 'multi-site and multiple mechanisms' concept. Curr.Opin.Anaesthesiol. 18, 386 - 391.

Hebel R and Stromberg, 1986. Nervous System. BioMed Verlag Worthsee, Gunzburg, Germany, 125.

Henry-Feugeas,M.C., Idy-Peretti,I., Blanchet,B., Hassine,D., Zannoli,G., Schouman-Claeys,E.,1993. Temporal and spatial assessment of normal cerebrospinal fluid dynamics with MR imaging. Magn Reson.Imaging. 11, 1107 - 1118.

Herdegen,T.,.Leah,J.D.,1998. Inducible and constitutive transcription factors in the mammalian nervous system: control of gene expression by Jun, Fos and Krox, and CREB/ATF proteins. Brain Res.Brain Res.Rev. 28, 370 - 490.

Hunt,S.P., Pini,A., Evan,G.,1987. Induction of c-fos-like protein in spinal cord neurons following sensory stimulation. Nature. 328, 632 - 634.

Hyder,F., Rothman,D.L., Shulman,R.G.,2002. Total neuroenergetics support localized brain activity: implications for the interpretation of fMRI. Proc.Natl.Acad.Sci.U.S.A. 99, 10771 - 10776.

Iadecola, C., 1997. Local and propagated vascular responses evoked by focal synaptic activity in cerebellar cortex. J Neurophys. 78, 651 – 659.

Inada,K., Okada,S., Phuchareon,J., Hatano,M., Sugimoto,T., Moriya,H., Tokuhisa,T.,1998. c-Fos induces apoptosis in germinal center B cells. J.Immunol. 161, 3853 - 3861.

Jennings,E.,.Fitzgerald,M.,1996. C-fos can be induced in the neonatal rat spinal cord by both noxious and innocuous peripheral stimulation. Pain. 68, 301 - 306.

Jezzard, P., Matthews, P. M., and Smith, S. M., 2001. Functional MRI: An Introduction to Methods. Oxford University Press, Oxford, 70, 80, 84, 86.

Jinks,S.L., Antognini,J.F., Martin,J.T., Jung,S., Carstens,E., Atherley,R.,2002. Isoflurane, but not halothane, depresses c-fos expression in rat spinal cord at concentrations that suppress reflex movement after supramaximal noxious stimulation. Anesth.Analg. 95, 1622 – 1628.

Kamondi,A., Acsady,L., Buzsaki,G.,1998. Dendritic spikes are enhanced by cooperative network activity in the intact hippocampus. J.Neurosci. 18, 3919 - 3928.

Kandel, E. R., Schwartz, J. H., and Jessell, T. M., 2000. Principles of Neural Science. McGraw-Hill, New York, 477, 715.

King,V.M.,.Apps,R.,2000. Somatotopical organization of fos-like immunoreactivity in rat cervical spinal cord following noxious stimulation of the forelimb. Neuroscience. 101, 179 - 188.

Kobayashi,M., Inoue,T., Matsuo,R., Masuda,Y., Hidaka,O., Kang,Y., Morimoto,T.,1997. Role of calcium conductances on spike afterpotentials in rat trigeminal motoneurons. J.Neurophysiol. 77, 3273 - 3283.

Kollias, S. S., Kwiecinkcki, S., and Summers, P., 2004. Functional MR Imaging of the human cervical spinal cord. American Society of Neuroradiology, Proceedings of the 42nd Annual Meeting. 227.

Kornelsen,J.,.Stroman,P.W.,2004. fMRI of the lumbar spinal cord during a lower limb motor task. Magn Reson.Med. 52, 411 - 414.

Lauterbur,P.C.,1973. Image formation by induced local interactions: examples employing nuclear magnetic resonance. Nature. 242, 190 - 191.

Lawrence,J., Stroman,P.W., Bascaramurty,S., Jordan,L.M., Malisza,K.L.,2004. Correlation of functional activation in the rat spinal cord with neuronal activation detected by immunohistochemistry. Neuroimage. 22, 1802 - 1807.

Lawrence,J., Stroman,P.W., Gruwel,M.L., Bascaramurty,S., Turner,A., Malisza K.L.,2004b. Comparing fMRI of the rat spinal cord in the alpha-chloralose and halothane anesthetized rat during electrical forepaw stimulation. Proceedings of the International Society for Magnetic Resonance in Medicine Twelveth Scientific Meeting and Exhibition. 1117.

Lawrence, J., Stroman, P. W., and Kollias, S., 2005. Functional MRI of the human cervical and lumbar spinal cord during vibration stimulation of different dermatomes. Organization for Human Brain Mapping, 11th Annual Meeting. 1399.

Li,G., Ng,M.C., Wong,K.K., Luk,K.D., Yang,E.S.,2005. Spinal effects of acupuncture stimulation assessed by proton density-weighted functional magnetic resonance imaging at 0.2 T. Magn Reson.Imaging. 23, 995 - 999.

Light,A.R.,.Perl,E.R.,1979. Spinal termination of functionally identified primary afferent neurons with slowly conducting myelinated fibers. J.Comp Neurol. 186, 133 - 150.

Lilja,J., Endo,T., Hofstetter,C., Westman,E., Young,J., Olson,L., Spenger,C.,2006. Blood oxygenation level-dependent visualization of synaptic relay stations of sensory pathways along the neuroaxis in response to graded sensory stimulation of a limb. J.Neurosci. 26, 6330 - 6336.

Liu,R.P.,1983. Laminar origins of spinal projection neurons to the periaqueductal gray of the rat. Brain Res. 264, 118 - 122.

Logothetis,N.K., Pauls,J., Augath,M., Trinath,T., Oeltermann,A.,2001. Neurophysiological investigation of the basis of the fMRI signal. Nature. 412, 150 - 157.

Logothetis,N.K.,.Pfeuffer,J.,2004. On the nature of the BOLD fMRI contrast mechanism. Magn Reson Imaging. 22, 1517 - 1531.

Logothetis, N.K., Wandell, B.A., 2004. Intrepreting the BOLD signal. Annu. Rev. Physiol. 66, 735 – 769.

Lund,T.E., Norgaard,M.D., Rostrup,E., Rowe,J.B., Paulson,O.B.,2005. Motion or activity: their role in intra- and inter-subject variation in fMRI. Neuroimage. 26, 960 - 964.

Majcher, K., Tomanek, B., Jasinski, A., Foniok, T., Kirk, D., Rushforth, D., Tuor, U. I., and Hess, G., 2006b. Functional Magnetic Resonance Imaging of the rat spinal cord after peripheral nerve injury. Proceedings of the International Society of Magnetic Resonance in Medicine 14th annual meeting. 2126.

Majcher,K., Tomanek,B., Jasinski,A., Foniok,T., Stroman,P.W., Tuor,U.I., Kirk,D., Hess,G.,2006a. Simultaneous functional magnetic resonance imaging in the rat spinal cord and brain. Exp.Neurol. 197, 458 - 464.

Malisza K.L.,.Stroman,P.,2002. Functional imaging of the rat cervical spinal cord. J Magn Reson Imag. 16, 553 - 558.

Malisza, K. L. and Stroman, P. W., 2001. Spinal fMRI of the rat cervical spinal cord.

Malisza,K.L., Stroman,P.W., Turner,A., Gregorash,L., Foniok,T., Wright,A.,2003. Functional MRI of the rat lumbar spinal cord involving painful stimulation and the effect of peripheral joint mobilization. J.Magn Reson.Imaging. 18, 152 - 159.

Malonek, D., Grinvald, A., 1996. Interactions between electrical activity and cortical microcirculation revealed by imaging spectroscopy: implications for functional brain mapping. Science. 272,551 – 554.

McGonigle,D.J., Howseman,A.M., Athwal,B.S., Friston,K.J., Frackowiak,R.S., Holmes,A.P.,2000. Variability in fMRI: an examination of intersession differences. Neuroimage. 11, 708 - 734.

Menetrey,D., Chaouch,A., Besson,J.M.,1979. Responses of spinal cord dorsal horn neurones to non-noxious and noxious cutaneous temperature changes in the spinal rat. Pain. 6, 265 - 282.

Menetrey,D., de,P.J., Besson,J.M.,1984. Electrophysiological characteristics of lumbar spinal cord neurons backfired from lateral reticular nucleus in the rat. J.Neurophysiol. 52, 595 - 611.

Menetrey,D., Gannon,A., Levine,J.D., Basbaum,A.I.,1989. Expression of c-fos protein in interneurons and projection neurons of the rat spinal cord in response to noxious somatic, articular, and visceral stimulation. J.Comp Neurol. 285, 177 - 195.

Molander, C. and Grant, G., 1995. Spinal Cord Cytoarchitecture. In: Paxinos, G. (Eds.), The Rat Nervous System. Academic Press, San Diego, 39.

Nahin,R.L.,.Micevych,P.E.,1986. A long ascending pathway of enkephalin-like immunoreactive spinoreticular neurons in the rat. Neurosci.Lett. 65, 271 - 276.

Nair, D.G., 2005. About being BOLD. Brain Res Rev. 50, 229 – 243.

Namiki,A., Collins,J.G., Kitahata,L.M., Kikuchi,H., Homma,E., Thalhammer,J.G.,1980. Effects of halothane on spinal neuronal responses to graded noxious heat stimulation in the cat. Anesthesiology. 53, 475 - 480.

Ng,M.C., Wong,K.K., Li,G., Lai,S., Yang,E.S., Hu,Y., Luk,K.D.,2006. Proton-density-weighted spinal fMRI with sensorimotor stimulation at 0.2 T. Neuroimage. 29, 995 - 999.

Nicoll,R.A.,.Madison,D.V.,1982. General anesthetics hyperpolarize neurons in the vertebrate central nervous system. Science. 217, 1055 - 1057.

Noga, B.R., Fortier, P.A., Kriellaars, D.J., Dai X., Detillieux, G.R., Jordan, L.M., 1995. Field potential mapping of neurons in the lumbar spinal cord activated following stimulation of the mesencephalic locomotor region. J. Neurosci. 15, 2203-2217.

Ogawa,S., Lee,T.M., Nayak,A.S., Glynn,P.,1990. Oxygenation-sensitive contrast in magnetic resonance image of rodent brain at high magnetic fields. Magn Reson.Med. 14, 68 - 78.

Ogawa,S., Tank,D.W., Menon,R., Ellermann,J.M., Kim,S.G., Merkle,H., Ugurbil,K.,1992. Intrinsic signal changes accompanying sensory stimulation: functional brain mapping with magnetic resonance imaging. Proc.Natl.Acad.Sci.U.S.A. 89, 5951 - 5955.

Ohta,S., Meyer,E., Fujita,H., Reutens,D.C., Evans,A., Gjedde,A.,1996. Cerebral [15O]water clearance in humans determined by PET: I. Theory and normal values. J.Cereb.Blood Flow Metab. 16, 765 - 780.

Pauling,L.,.Coryell,C.D.,1936. The Magnetic Properties and Structure of Hemoglobin, Oxyhemoglobin and Carbonmonoxyhemoglobin. Proc.Natl.Acad.Sci.U.S.A. 22, 210 - 216.

Raichle, M.E., Mintun, M.A., 2006. Brain work and brain imaging. Annu Rev Neurosci. 29, 449-476.

Ramsey,N.F., Kirkby,B.S., van,G.P., Berman,K.F., Duyn,J.H., Frank,J.A., Mattay,V.S., Van Horn,J.D., Esposito,G., Moonen,C.T., Weinberger,D.R.,1996. Functional mapping of human sensorimotor cortex with 3D BOLD fMRI correlates highly with H2(15)O PET rCBF. J.Cereb.Blood Flow Metab. 16, 755 - 764.

Rexed,B.,1952. The cytoarchitectonic organization of the spinal cord in the cat. J.Comp Neurol. 96, 414 - 495.

Rexed,B.,1954. A cytoarchitectonic atlas of the spinal cord in the cat. J.Comp Neurol. 100, 297 - 379.

Rick Hansen Foundation, 2004. Obtained from www.rickhansen.com/Foundation/foundation_scilinks.htm on June 17, 2006.

Schaible, H.G., Schmidt, R.F., Willis, W.D., 1986. Responses of spinal cord neruones to stimulation of articular afferent fibres in the cat. J Physiol. 372, 575 - 593.

Scremin, O. U, 1995. Cerebral Vascular System. In: Paxinos, G. (Eds.), The Rat Nervous System. Academic Press, San Diego, 28.

Shapiro,H.M., Greenberg,J.H., Reivich,M., Ashmead,G., Sokoloff,L.,1978. Local cerebral glucose uptake in awake and halothane-anesthetized primates. Anesthesiology. 48, 97 - 103.

Sheng,H.Z., Fields,R.D., Nelson,P.G.,1993. Specific regulation of immediate early genes by patterned neuronal activity. J.Neurosci.Res. 35, 459 - 467.

Sherrington, C.S. 1906. Integrative Actions of the Nervous System. Yale University Press. New Haven, CT.

Smith,S.M., Beckmann,C.F., Ramnani,N., Woolrich,M.W., Bannister,P.R., Jenkinson,M., Matthews,P.M., McGonigle,D.J.,2005. Variability in fMRI: a re-examination of inter-session differences. Hum.Brain Mapp. 24, 248 - 257.

Stroman,P.W.,2005. Magnetic resonance imaging of neuronal function in the spinal cord: spinal FMRI. Clin.Med.Res. 3, 146 - 156.

Stroman, P. W., 2006. Improved sensitivity of spinal fMRI by using physiological recordings in general linear model analysis. Proceedings of the International Society of Magnetic Resonance in Medicine 14th annual meeting. 2828.

Stroman, P. W. and Cahill, C. M., 2006. Functional Magnetic Resonance Imaging of the human spinal cord and brainstem during heat stimulation. Proceedings of the International Society of Magnetic Resonance in Medicine 14th annual meeting. 1144.

Stroman,P.W., Kornelsen,J., Bergman,A., Krause,V., Ethans,K., Malisza,K.L., Tomanek,B.,2004. Noninvasive assessment of the injured human spinal cord by means of functional magnetic resonance imaging. Spinal Cord. 42, 59 - 66.

Stroman,P.W., Kornelsen,J., Lawrence,J.,2005a. An improved method for spinal functional MRI with large volume coverage of the spinal cord. J.Magn Reson.Imaging. 21, 520 - 526.

Stroman,P.W., Kornelsen,J., Lawrence,J., Malisza, K.L. 2005b. Functional magnetic resonance imaging based on SEEP contrast: response function specificity. Magn Reson Imaging. 23, 843-50.

Stroman, P. W. and Krause, V., 2000. Spinal fMRI of the Human Cervical Spinal Cord with Stimulation of Different Sensory Dermatomes.

Stroman,P.W., Krause,V., Malisza,K.L., Frankenstein,U.N., Tomanek,B.,2002. Functional magnetic resonance imaging of the human cervical spinal cord with stimulation of different sensory dermatomes. Magn Reson.Imaging. 20, 1 - 6.

Stroman,P.W., Malisza,K.L., Onu,M.,2003. Functional magnetic resonance imaging at 0.2 Tesla. Neuroimage. 20, 1210 - 1214.

Stroman,P.W., Nance,P.W., Ryner,L.N.,1999. BOLD MRI of the human cervical spinal cord at 3 tesla. Magn Reson.Med. 42, 571 - 576.

Stroman,P.W.,.Ryner,L.N.,2001. Functional MRI of motor and sensory activation in the human spinal cord. Magn Reson.Imaging. 19, 27 - 32.

Stroman,P.W., Tomanek,B., Krause,V., Frankenstein,U.N., Malisza,K.L.,2002b. Mapping of neuronal function in the healthy and injured human spinal cord with spinal fMRI. Neuroimage. 17, 1854 - 1860.

Sugiura,Y., Lee,C.L., Perl,E.R.,1986. Central projections of identified, unmyelinated (C) afferent fibers innervating mammalian skin. Science. 234, 358 - 361.

Svoboda, J. and Sykova, E., 1991. Extracellular space volume changes in the rat spinal cord produced by nerve stimulation and peripheral injury. Brain Res. 560, 216-224.

Sykova, E. 1987. Modulation of spinal cord transmission by changes in extracellular K+ activity and extracellular volume. Can.J.Physiol Pharmacol. 65, 1058-1066.

Sykova, E., Vargova, L., Kubinova, S., Jendelova, P., and Chvatal, A, 2003. The relationship between changes in intrinsic optical signals and cell swelling in rat spinal cord slices. Neuroimage. 18, 214-230.

Talairach, J. and Tournoux, P., 1998. Co-planar sterotaxic atlas of the human brain. Thieme Medical Publishers, Stuttgart.

Takahashi,Y.,.Nakajima,Y.,1996. Dermatomes in the rat limbs as determined by antidromic stimulation of sensory C-fibers in spinal nerves. Pain. 67, 197 - 202.

Thomason,M.E., Foland,L.C., Glover,G.H.,2006. Calibration of BOLD fMRI using breath holding reduces group variance during a cognitive task. Hum.Brain Mapp. May 2 [Epub ahead of print],

Thulborn,K.R., Waterton,J.C., Matthews,P.M., Radda,G.K.,1982. Oxygenation dependence of the transverse relaxation time of water protons in whole blood at high field. Biochim.Biophys.Acta. 714, 265 - 270.

Ueki,M., Mies,G., Hossmann,K.A.,1992. Effect of alpha-chloralose, halothane, pentobarbital and nitrous oxide anesthesia on metabolic coupling in somatosensory cortex of rat. Acta Anaesthesiol.Scand. 36, 318 - 322.

Willis, W. D. and Coggeshall, R. E., 2004. Sensory mechanisms of the spinal cord: Ascending sensory tracts and their descending control. 3rd ed. Kluwer Academic/Plenum Publishers, New York, 735, 833.

Willis, W. D., Westlund, K. N., and Carlton, S. M., 1995. Pain. In: Paxinos, G. (Eds.), The Rat Nervous System. Academic Press, San Diego, 732-735.

APPENDIX A

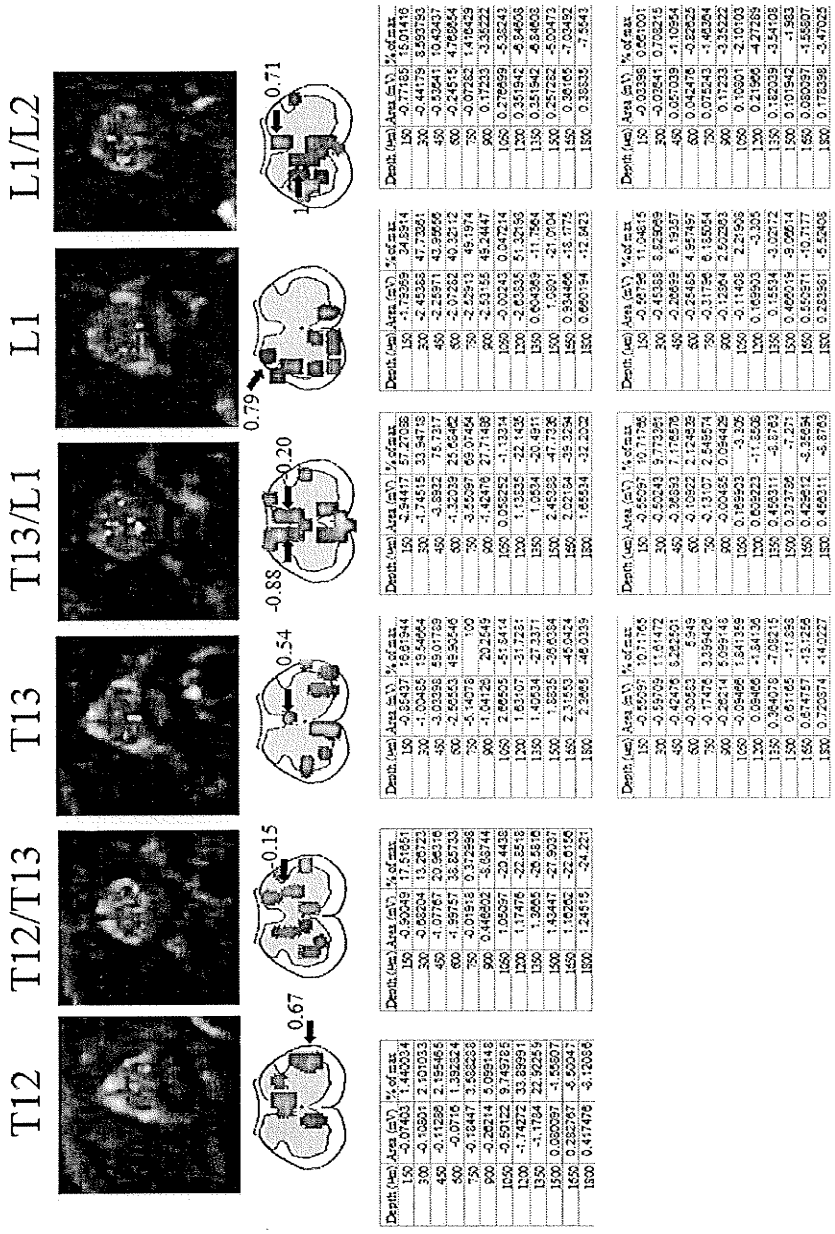

Figure 1. FMRI and electrophysiology from Animal 1. All active pixels from 3 fMRI experiments were overlaid onto one map. Labels indicated the vertebral level of the slice. The images are oriented with dorsal up, ventral down, left side of the animal is on the left side of the image, and the right side of the animal is on the right side of the image. The top row of tables are measurements taken on the right side of the spinal cord. The bottom row of tables are measurements taken on the left side of the spinal cord.

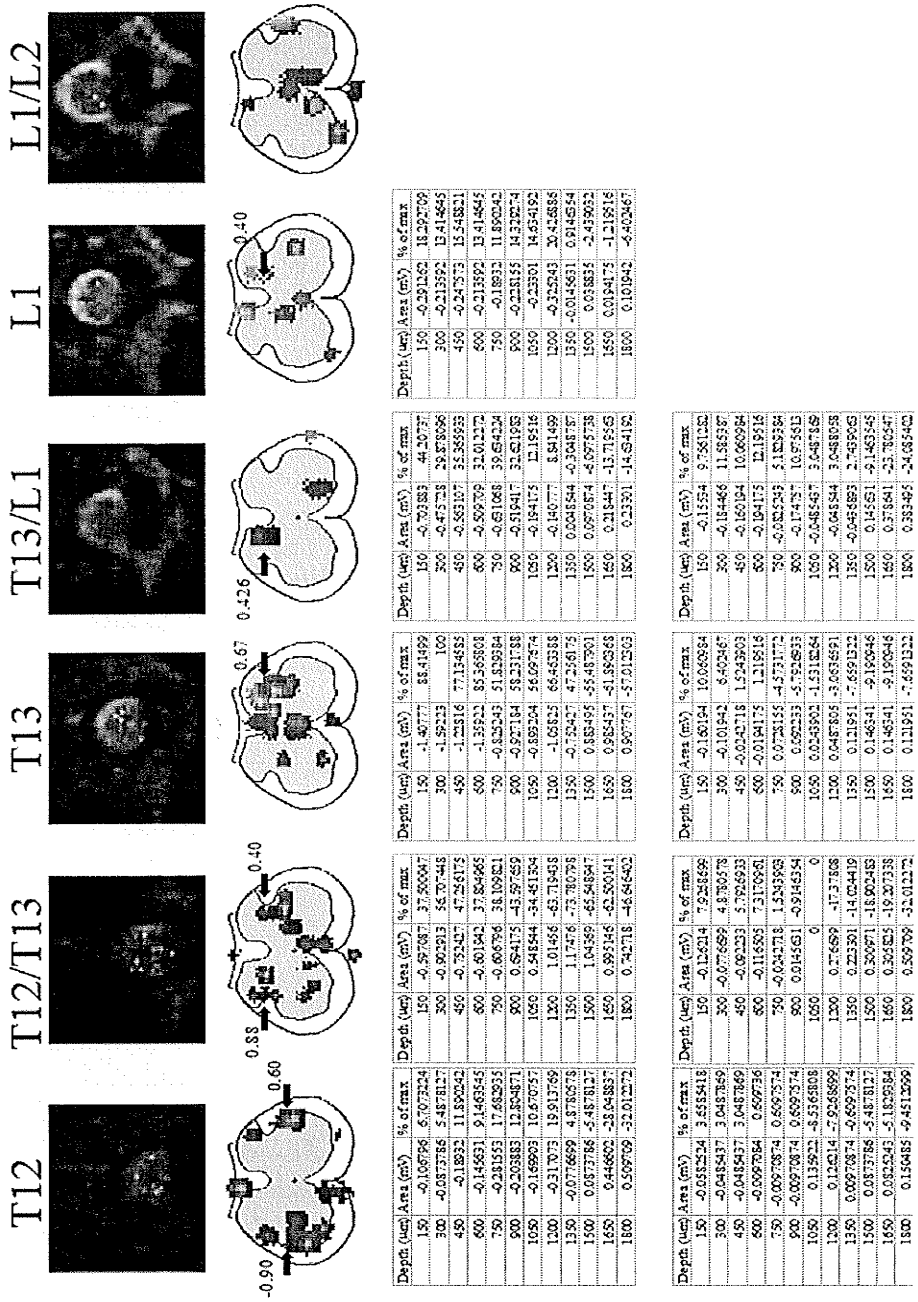

Figure 2. FMRI and electrophysiology from Animal 2. All active pixels from 3 fMRI experiments were overlaid onto one map. Labels indicated the vertebral level of the slice. The images are oriented with dorsal up, ventral down, left side of the animal is on the left side of the image, and the right side of the animal is on the right side of the image. The top row of tables are measurements taken on the right side of the spinal cord. The bottom row of tables are measurements taken on the left side of the spinal cord.

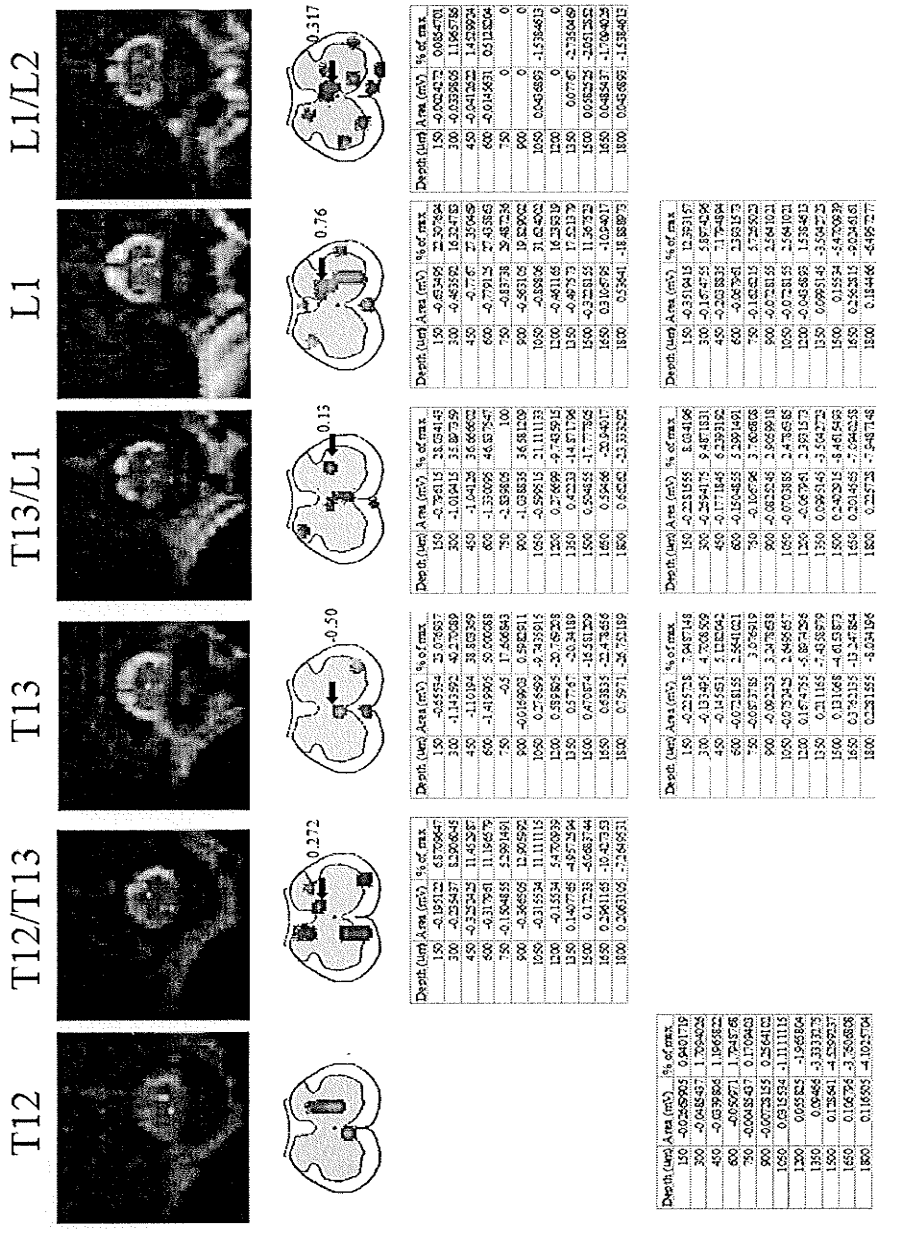

Figure 3. FMRI and electrophysiology from Animal 3. All active pixels from 3 fMRI experiments were overlaid onto one map. Labels indicated the vertebral level of the slice. The images are oriented with dorsal up, ventral down, left side of the animal is on the left side of the image, and the right side of the animal is on the right side of the image. The top row of tables are measurements taken on the right side of the spinal cord. The bottom row of tables are measurements taken on the left side of the spinal cord.

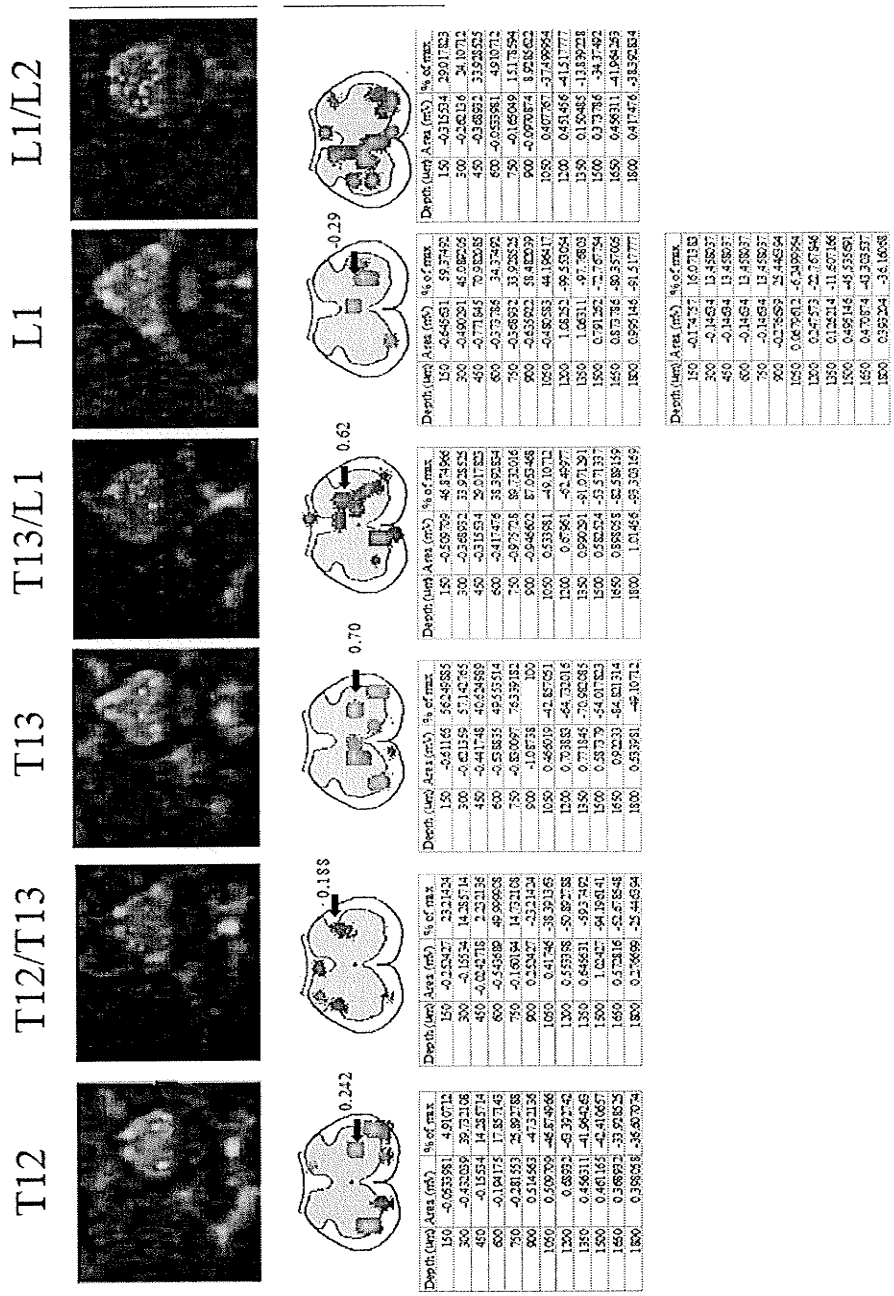

Figure 4. FMRI and electrophysiology from Animal 4. All active pixels from 3 fMRI experiments were overlaid onto one map. Labels indicated the vertebral level of the slice. The images are oriented with dorsal up, ventral down, left side of the animal is on the left side of the image, and the right side of the animal is on the right side of the image. The top row of tables are measurements taken on the right side of the spinal cord. The bottom row of tables are measurements taken on the left side of the spinal cord.

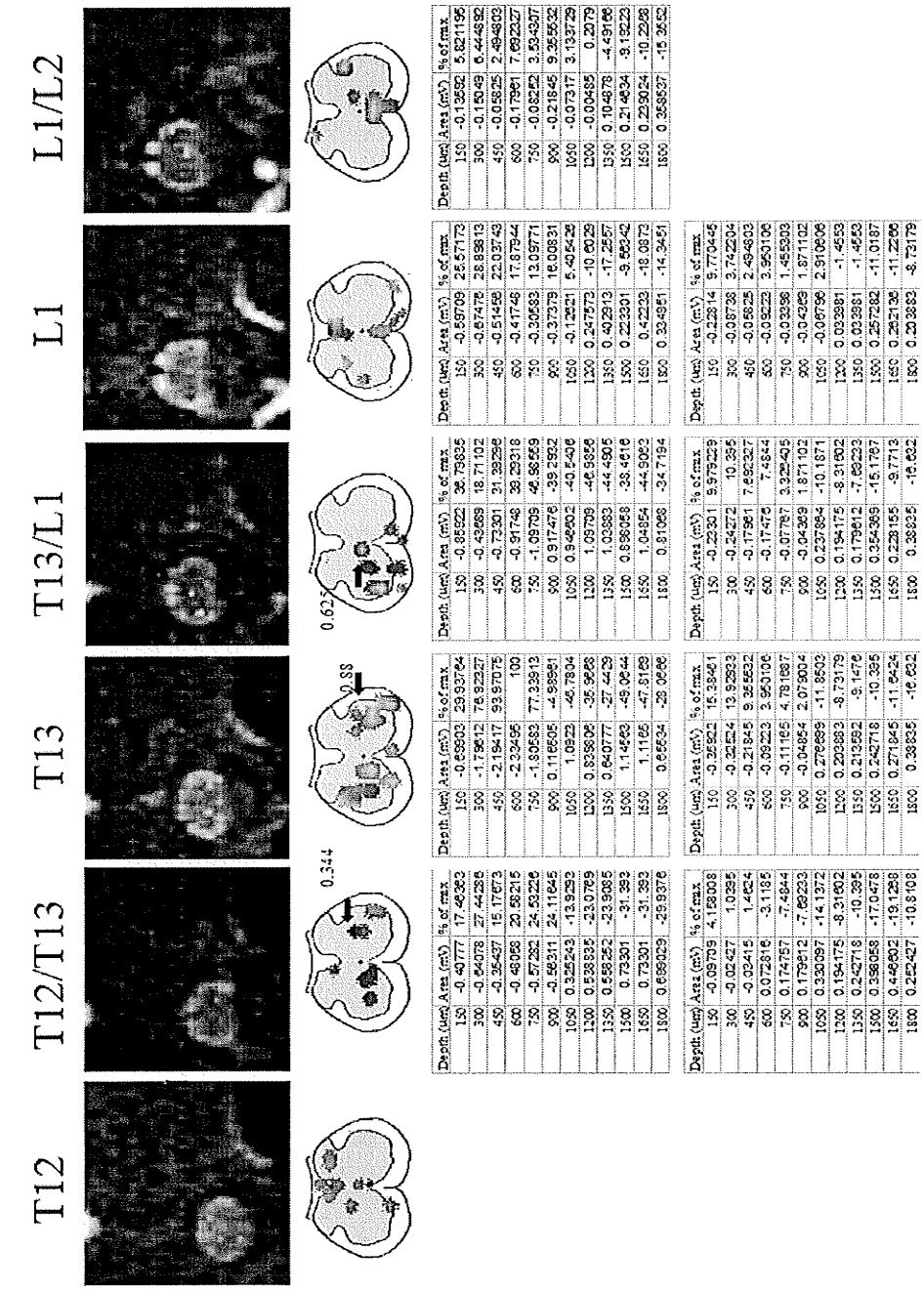

Figure 5. FMRI and electrophysiology from Animal 5. All active pixels from 3 fMRI experiments were overlaid onto one map. Labels indicated the vertebral level of the slice. The images are oriented with dorsal up, ventral down, left side of the animal is on the left side of the image, and the right side of the animal is on the right side of the image. The top row of tables are measurements taken on the right side of the spinal cord. The bottom row of tables are measurements taken on the left side of the spinal cord.

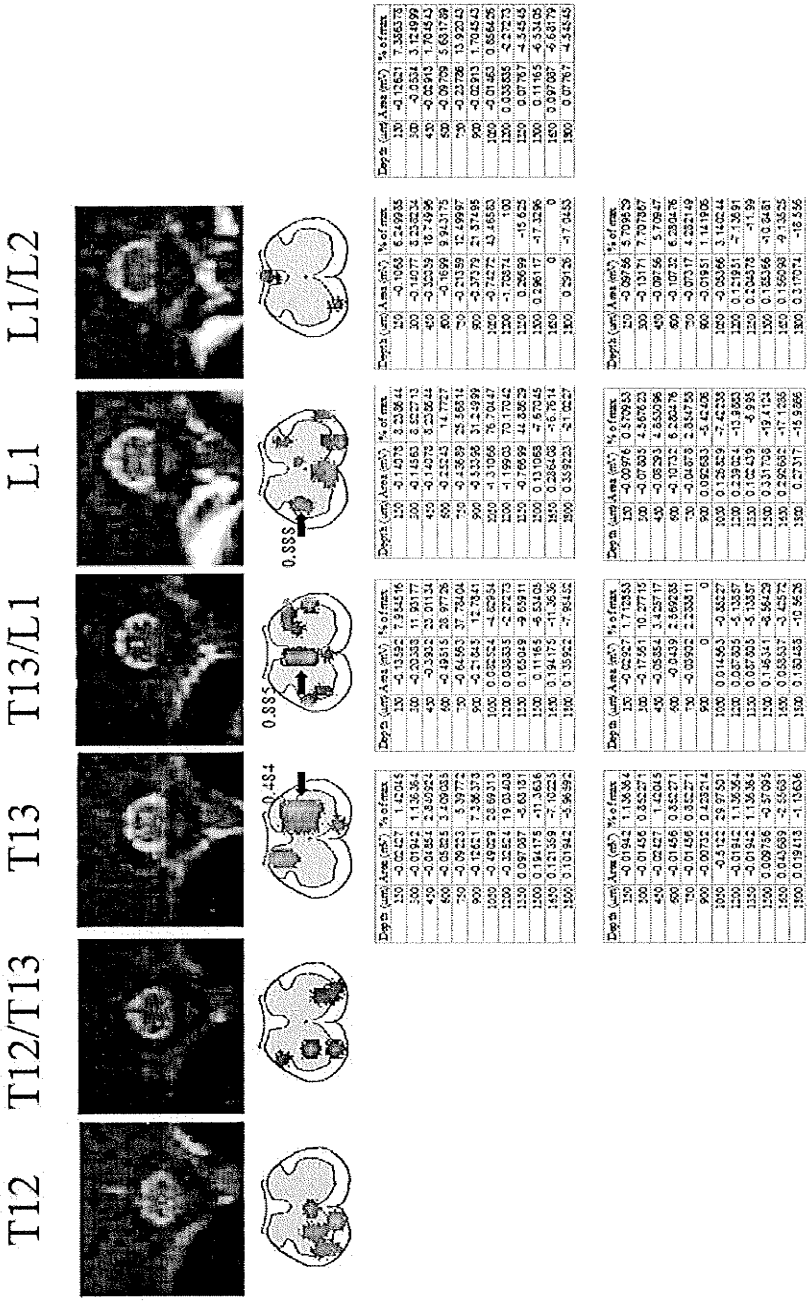

Figure 6. FMRI and electrophysiology from Animal 6. All active pixels from 3 fMRI experiments were overlaid onto one map. Labels indicated the vertebral level of the slice. The images are oriented with dorsal up, ventral down, left side of the animal is on the left side of the image, and the right side of the animal is on the right side of the image. The top row of tables are measurements taken on the right side of the spinal cord. The bottom row of tables are measurements taken on the left side of the spinal cord.

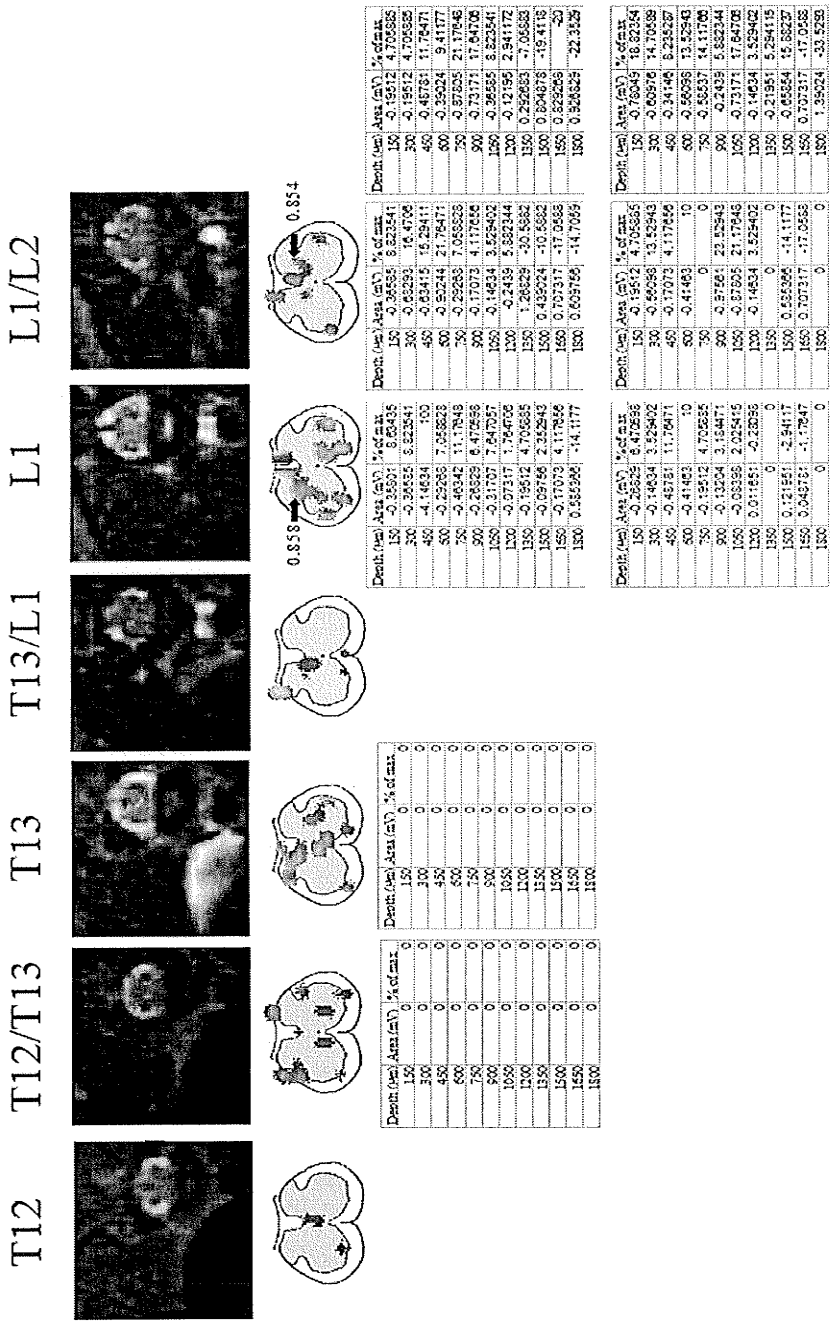

Figure 7. FMRI and electrophysiology from Animal 7. All active pixels from 3 fMRI experiments were overlaid onto one map. Labels indicated the vertebral level of the slice. The images are oriented with dorsal up, ventral down, left side of the animal is on the left side of the image, and the right side of the animal is on the right side of the image. The top row of tables are measurements taken on the right side of the spinal cord. The bottom row of tables are measurements taken on the left side of the spinal cord.

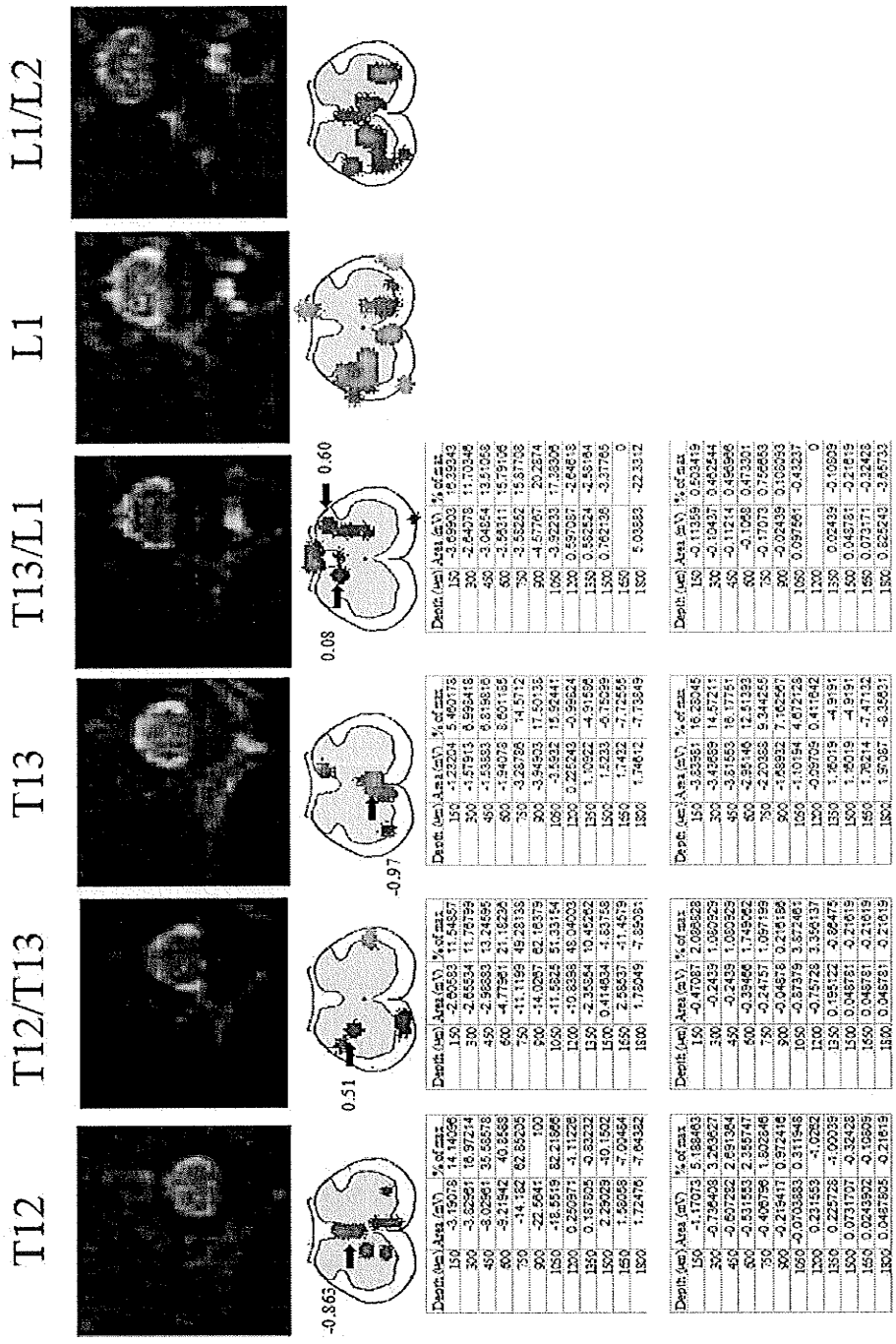

Figure 8. FMRI and electrophysiology from Animal 8. All active pixels from 3 fMRI experiments were overlaid onto one map. Labels indicated the vertebral level of the slice. The images are oriented with dorsal up, ventral down, left side of the animal is on the left side of the image, and the right side of the animal is on the right side of the image. The top row of tables are measurements taken on the right side of the spinal cord. The bottom row of tables are measurements taken on the left side of the spinal cord.

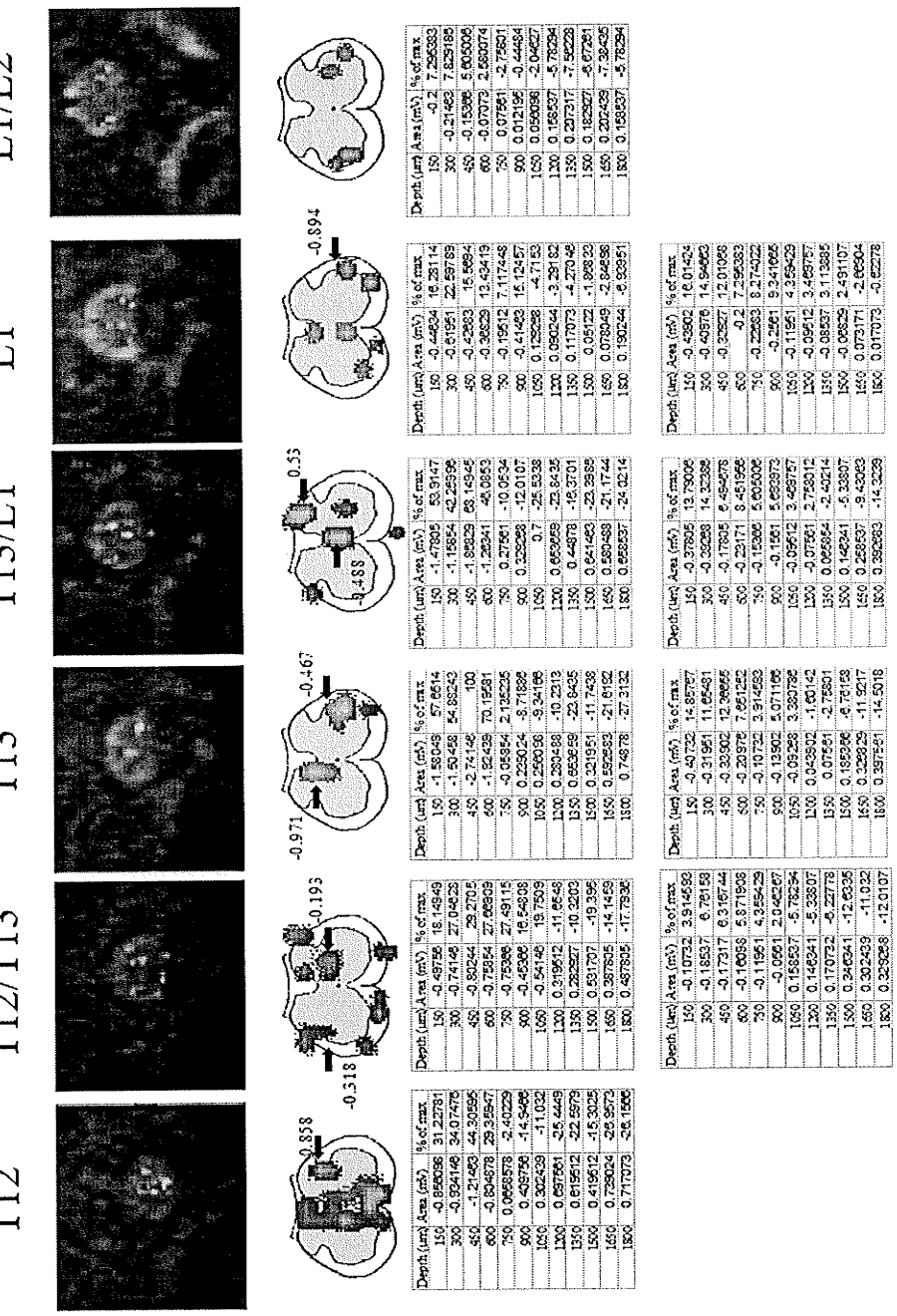

Figure 9. FMRI and electrophysiology from Animal 9. All active pixels from 3 fMRI experiments were overlaid onto one map. Labels indicated the vertebral level of the slice. The images are oriented with dorsal up, ventral down, left side of the animal is on the left side of the image, and the right side of the animal is on the right side of the image. The top row of tables are measurements taken on the right side of the spinal cord. The bottom row of tables are measurements taken on the left side of the spinal cord.